

Automated determination of
the theoretical range of hip motion
prior to total hip arthroplasty
using 3-D models created from pelvic
CT scans

By Ségolène Walter

A thesis submitted in partial fulfilment for the
degree of Master of Science

in the

Department of Biomedical Engineering

University of Strathclyde

August 2015

Declaration of Authenticity and Author's Rights

This thesis is the result of the author's original research. It has been composed by the author and has not been previously submitted for examination which has led to the award of a degree.

The copyright of this thesis belongs to the author under the terms of the United Kingdom Copyright Acts as qualified by University of Strathclyde Regulation 3.50. Due acknowledgement must always be made of the use of any material contained in, or derived from, this thesis.

Signed: Ségolène WALTER

Date: 21st August 2015

A handwritten signature in black ink, appearing to be 'Ségolène WALTER', written in a cursive style.

Acknowledgements

I would like to thank deeply my supervisor Angela Deakin for her support. Through the many difficulties that emerged during the project, she was always available, supportive, and most of all she gave me the right advices at the right time. I would also like to thank Jon Clarke, Alistair Ewen and all members of the Golden Jubilee National Hospital who helped me emerge from several problems I encounter during the last months.

I also am thankful to the Biomedical Engineering Department professors, lecturers and staff for their work during the past year. I realise how much I learned during this Master of Science and hope to be as passionate in my future work as the people I met at Strathclyde.

Finally, I thank my family and friends for their support, especially the ones who took the time to cheer me up even when they were thousands of kilometres away from Glasgow.

Abbreviations

CAD	Computed Aided Design
CT	Computed Tomography
DICOM	Digital Imaging and COmmunications in Medicine
IGES	Initial Graphics Exchange Specification
MCS	Mimics project format
THA	Total Hip Arthroplasty

Abstract

One of the major concerns following a total hip arthroplasty (THA) is the risk of dislocation: the artificial femoral head pops out of the replaced acetabulum due to a leverage effect. It affects about 4,000 patients a year in the UK, for 80,000 THA¹. To prevent this complication, surgeons would benefit from estimating the range of angular hip motion that can be achieved by their patient without impingement between the femur and the pelvis. It would allow them to position more accurately the hip implant during the surgery.

During the project, functional specifications have been established first and analysed before choosing a coherent solution. Then 2-D CT-scans of the hip have been converted to 3-D models with the Mimics software, which is specialised in DICOM (Digital Imaging and Communications in Medicine) data post-processing. The hip centre was measured by locating the centre of extrapolated spheres fitted on the acetabulum and femoral head. The 3D volume models generated were then decomposed into several surface files and exported to the Solidworks software, then reunited into two bone surface structures. The pelvic part being fixed, the femur has been added and located in anatomical position. The motion study manager of Solidworks was then used to set a motion analysis until impingements occurred in different directions. The angular position of the femur at impingement times was measured using the femoral neck axis and the anatomical planes (sagittal, coronal and transverse) centred on the hip joint centre. Then the range of motion in those planes was then deducted.

The types of impingements that occurred during simulation are consistent with clinical findings about dislocation. Therefore the simulation was accurate and should be developed in order to explore more paths like projecting the different femoral angles on radiological planes.

Table of contents

Declaration of Authenticity and Author's Rights	2
Acknowledgements	3
Abbreviations.....	4
Abstract	5
Table of contents	6
Table of figures.....	8
Part 1	14
Introduction	14
1.1 Etiology of Total Hip Arthroplasty (THA)	16
1.2 Contents of thesis	17
Part 2	19
Literature review.....	19
2.1 Etiology of dislocations	20
2.11 Surgical techniques	20
2.12 Implants and bearing surfaces	22
2.13 Component positioning.....	24
2.2 Assessing the risk of dislocation	27
2.21 3D hip reconstruction.....	27
2.22 Steps to 3D reconstruction	28
Part 3	31
Functional specifications	31
3.1 Perimeter.....	32
3.2 Functional expression of needs	34
3.21 Defining the needs for the product	34
3.22 Functions of the product	36
3.3 Search for solutions	37
3.31 SF1 Determine automatically the range of motion from the 3D files	39
3.32 C1: Be compatible with the 3D format.	47
3.33 C2: Display the results to the user.	48
3.34 C3: Cost nothing.	50
3.35 C4: Be compatible with the computer capacities.....	51

3.36 Review of the solutions.....	52
Part 4.....	55
Project progression.....	55
4.1 DICOM viewer and analysis of CT images	56
4.11 First set of CT scans.....	56
4.12 Second set of CT images.....	62
4.2 Mimics Software	63
4.21 Principle of Mimics	63
4.22 Importing the images	64
4.23 Understanding the Mimics interface.....	65
4.24 Creating a mask	67
4.25 Isolating the femur.....	70
4.26 Processing the pelvis.....	73
4.27 MedCAD module	78
4.3 CAD modelling with Solidworks	89
4.31 Basic principle of Solidworks	89
4.32 Reconstruction of the pelvic part.....	91
4.33 Reconstruction of the femur part.....	94
4.34 Assembling the articulation.....	97
4.35 Cinematic analysis	100
4.36 Results of simulation.	103
Part 5.....	108
Discussion	108
5.1 Available CTs	109
5.2 Mimics software.....	109
5.3 Solidworks software	111
Part 6.....	114
Further work and conclusion	114
Associated video files	118
References	119

Table of figures

Figure 1: Modifications of the joint due to severe osteoarthritis (http://www.arthritisresearchuk.org)	16
Figure 2: Modifications of the joint due to rheumatoid arthritis (http://www.arthritisresearchuk.org)	17
Figure 3: Steps for hip replacement surgery (from http://www.medlegalvisuals.com)	20
Figure 4: Incision sites for hip arthroplasty (adapted from http://www.orthopaedicswa.com.au)	21
Figure 5: Structure of a hip implant (from http://evertsmith.com/)	23
Figure 6: A scatter-diagram of the orientation of the acetabular components, showing the “safe zone” (square) determined by Lewinnek et al.	25
Figure 7: Relationship between the angles of cup implantation and head-to-neck ratio, K-H Widmer	26
Figure 8: Evolution of the project planning between the beginning and the end of the project.....	33
Figure 9: Defining the needs with a standardised APTE diagram	35
Figure 10: Standardised « octopus diagram » allowing to define the relationships between the product and its environment.....	36
Figure 11: « octopus diagram » of the current project.....	37
Figure 12: How to find concrete solutions by breaking down a service function or constraint into several technical functions	38
Figure 13: Two first levels of technical functions describing the “SF1: Determine automatically the range of motion from the 3D files”	39
Figure 14: Breakdown of the first degree technical function “Differentiate the femur from the femur” into second degree technical functions leading to concrete solutions	40
Figure 15: Neck axis (C line), long axis (A line) and neck angle (B) of a left femur, anterior view	42

Figure 16: Lateral view of a 3D right pelvis showing the anatomical position (adapted from https://commons.wikimedia.org)	43
Figure 17: Breakdown of the first degree technical function “Identify the hip centre” into second degree technical functions leading to concrete solutions	43
Figure 18: Breakdown of the first degree technical function “Find the range of motion” into second degree technical functions leading to concrete solutions.....	45
Figure 19: Analysis of the constraint “C1: Be compatible with the 3D format” by using technical functions leading to concrete solutions.....	47
Figure 20: Analysis of the constraint “C2: Display the results to the user” by using technical functions leading to concrete solutions	48
Figure 21: Analysis of the constraint “C3: Cost nothing” by using technical functions leading to concrete solutions	50
Figure 22: Analysis of the constraint “C4: Be compatible with the computer capacities” by using technical functions leading to concrete solutions	51
Figure 23: Frontal views of the CT207 (left) and CT208 (right) centred on the knee implants	56
Figure 24: A low-quality slice from CT208 (series 2) displaying the CT parameters on each side and corner	57
Figure 25: Explanation of the parameters displayed on a CT slice	59
Figure 26: Default settings (top) and bone settings (bottom) of series 2 (left) and 3 (right), CT208. The bone settings improve the visualisation of the bone structures..	60
Figure 27: Default settings (top) and bone settings (bottom) of series 2 (left) and 3 (right), CT207. The bone contours appear sharper in the series 2 than in the series 3.	61
Figure 28: High quality of details shown by a CT slice from the second data set	63
Figure 29: Main windows of the Mimics software showing the original CT slices (top right) and the reconstructed coronal (top left) and sagittal (bottom left) views of the patient. The bottom right window shows the same views in 3D.	65
Figure 30: Main control windows of Mimics. The window 1 shows the work made directly on the CT slices, the window 2 shows the extrapolated 3D structures, the window 3 allows the user to generate contours and surfaces and the window 4 allow managing the visualisation parameters.	66

Figure 31: The main tools are displayed in the top toolbars of Mimics	67
Figure 32: The thresholding command as displayed in Mimics. The threshold limits can be adjusted between -1023 and 3071 Hounsfield units manually or selected from predefined thresholds sets.	68
Figure 33: Generated 3D model after first thresholding. Many artefacts are scattered through the model, the table appears posteriorly to the skeleton and the model is not limited to the hip articulation.	69
Figure 34: Cropped 3D model of the right femur. Abnormal holes appear on the femoral head, and fused areas are visible between the femur and the pelvis.	70
Figure 35: The first polylines set (bottom) shows the contours generated from the first 3D model. It allows the new mask being edited (top) to suppress the pelvis in the next 3D model.	71
Figure 36: The new set of polylines (left) does not include the pelvis. It is then converted to a new 3D model (right) generated from a new mask.	72
Figure 37: Evolution of the 3D model before (left) and after (right) one iteration of the refine process. The surface is more detailed after the iteration, but the difference is subtle, so many iterations are necessary to have a good model.	73
Figure 38: Views of 3D model of the left femur after the final iteration, showing a good surface grain and an anatomically accurate bone.	73
Figure 39: “Crop mask” operation on pelvis preserving the pelvic asperities susceptible to lead to impingements with the femur during the motion simulation. ..	74
Figure 40: The first mask (light green, top) includes many different bone structures and shows numerous holes that should not appear. The polylines extrapolated from this mask (yellow lines, top and bottom) reflect this problem.	75
Figure 41: The first iteration consists in a removal of the femurs, the sacrum and the main artefacts. The polylines are recalculated and shown here: the model is clearer.	75
Figure 42: From the rough CT slice (top left) the extrapolated polylines define automatically the contours of the bone (middle), but the process is far from perfect (holes and inadequate shapes). Therefore the user has to recreate the mask manually (bottom right) based on the polylines and measurements on the CT slices.	76

Figure 43: There is a clear improvement in the quality of the 3D model of the pelvis before (top) and after an iteration (bottom). The surface is smoother, artefacts are removed and abnormal holes are filled.	77
Figure 44: Smoothened model of the pelvic bone showing a realistic rendering of the bone surface.....	78
Figure 45: By zooming on polylines calculated from the new pelvic model, we can see how they are extrapolated directly from the 3D model.....	79
Figure 46: By doing a polyline growing (green lines) from polylines of the left pelvis (red lines), only a part of the pelvis is selected.	80
Figure 47: Definitive location of the different polyline growing sets for the left femur (top) and left pelvis (bottom). This segmentation has to be done with horizontal limits since it is based on polylines which are in the transverse plane.	81
Figure 48: Selection of a polyline in a slice during polyline growing process. If two different closed contours were selected in the same slice of a single polylines set, the following surface generation could not be solved by the Mimics algorithm.	82
Figure 49: Freeform surface fitting interface allowing the user to choose the order and number of control points to be used for the surface fitting.....	83
Figure 50: Surface artefact due mainly to an inaccurate number of control points, making the generated surface inadequate for further analysis.	84
Figure 51: Gap between superior and medial part of left pelvis due to lack of polylines overlap. The resulting assembly is not suitable for analysis since there is a lack of surface information.....	84
Figure 52: Fitted surface before (left) and after (right) “order” and “control point” adjustments. After the adjustments, the surface is fitted closer to the 3D model hence it is a better representation of the real surface.	85
Figure 53: Extracted surfaces of the left pelvis (left) and the left femur (right) shown with (top) or without the original 3D model (bottom). For these surface models, the important parameter is to fit closely to the 3D model regardless the surface rendering.....	86
Figure 54: Sphere fitted on the acetabular surface and its projection in coronal (top left), transverse (top right) and sagittal plane (bottom left). Simple measurements on the slices allow positioning the sphere accurately in the different planes.	87

Figure 55: Measurements on the acetabular (top) and femoral sphere (bottom). The location of the hip centre based on the femoral head is consistent with the one based on acetabular cavity. The acetabular fitted sphere is logically slightly larger than the femoral head one.....	88
Figure 56: Fitted sphere, cylinders and axes on left femur 3D model defining the geometrical parameters of the bone.	89
Figure 57: Early assembly tree of a 2-parts assembly (“superior” part partially blue and “lateral” part partially pink) in Solidworks. Many parameters already appear in the tree despite the simplicity of the overall structure, and must be managed to ensure the stability of the assembly.	90
Figure 58: Import diagnostic window analysing the "medial" surface of left pelvic bone. The “faulty faces” are unwanted defects of the Mimics generated surfaces whereas the “gaps between faces” are to be connected with the “superior” and “inferior” parts of the pelvis.	92
Figure 59: Assembly of the four pelvic surfaces and associated assembly tree. At the bottom of the tree, we see the four “Lock” mates that ensure the immobility of the pelvis.	93
Figure 60: Complete left pelvic bone with fitted sphere. The centre of mass has been recalculated within Solidworks to redefine the centre of the hip articulation.	94
Figure 61: "Patch boundary" being performed on the upper limit of the "crest" part. This will repair the surface by closing a residual hole on the model.....	95
Figure 62: Femoral sphere positioning, anterior view of coronal plane. The translation is very carefully controlled by the left window (up to 0.1nm precision)..	96
Figure 63: Geometrical parameters leading to the reconstruction of the neck axis. The neck centre is extrapolated from two neck points (A and B) which coordinates were measured on CT slices and the plane normal to the AB axis that passes through the head centre.....	97
Figure 64: Hip articulation assembly and associated mates The “Multi-Mates” 1 to 4 are the “Lock” mates that fix the pelvis. The last mate (“Coincident”) is the coincidence of the femoral head centre and the acetabular centre.	98

Figure 65: Anatomical planes passing through the hip centre. These planes are to be used for projecting the measured angles of the hip articulation after the motion simulation.	99
Figure 66: Hip articulation with new axes and anatomical planes. These new axes are designed to be used as rotation axes for the femur during the motion simulation.	99
Figure 67: Updated mates showing the three new angular parameters (bottom) that can be modified in order to control the displacements of the femur during the motion analysis.	100
Figure 68: Setting the default value of the angle between the neck axis and the vertical axis (SagCorAxis). We see that the default anatomical angle is set at 136.04° in the coronal view.	101
Figure 69: Full Solidworks screenshot showing the Motion Study manager (red frame). This module must be managed in time, hence the blue and brown lines extending in front of each parameter that represent the setting changes in time.	102
Figure 70: First impingement during simulation between the greater trochanter and the antero-superior iliac spine, coronal view.	103
Figure 71: Angular measure between neck axis and sagittal plane at first impingement, superior view. The femur has rotated internally around the hip centre towards the pubis from the anatomical position.	104
Figure 72: Second impingement, between the lesser trochanter and the ischium, during the simulation.	105
Figure 73: Maximum angles between neck axis and sagittal plane measured in a transverse view. The total range of motion in this view is 75.59° if we consider the two impingement angles as the extremums.	106
Figure 74: Maximum angles between neck axis and sagittal plane in a coronal view. The range of motion is 94.66° between the initial angle and the first impingement angle. The second impingement angle is inferior to the initial angle because of a rotation of the femur around its neck axis restricting the motion of the bone.	107

Part 1

Introduction

The life expectancy nowadays is significantly increasing while the population in the UK is ageing rapidly, according to the Office for National Statistics². This situation leads to an increase in the number of articular diseases (often linked to age) and therefore more and more total hip arthroplasties (THA) are performed. The aim of THA is to replace the deficient articulation by a prosthesis that mimics the physiological behaviour of the hip. If this operation is performed as a routine, it remains major surgery with possible complications that can become serious.

One of the most common complications is the hip dislocation. This is a multifactorial phenomenon that occurs when the head of the femoral component comes out of the acetabular socket. The main causes of dislocation are related to 3 parameters: the surgeon, the patient and the implant. Obviously, it is not possible to modify the patient factor when it comes to anatomical or physiological parameters. However, it is possible to educate the patient to lower the risk of dislocation. The remaining challenge is then to choose the implant carefully and to optimise the positioning of the implant by the surgeon. By estimating the range of hip motion that can be achieved by the patient before the operation, surgeons can have a better understanding of how the new hip must be implanted in order to minimise this risk of dislocation, especially regarding the angle of implantation.

The present project is designed to support this task by finding a way to reconstruct 3D hip models from CT scans and then simulate the articulation movements in order to evaluate the achievable range of motion without impingement. No previous work on this subject has been done within the Department of Biomedical Engineering or at the Golden Jubilee National Hospital; therefore the path to this simulation is part of the project in itself.

1.1 Etiology of Total Hip Arthroplasty (THA)

Total hip arthroplasty (THA) has become a routine operation. According to the National Joint Registry³, about 80,000 hip replacements are performed each year in England and Wales in nearly 400 hospitals. The dislocation prevalence following THA ranges from 0 to 4.1% according to a 2012 study by Nutt *et al*⁴. Higher rates of dislocation are generally associated with revision surgery (when a patient must be operated again).

THA is performed in order to replace a deficient hip articulation, when the patient's life conditions are significantly impacted by the underlying disease. The 2013 publication of Pivec *et al*.⁵ explains that this impact can be pain or difficulty to walk, but often patient experience both problems. However, THA is usually performed as late as possible since doctors prefer to rely as much as they can on the real articulation. It allows diminishing the time, during which the patient will live with an artificial hip. Hence, the risk of degradation of the prosthesis will be lowered, and so will the probability of a revision surgery.

The main causes of hip degradation that lead to a hip replacement are osteoarthritis (shown figure 1), rheumatoid arthritis and hip fracture, as reported by the NHS⁶. Pivec *et al*. report that more than 90% of THA are in direct relation to advanced osteoarthritis.

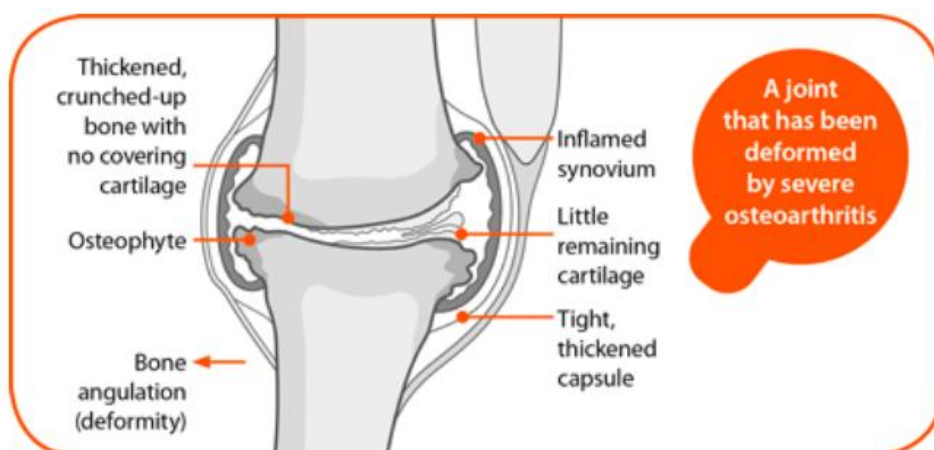


Figure 1: Modifications of the joint due to severe osteoarthritis
(<http://www.arthritisresearchuk.org>)

Osteoarthritis is a degradation of the articulation that has many causes; mainly age, genetics, trauma or obesity are involved. Several abnormalities take place in the joint, causing pain as well as tissue modifications that limit the range of motion the patient can achieve.

The second most common cause of THA is rheumatoid arthritis, an autoimmune disease that also damages the inner structure of the joint (figure 2). The immune reaction of the patient's antibodies against its own joints generates an inflammation that results in degradation and a swelling of the articulation.

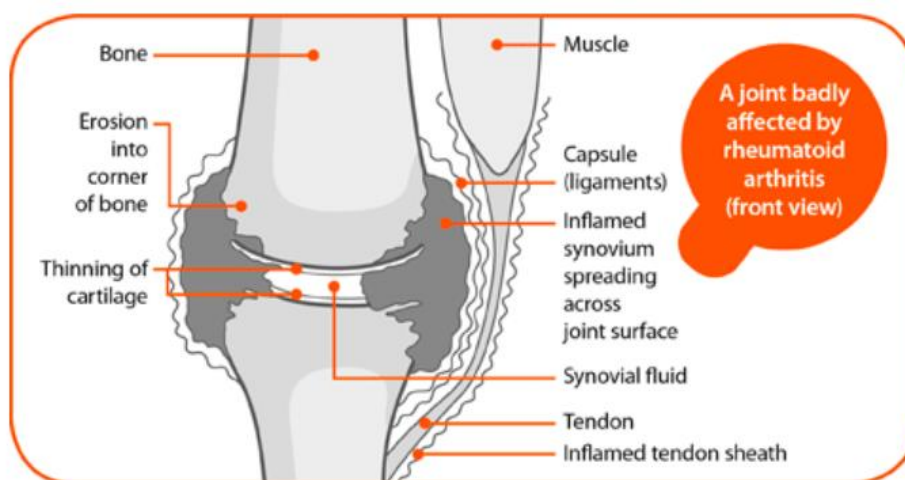


Figure 2: Modifications of the joint due to rheumatoid arthritis
(<http://www.arthritisresearchuk.org>)

Finally, hip fractures mainly result from falls in the elderly population. It concerns more women than men as a consequence of osteoporosis.

Some of the less common causes of hip degradation that require hip replacement are tumours, femoral necrosis, infections or genetic diseases like dysplasia.

1.2 Contents of thesis

This thesis is composed of the following sections: the literature review, the functional specifications, the project progression, the discussion and finally the conclusion and recommendations for future work.

The literature review aims to inform the reader on previous studies and scientific publications that are useful to the project. The first part is focused on the etiology of dislocations and how it is possible to reduce their frequency. This section will discuss the existing surgical techniques, the types of implant that are available and the way they are positioned during the operation. The second part of the literature review tends to describe how the risk of dislocation is assessed with numerical tools. Since the final objective of the project is to assess this risk with a custom-made 3D simulation, we will first ensure that such work has not been done elsewhere. After this verification, we will then take a particular interest in the steps that can allow us to perform an accurate motion simulation of the hip articulation.

The functional specifications are a very important part of this project. Since it has no pre-existing bases in the Department or at the Golden Jubilee, an in-depth analysis of the requirements for the final product was necessary. This section therefore attempts to ensure the viability of the project, and then does a systematic functional analysis to consider any aspects of the project development. The principle is to start from the functions we want to achieve and develop them, and then break the result into technical functions that we can associate with concrete results. All we have to do then is choose the best solution by combining the optimal results in a logical way. This functional analysis is therefore supposed to convert ideas to practical solutions.

The project progression will be a chronological display of the project advances, explaining the difficulties as well as the successes of the computational work. Some scientific notions will also be explained where needed, in order to enlighten the reader.

The discussion aims to critically review the project. It is a useful measure for personal improvement as well as a necessary step to pursue the project. This continuation of the project will then be developed in the last part of the thesis, in the “further work” section included in the conclusion.

Part 2

Literature review

2.1 Etiology of dislocations

2.11 Surgical techniques

Regardless of the cause, the natural evolution of the diseases that degrade the hip articulation will commonly imply that the patient undergo a hip replacement. This operation is performed daily in many hospitals and is usually very successful. The basic principle is to remove the damaged structures of the joint and replace them with an artificial prosthesis as shown in figure 3.

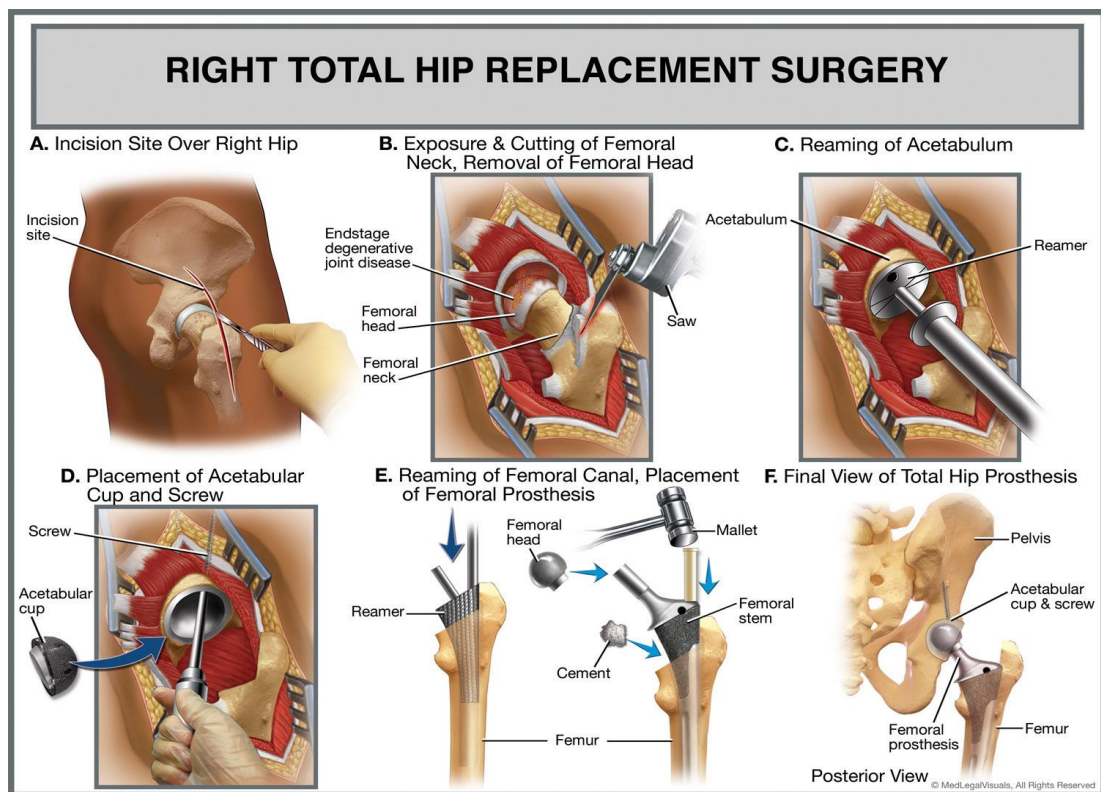


Figure 3: Steps for hip replacement surgery (from <http://www.medlegalvisuals.com/>)

The surgeon can operate with several different entry points. To reach the articulation, it is necessary to go through muscles that surround the hip. The two major differences between the four principal surgery techniques are on one hand which muscles groups are crossed during the operation and on the other hand whereas the muscles are incised or just pushed aside during the operation (Hosack *et al.*, 2009⁷).

The direct anterior (or Smith-Petersen) and the anterolateral minimal (or Watson-Jones) approaches do not require to cut through the muscles. The operation is then performed by entering in intervals between muscle groups of the thigh. Specifically, the direct anterior entry point is between the tensor fascia latae and the sartorius (Nogler, 2009⁸), and the anterolateral approach gives access to the intermuscular space between the gluteus medius and tensor fascia latae (Garbuz *et al.*, 2009⁹), as shown in figure 4.

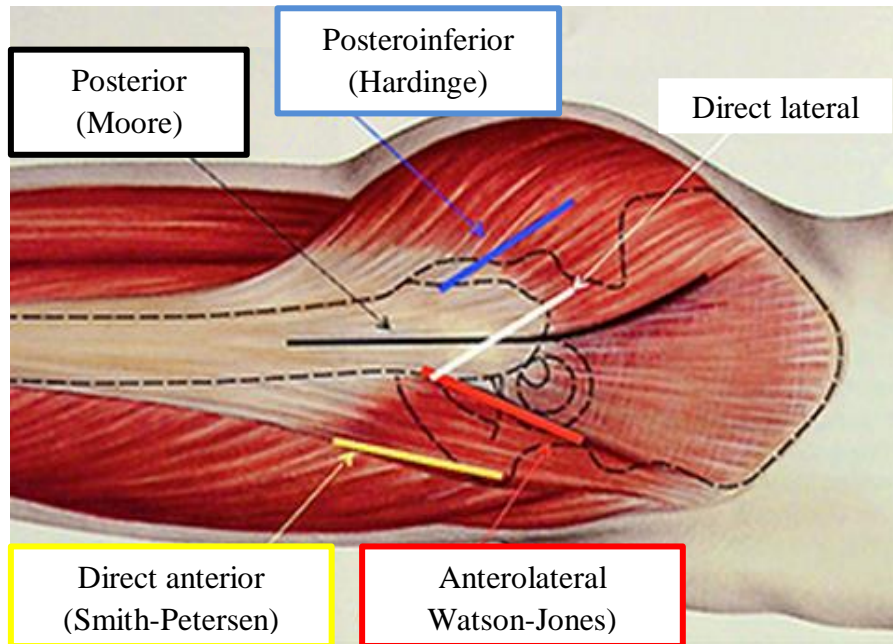


Figure 4: Incision sites for hip arthroplasty (adapted from <http://www.orthopaedicswa.com.au>)

At the contrary, the direct lateral and posterior approaches require to cut through muscles, essentially the tensor fascia latae and gluteus maximus (Ormonde *et al.*, 2009¹⁰ and Lusty *et al.*, 2009¹¹).

Many controversies exist about these different techniques. Therefore, a great amount of studies have been performed in order to determine which entry point led to the minimal dislocation rate after the operation.

According to Palan *et al.* (2009)¹², the operation was historically performed from a posterior entry point (Moore approach) through the gluteal muscles, but nowadays the direct lateral or transgluteal (Hardinge) approach is used as often. Ploumis *et al.*

(2003)¹³ state that this method is related to a greater number of complications following the operation compared to the Hardinge one. It seems that the damaging of the gluteus that occurs with the posterior entry point results in an increase of muscle weakness that might lead to an increase of postoperative dislocations among other complications. However, this point of view has not been confirmed, and both approaches are still equally performed, suggesting that there is no significant difference. This point of view is supported by M.S. Kwon *et al.* (2006)¹⁴ in a publication that cross-references several studies on this subject. Their conclusion is that there is no significant difference regarding the dislocation rate depending on the type of entry point, as soon as adequate soft tissue repair has been performed during surgery. The absence of significant change (minor difference considered as “not clinically relevant”) in dislocation rate after the posterior or direct lateral approach was also depicted by Witzleb *et al.* (2009)¹⁵. But some papers have opposite conclusions. For instance, a study by Demos *et al.* (2001)¹⁶ concluded that the direct lateral approach eliminated almost all dislocations after primary hip arthroplasty.

2.12 Implants and bearing surfaces

The implants are composed of two main parts. One is the acetabular cup, which is designed to replace the anatomical acetabulum and must be inserted in the pelvis. The complementary part is the femoral component. Its head fits into the cup, whereas the stem is inserted in the femur after resection of the proximal extremity of the bone (see figure 5). The bearing surfaces that are in contact between those two parts are transmitting the mechanical loads through the articulation.

There is a large variety of hip implants used to replace the disease joint.

The materials used for the different part vary, but their mechanical characteristics always remain quite similar. Kaivosoja *et al.*(2013)¹⁷ explain that they are designed to resist high pressures and minimise the friction, so they can support the body weight and promote a smooth motion of the joint. Resistance to degradation and remodelling processes is also fundamental.

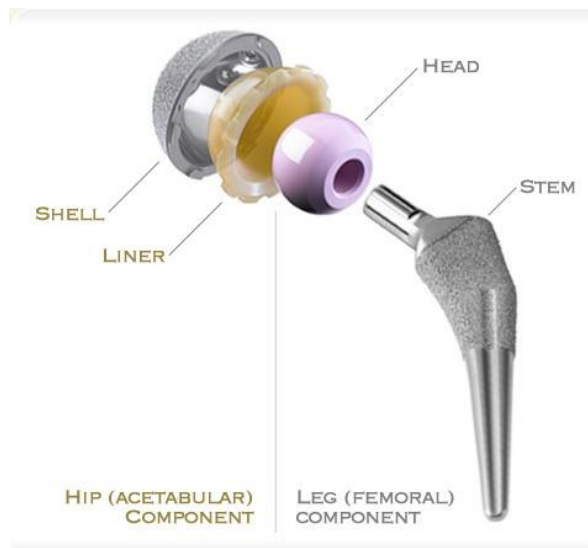


Figure 5: Structure of a hip implant (from <http://evertsmith.com/>)

The acetabular and femoral bearing surfaces may be composed of the same material, but it is not always the case. The main types materials used for these surfaces are polymers, metals and ceramics (Sonny and Vallurupalli, 2013)¹⁸. These materials can be used for both femoral and acetabular bearing surfaces like metal on metal (MoM, often cobalt-chromium or titanium alloys) or ceramic on ceramic (CoC, generally alumina or zirconia) implants, but it is also possible to combine different materials. Ceramic on plastic (Ultra High Molecular Weight Polyethylene, UHMWPE) or metal on plastic (polyethylene or UHMWPE) are the most common mixed implants nowadays Kaivosoja *et al.*(2013)¹⁹.

The type of fixation also varies. As it is described by Pedersen *et al.* (2014)²⁰ it can be a cemented fixation that grouts the stem into the femur with polymethylmethacrylate (PMMA), a biocompatible type of polymer. The other possibility is to use a cementless fixation. The stem of the implant is longer, and has a porous structure allowing in-growth (inside the stem) or on-growth (on the surface) fixation when the patients cells migrate inside the structure and form new bone. This phenomenon anchors the stem into the bone. The last technique used for total hip arthroplasty is called hybrid fixation: one element (generally the acetabular cup) is cementless whereas the stem is cemented.

It is important to notice that many studies like the one realised by Pedersen *et al.* (2014) have been conducted in order to compare these types of implants (also see for example Wear of materials used for artificial joints in total hip replacements by Wilches, Uribe and Toro²¹) but in the majority of these studies there are no findings that are significant regarding the rate of hip dislocation of these different implants, even if Pedersen *et al.* (2014) suggest that the cemented prostheses “perform better in relation to long-term risk of aseptic loosening”.

The last variation between the different hip prosthesis is the size. The acetabular cup and femoral head are available in many diameters in order to fit the patient. The neck of the femoral part, which connects the ball to the stem, also may have various sizes. The size of the components itself does not seem to influence that much the dislocation rate. A bigger head seems safer however. But another important parameter explained in latest studies is the head-to-neck ratio which is of particular interest regarding the impingement possibility (D’Lima *et al.*, 2000²²).

The head-to-neck ratio is the relationship between the diameter of the femoral head and the diameter of the neck²³. It is well known that the augmentation of the head-to-neck ratio allows increasing the range of motion that can be achieved without prosthetic impingement. It is supported for example by D’Lima *et al.* in 2000 and by Widmer and Zurfluh in their 2003 publication²⁴. This is really important, because the impingement leads to the possibility of dislocation. It happens most often between the neck and cup. An optimised head-to-neck ratio allows therefore minimising the risk of dislocation.

2.13 Component positioning

The positioning of the acetabular component seems to be fundamental in the dislocation problematic (Veitch and Jones, 2009²⁵). This subject has been assessed in 1978 by Lewinnek *et al.*²⁶ in a publication that support the idea of a “safe zone” that

would minimise the risk of dislocation. This “safe zone” is delimited by a range of angular positions of the acetabular cup. In this publication, the authors define two angles of interest:

- α , the anteversion angle
- ϑ , the lateral opening angle.

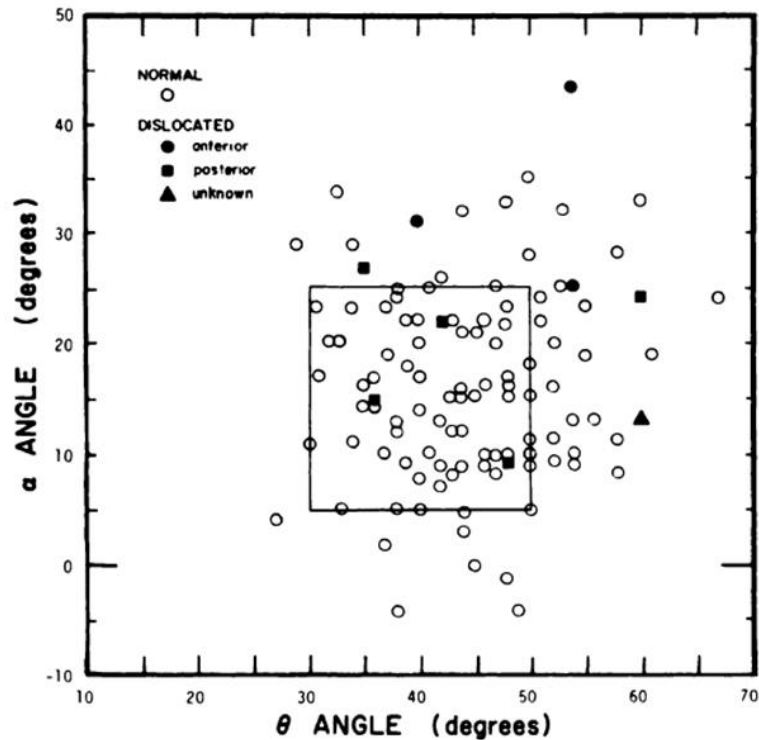


Figure 6: A scatter-diagram of the orientation of the acetabular components, showing the “safe zone” (square) determined by Lewinnek et al.

We can see in figure 6 the “safe zone” which is represented by the square. According to the authors, the dislocation rate in this square is four times less than outside (1.5% against 6.1%). Therefore, the recommended angles of acetabular implantation would be as follow:

15 ± 10 degrees for α and 40 ± 10 degrees for ϑ .

These findings are now controversial, mainly because the study took only one parameter into account, the angle at which the cup was oriented. The most recent papers tend to include numerous parameters and cross the results to have a more complete overview on the dislocation origin. Karl-Heinz Widmer produced in 2006 a very interesting paper²⁷ addressing this issue. He insists on the fact that the angular

positioning of the acetabular cup should be linked to the prosthesis design, included the head-to-neck ratio, as shown in figure 7.

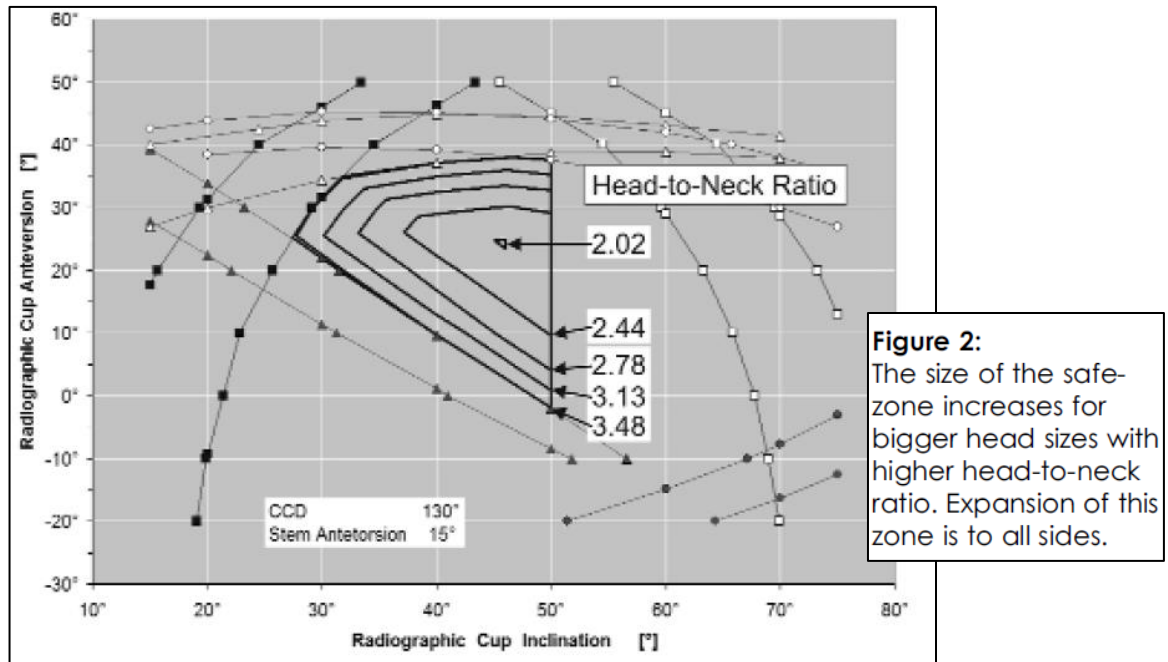


Figure 7: Relationship between the angles of cup implantation and head-to-neck ratio, K-H Widmer

The conclusion is that there is no universal “safe zone”, but a conjunction of parameters that minimise the risks of dislocation, and reduce the impingement possibility to nearly zero. To achieve this goal, it is very important for surgeons to have a maximum of information prior to surgery, which can help them positioning the implant in the most efficient way. Abe *et al.* (2015)²⁸ insist on the importance of stem and cup alignment to minimise the dislocations, in addition to the cup “safe zone” concept which can still be a good start for component positioning. Some researchers like Widmer and Zurfluh (2004)²⁹ also suggest that other parameters like stem-neck angle and the design of the acetabular opening are susceptible to influence the hip stability after arthroplasty.

2.2 Assessing the risk of dislocation

2.21 3D hip reconstruction

The determination of hip motion prior to surgery is a crucial parameter to reduce the risk of hip dislocation. It allows the surgeons to optimise the angular positioning of the prosthesis regarding their choice of implant.

Some individuals have already tried to create an automated determination of hip motion, but their findings are generally kept secret since they exploit the result in a lucrative way. One example is Clinical Graphics³⁰, a company located in the Netherlands that offers a 3D hip impingement analysis from MRI or CT scans, for €249 plus 21% BTW (Dutch value added tax), equivalent to a total of £212. However, a number of publications address the issue of hip motion range determination, like a 2007 article by Arbabi, Boulic and Thalmann³¹ but they detail the mathematical solution of the computer-based method. Therefore, we have access to the mathematical operations that happen inside the computer, but not to the practical use of the computer language. This is of limited interest if we want to use a CAD software-based approach, since we will not have access to the underlying code.

Some publications are strictly limited to a mathematical point of view. The publication of Yoshimine and Ginbayashi published in 2002³² might be a good start for us to try to create an original algorithm, since the analysis of motion is only based on angles and trigonometry. The limitation of this method is that it requires a measurement of many parameters (angles and axes) which are not always directly accessible with a simple batch of CT scans; furthermore, it is based on measurements on the prosthetic elements too, hence the theoretical range of motion calculated applies *after* the operation. It is not a method used for assessing the movements prior to surgery, which is the aim of this project.

Some work has been done on the MRI computation in order to define the range of hip motion, but it relates to dynamic studies and not static data like the ones we

obtain from CT scans. See for example Calculation and Visualization of Range of Motion of Hip Joint from MRI³³ which is a thesis submitted in 2014 and uses the dynamic possibilities of MRI. Some work has also been done by Hagio *et al.* in 2004³⁴ in this area. They realised what they called a four-dimensional analysis (3D plus time): this study aimed to assess the range of hip motion after hip arthroplasty by combining CT data and an open MRI motion capture system. Recording the real movements of each patient seems a good way to guide the re-education after the hip arthroplasty, but it is not the same as trying to estimate these movements before the operation.

The very limited amount of publications regarding an actual computer-based method of analysing CT scans to evaluate the hip motion range confirms that there is a need for elaborating a new, fast method that would help surgeons to perform better surgery, and therefore decreasing the dislocation rate after THA.

2.22 Steps to 3D reconstruction

If no specific solution has been found for 3D assessment of the range of motion, some steps can be individually identified and investigated. To be able to perform a 3D-analysis from a simple batch of CT scans, we will have to take interest into the quality of the 3D models, the location of the hip centre and the accuracy of the numerical data compared to the clinical results.

2.221 Quality of 3D reconstruction from CT scans

The accuracy of the 3D models we can reconstruct from CT slices is obviously a fundamental parameter to obtain coherent results. Some investigations have been performed by Wang *et al.* in 2009³⁵ to determine the precision of the cortical bone 3D reconstruction. This study was not only investigating the numerical 3D model, but also the physical 3D model obtained by machining from the 3D numerical data. The errors they measured in the coronal, sagittal and axial directions had a mean of 0.21 mm, with standard a deviation of 0.12 mm and a maximum error of 0.47 mm.

The researchers concluded that 70% of the errors were due to the image processing, therefore the way the CT slices are processed has a very important role in the accuracy of the 3D models.

Rathnayaka *et al.* (2012)³⁶ compared the accuracy of MRI-based and CT-based 3D models, and found that no statistical difference emerge from this analysis. Furthermore, the study has been conducted on ovine cadavers, which allowed a comparison between the CT-based models deduced from CTs of the complete limb (bone surrounded by soft tissues) with the real isolated bone (after removal of soft tissues). They found only a 0.15mm average error between the estimated bone structure and the 3D model of the femur, which seems a good approximation.

For those studies, the method of 3D modelling is not explicit. It is interesting to see that the 3D reconstruction requires a process called thresholding (Starzynski *et al.*, 2015)³⁷. Basically, it consists in an automatic selection of the bone structure by filtering the voxels (volume pixels) of the CT slices. This selection relies mostly on the operator, but Starzynski *et al.* created an algorithm that allegedly makes this selection almost automatic. Unfortunately, this technique is very recent (2015) and many parameters need to be improved. It remains an experimental study, and the authors indicate that at this stage their algorithm “is not sufficient for skeleton structure extraction and selection of the individual bones”.

Therefore, it remains a delicate task to select the right data and realise the most accurate thresholding on the CTs. It still relies on the operator’s skills and what Starzynski *et al.* referred to as “an expert knowledge” of the bone structure, especially the cancellous parts. Moreover, the sliced nature of the CT data leads inevitably to approximations. To obtain smooth 3D models, some estimation must be done about the real bone geometry. In a 2011 study, Kels and Dyn³⁸ indicate that an iterative process of interpolation and extrapolation of the data would benefit to the 3D model. In simplest terms, it suggests that successive operations would lead to a better structural accuracy than a single complex numerical reconstruction of the missing data between the different CT slices.

2.221 Location of the hip centre

In order to properly estimate the range of motion of the hip articulation, the hip centre must be located accurately. It is the only way the impingement risk can be assessed with a good reliability. Since the aim of this project is to use CTs to do the 3D model, it seems logical to find out if it is possible to locate precisely this centre with the CT slices.

A study by Viste *et al.* (2013)³⁹ compared the precision of CT-based location of the hip centre compared to motion analysis (3D palpation of the bone) on dried femurs. By doing a least square regression on the CT data, they determined that no statistical difference could be detected between these different methods. Therefore it tends to prove that CTs are good material to estimate the hip centre.

This result is also corroborated by Kainz *et al.* (2015)⁴⁰ in an extensive comparison between numerous methods allowing finding the hip joint centre. They conclude that CTs (along with X-rays and MRI) remain the “gold standard” for finding this point. The interesting information that is displayed in addition to this confirmation is the method used for estimating this centre. Kainz *et al.* state that a sphere fitting is the most accurate functional technique whereas the most precise regression method is the use of Harrington equations. These equations are explained by Harrington *et al.* in a 2007 publication⁴¹. They are based on several physiological measurements (from MRI images with external markers in this study) used in three linear regression equations that end up to a pretty accurate location of the hip joint centre. However, a limitation of this method lies in the necessity to access extended measurements. Without the external measures, it is not possible to rely only on the CT slices, and therefore it would surely be more appropriate to prefer either a least square regression or a sphere fitting to find the hip centre based on CT slices.

This point of view is confirmed by Sanding *et al.* (2012)⁴² who claim that it is more efficient to first adjust circles to the femoral head because of its quasi-circular shape. Their results are refined by integrating the location of the head-neck intersection into their estimation.

Part 3

Functional specifications

This section aims to describe clearly the final product and its specifications, by setting a perimeter, describing the initial hypothesis and associated constraints of the product.

The functional analysis is based on the APTE method (méthode APTE⁴³) that emerged in France in the 1960's to improve the quality of industrial products. The principle of this method is to focus on the client's expectations and needs to create the adequate result. It is a customer-based approach that contrasts with the old product-based one.

With this method, it is important not to be restrained by preconceived ideas about the final product, in order to be as creative and effective as possible. The concept of the product and its solutions should emerge from the analysis and not the other way around; therefore, it is called "the product" through the entire section to allow us to remain neutral.

Here, the product must be an answer to the following part of the project: "**Automated determination of the theoretical range of hip motion** prior to total hip arthroplasty using 3-D models created from pelvic CT scans". The conversion from pelvic CTs to 3-D models is not included, because the use of the Mimics software was set to achieve this goal from the very beginning of the project.

3.1 Perimeter

The perimeter sets the limits of the project. It is usually composed of three parameters: time, resources and cost. They must be defined from the start of the project, and should not be changed afterwards. However, it might be necessary to adjust one of those parameters at some point, but it is important to bear in mind that the three limits are interconnected: the extension of one of them leads to the extension of the two others. For instance, if more resources are needed, then it will take more time and money to achieve the project.

In this MSc project, the time is set from the beginning as well. It cannot be extent further than August 13th 2015, with a full-time beginning on June 1st 2015. The duration of the project is therefore 10 full weeks. The initial organisation of the workload compared to the real schedule is shown in figure 8. We can see here that there is an important evolution over time, because unexpected difficulties or changes always interfere with the planned organisation. A project is always evolving, so it is important to adapt and reorganise the workload on a weekly basis.

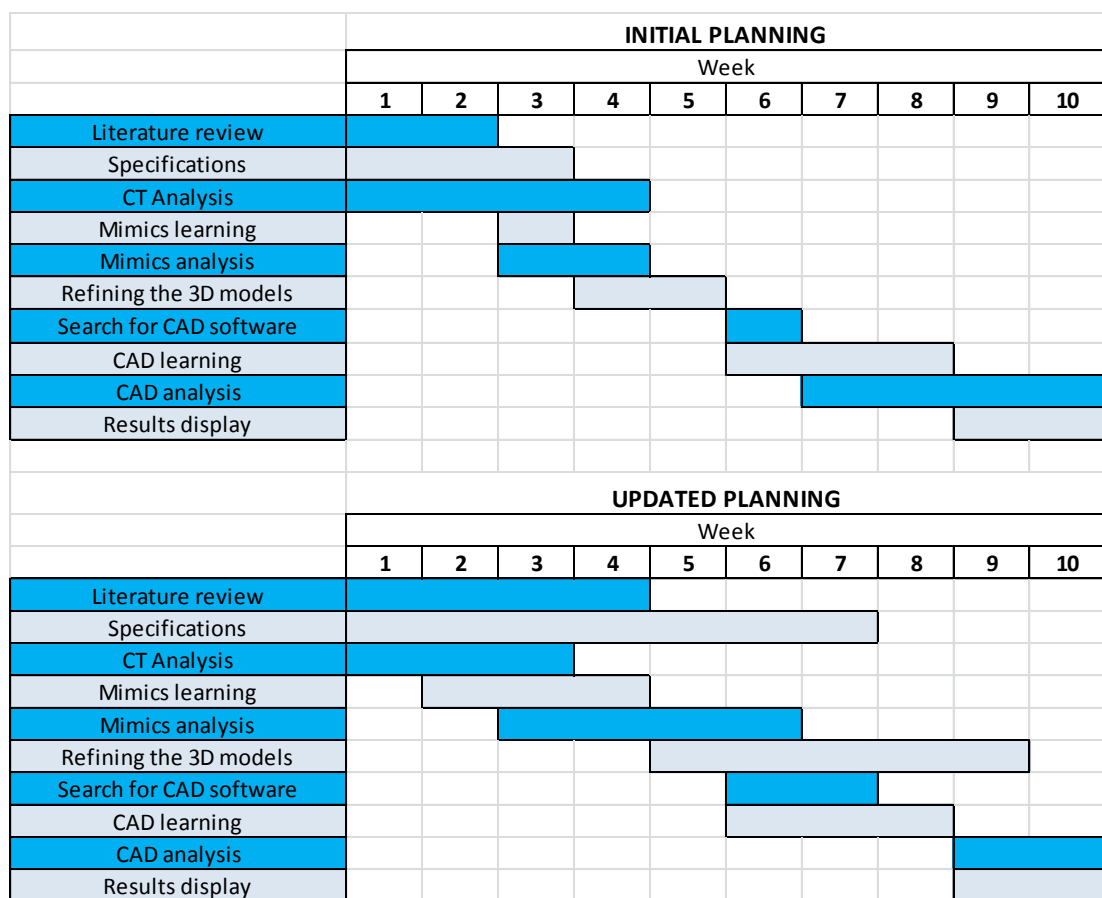


Figure 8: Evolution of the project planning between the beginning and the end of the project

The available resources include both people and physical or numerical resources. The people involved in the project are either from the Department of Orthopaedics of the Golden Jubilee National Hospital or the Department of Biomedical Engineering

of the University of Strathclyde. The physical resources include all materials relevant to the project, CT scanners and computers mainly. The numerical resources are self-explaining. CT scans, Mimics and other software enter this category. The limitation is the availability of the software: it must be either software which licence is owned by the University or the Hospital or a freeware. It also requires access to the computer on which the necessary software are installed. For instance, Mimics is only available through a single computer in the Biomedical Engineering department, and other students need it for their project as well, so the access is restricted.

The cost is implicit; there is no specific donation for the project. The only “cost” will be included in the time and resources attributed to the project, and it cannot benefit from any other funding.

3.2 Functional expression of needs

3.21 Defining the needs for the product

The utility of the product must be proved in order to start a project to develop it. Therefore we need to check whereas the need for the product will be perennial or not based on the basic graphical description shown figure 9.

Who needs the product?

The medical staff, especially orthopaedic surgeons and possibly the medical staff working with them.

Why do they need the product?

To allow an estimation of the range of hip motion after arthroplasty, in order to decrease the risk of dislocation.

What might decrease or suppress the need for the product? In what extent?

An integrated 3D-analysis tool integrated to the CT output would decrease the need for the product. Technologically, this could be achieved within a few years, but the costs involved in such an evolution make it unlikely to happen.

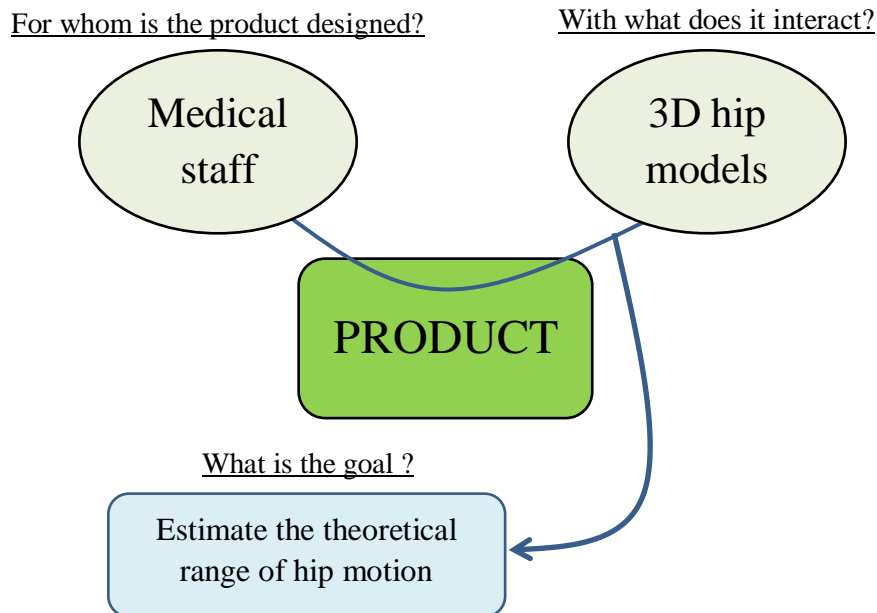


Figure 9: Defining the needs with a standardised APTE diagram

In the same way, external assessment of the anatomical range of motion of the patient would impact the need for the product. This could be high-quality ultrasound measurements for instance, but this is not an easy transition to make since the reference imaging before hip surgery remains CT scans. Furthermore, this kind of external assessment would still require image processing, so automated determination would not be operational. Therefore it is not before years that this kind of change would impact our project.

We can then conclude that there is a real need for the automated determination of hip motion based on 3D reconstruction from CT scans.

3.22 Functions of the product

Now that we ascertained the need for our product, we must define it as accurately as possible by describing the functions that must be performed by the product. Two types of functions coexist in any product:

- Service function (SF), which justify the existence of the product. It relates two of the external elements to the product.
- Constraints (C), which limits the use of the product. It relates one external element to the product.

All these functions are displayed in a standardised format called “octopus diagram” as shown in figure 10.

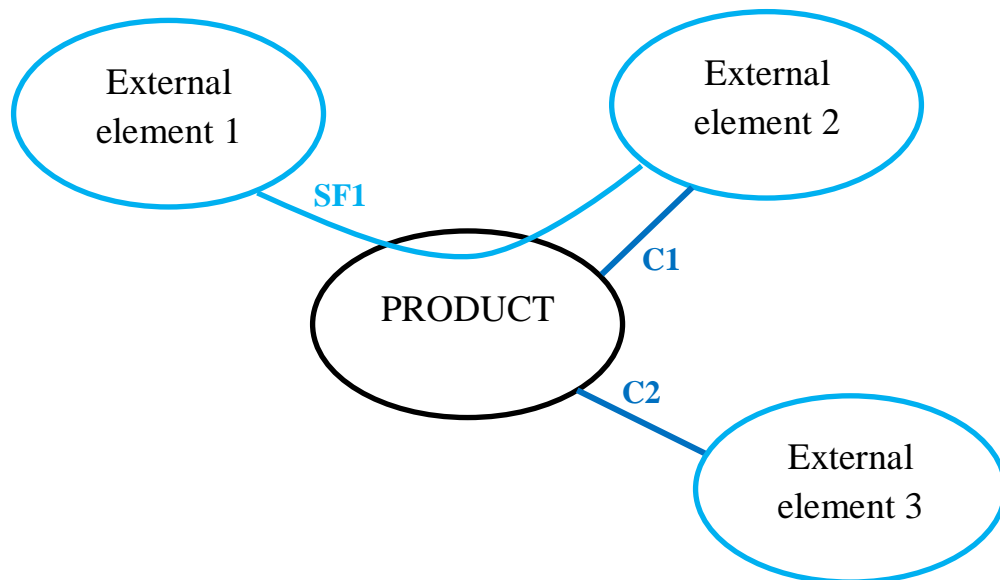


Figure 10: Standardised « octopus diagram » allowing to define the relationships between the product and its environment

The external elements are all the items that are different from the product. It generally includes the user. The functions are then described one by one with a simple phrase. All functions must begin with an infinitive verb that is virtually preceded by “The product must”, and should not be in a negative form. They must not suggest any concrete solution or contain any technological information. This

formalism might seem a little onerous, but it is a necessary base for a well-structured analysis in the next step.

In the current project, the “octopus diagram” in figure 11 covers the essential functions of the product.

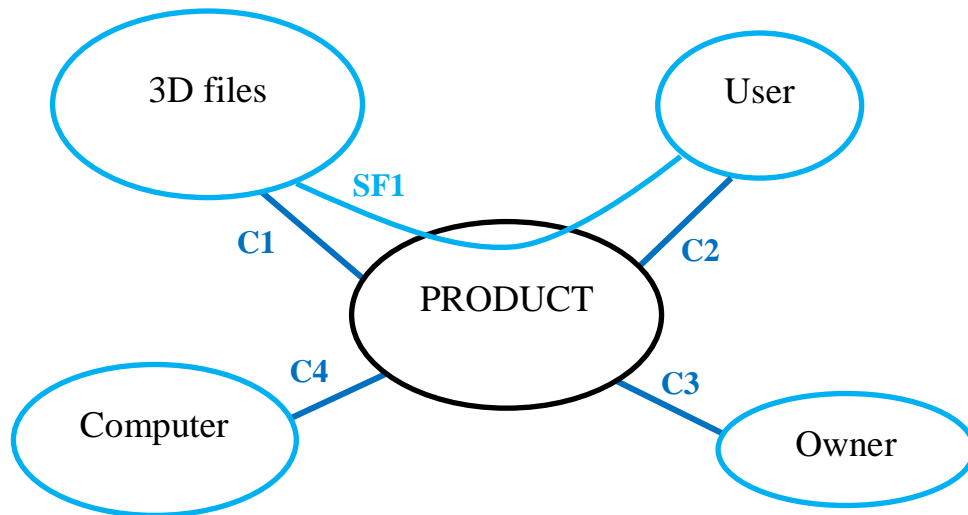


Figure 11: « octopus diagram » of the current project

SF1: Determine automatically the range of motion from the 3D files.

C1: Be compatible with the 3D format.

C2: Display the results to the user.

C3: Cost nothing.

C4: Be compatible with the computer capacities.

3.3 Search for solutions

Once the constraints and service functions have been defined, it is time to develop them to try to reach a coherent solution. Every function must be subdivided into simpler technical functions, until different possible solutions emerge for each technical function. As shown on figure 12, two technical functions on the same level can either be connected with a single line, which mean the two functions must be

simultaneously realised, or with two separate lines, which means one or the other function must be realised.

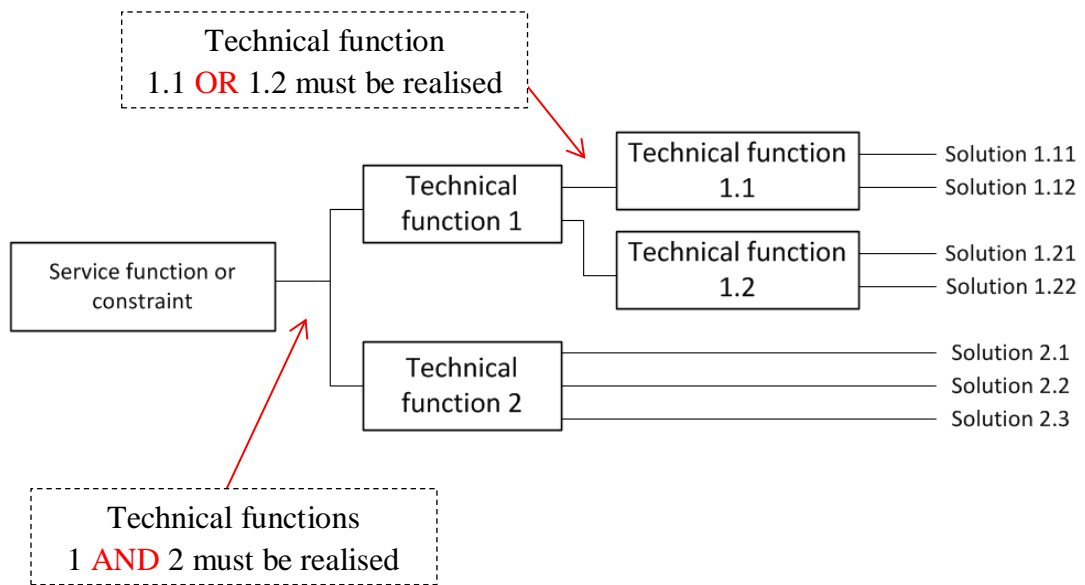


Figure 12: How to find concrete solutions by breaking down a service function or constraint into several technical functions

In this example, we will then have to choose a complete solution by selecting the following combination of solutions:

[[1.11 OR 1.12] OR [1.21 OR 1.22]] AND [2.1 OR 2.2 OR 2.3]

It is then our responsibility to reach the best possible product by choosing the most appropriate group of solutions. Therefore, it is more about making the best possible *combination* of individual solutions than selecting all the best *individual* solutions.

In a practical point of view, the complete decomposition of the functions might be displayed on several pages due to their length. Also note that no solution should be excluded from this analysis, even if it seems unlikely or eccentric, because this step is designed to find both creative and efficient solutions.

3.31 SF1 Determine automatically the range of motion from the 3D files

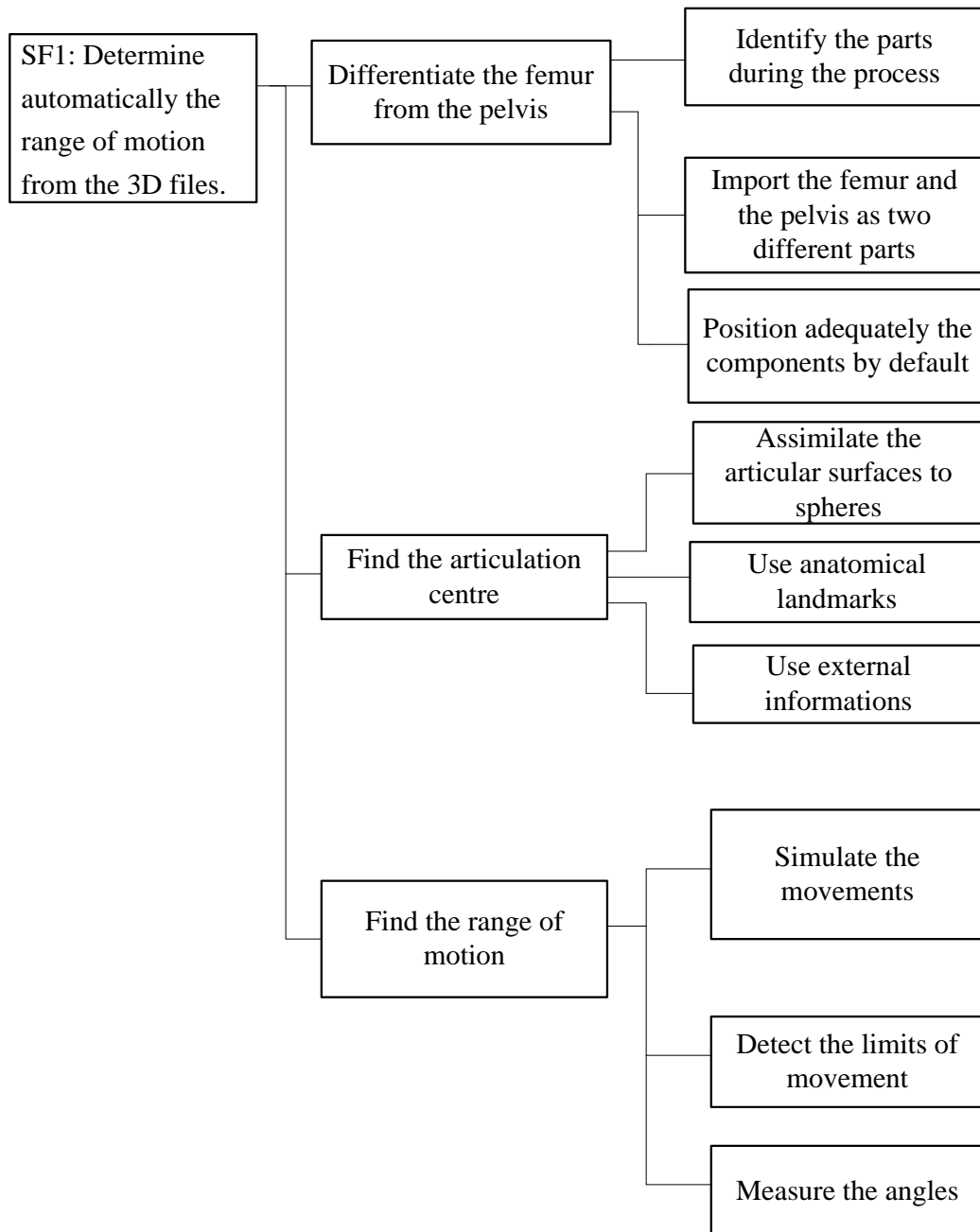


Figure 13: Two first levels of technical functions describing the “SF1: Determine automatically the range of motion from the 3D files”

For the service function of our product, three main technical functions can be identified in the figure 13: differentiate the femur from the pelvis, find the articulation centre and find the range of motion. Here these three functions must be

realised for the service function to be properly achieved. They are detailed in the next three paragraphs.

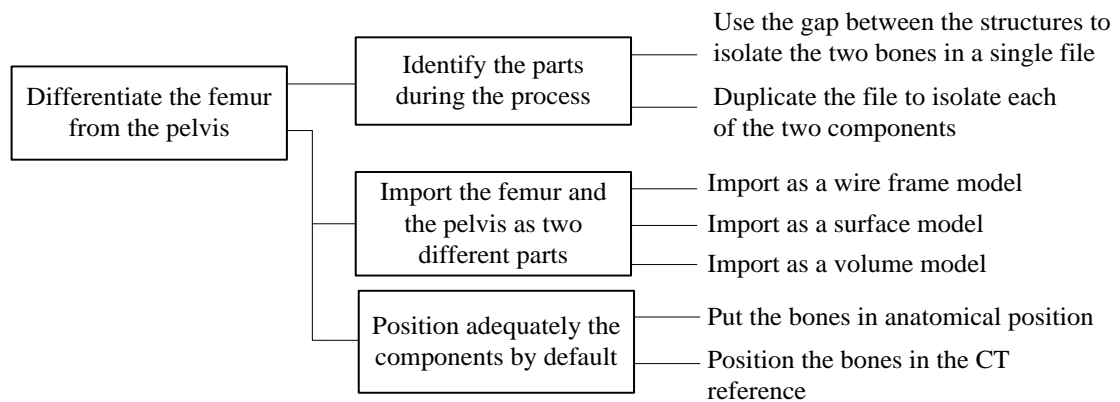


Figure 14: Breakdown of the first degree technical function “Differentiate the femur from the femur” into second degree technical functions leading to concrete solutions

The first technical function that needs to be realised to estimate the range of motion is shown figure 14. Differentiate the femur from the pelvis is required in order to allow movement between these two articular components.

It can be done by **identifying the different bones during the process**, which means the output 3D file from Mimics is a single bloc containing the two bones. Two solutions are then possible. The first one consists in a separation of the two elements. This is possible for instance by using the gap that exists between the articular surfaces. The space can be used to create a surface delimiting the two components. The two parts could then be treated separately if we accurately describe them as two different entities. It implies for instance to have two different “part origins”, one being assigned to each part, in order to move them independently in 3D. Then we will have one file with two separate parts. The second solution would be to duplicate the single bloc and then erase one of the two elements in each file, to end up with two files containing the pelvis and the femur. It is then necessary to reunite them in a single file within an assembly.

The advantage of these solutions is that no repositioning of the parts is necessary. The file being the same at the origin, the position of one bone in relation to the other

remains the same as it was in the 3D file, and therefore it is the same as in the CTs. The position is therefore very close to the anatomical one. On the other hand, it requires a lot of post-processing to distinguish the different parts of the articulation which can be rather time-consuming and difficult to computerise.

But the technical function “differentiate the bone from the femur” can also be achieved by **importing the femur and the pelvis as two separate parts** and then put them in the right position. The decision that needs to be made about the 3D files is the input format. It is chosen while exporting the 3D files from Mimics. Many different output formats are available, but only a few might be of interest in this project. Basically, it is possible to choose between a wire frame, a surface or a volume model. The wire frame model is the simplest of the different models and therefore requires a minimal amount of memory space and its processing takes a minimal computing time. The shape of the 3D object is shown only with a discrete number of points, lines and curves. With Mimics, it is possible to generate such a model, but it means that we have very few information about the spatial geometry of the object. A surface model only depicts the outside shape of an object. Like the wire frame model, it only depicts the geometry and cannot contain material properties about the part it describes. Nevertheless, the surfaces are much more complex than with the wire frame model. Two main systems can be used: the STL or the IGES. The STL is more adapted for finite element analysis (FEA), whereas the IGES is the standard format for computer-aided design (CAD). The volume model is the most complex one. It contains information about the external shape, the volume inside, and can be associated with any material and mechanical properties: density, Young’s modulus, anisotropy, Poisson’s ratio... Because of the high level of details depicted, the files describing a volume model are often quite big, and imply a significantly larger amount of time required to process them.

For the current project, it seems unnecessary to rely on a volume model. We do not need the material or mechanical properties and only require identifying the range of motion that can be achieved without having collisions between the different anatomical structures. Therefore, the most important thing is to have an accurate

description of the outer surface of the bones. The more details we have about this surface, the more appropriate the motion estimation will be. This encourages us to use a surface model instead of a wire frame model, which would be really weak in terms of details. Moreover, the IGES would be more accurate than the STL format, because it seems very likely that we will use a CAD approach. The FEA is designed to analyse displacements and deformations of mechanical structures under loads, which is not really our interest here.

After importing the femur and the pelvis as two separate files, it is then important to **put them in an adequate position**. It is possible to attempt to put the parts in the anatomical position. We would then have to rely on the main femoral axes, especially the angle (B) shown in figure 15 between the long axis of the femur (A) and the neck (C), since it is known for having very few variation between individuals (Yoshioka *et al.*, 1987⁴⁴).

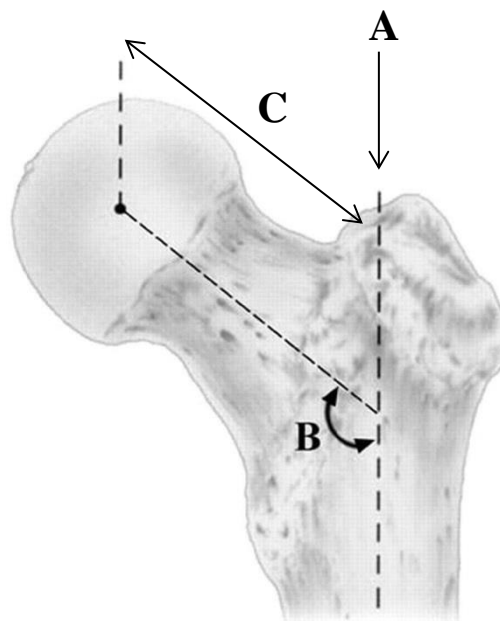


Figure 15: Neck axis (C line), long axis (A line) and neck angle (B) of a left femur, anterior view

To put the pelvis in an anatomical reference, the anterior superior iliac spine must be vertically aligned with the pubic tubercle in the lateral and medial views (see figure 16). If the pelvic part includes the right and the left articulations, this is sufficient to

put the model into the right position. Once each bone is oriented, the assembly of the two parts must be achieved. We might have then to take measurements directly on the CTs to estimate the effective distance between the femoral head and the acetabulum.

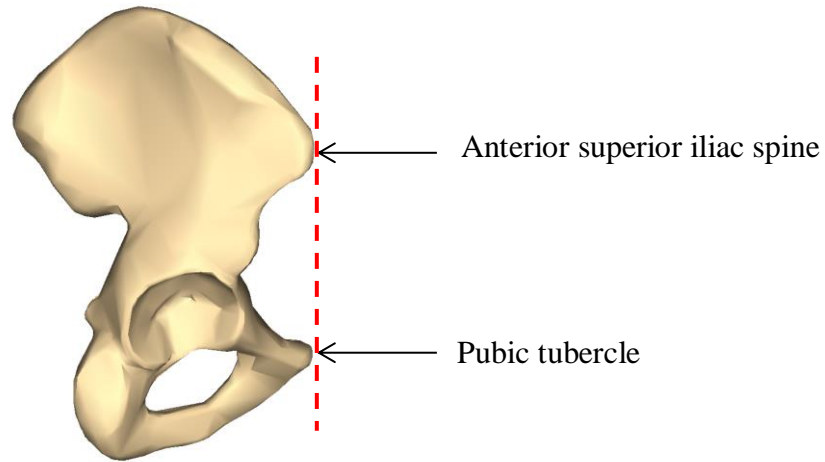


Figure 16: Lateral view of a 3D right pelvis showing the anatomical position (adapted from <https://commons.wikimedia.org>)

Another possibility would be to use the CT reference once again; it would simply rely on the default part positioning that is automatically generated while exporting a 3D file. The femur and the pelvis would be in the same orientation as in the CT, the only remaining work would be to position them relatively to each other. Once again, measurements on the CT slices would surely be the quickest solution to reproduce the distance between the femoral head and the acetabulum.

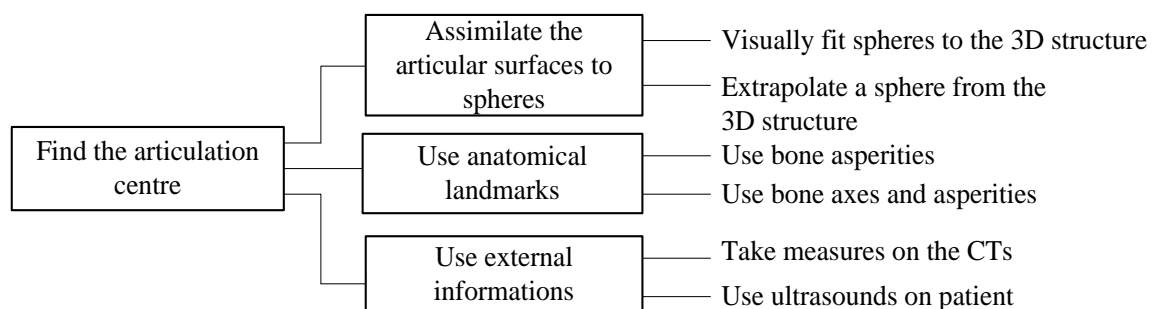


Figure 17: Breakdown of the first degree technical function “Identify the hip centre” into second degree technical functions leading to concrete solutions

If we want to properly rotate the femur in the acetabular cavity, we must find a rotation centre (figure 17). This should attempt to be as close as the real rotation centre as possible. Of course, it is an approximation already, since the real hip articulation might have more than one rotation centre: the presence of soft tissue surrounding the articulation possibly modify this centre during the movements, making it more like an instant rotation centre whose trajectory could depend on the direction of the movement. But it is strictly impossible to extrapolate such elements from a static series of CT scans, therefore we will consider that a fixed rotation centre exists in the hip.

We can find this specific point by using three distinct methods. The first one would allow us to find this centre by **assuming the anatomical surfaces of the articulation are spherical**. Then we have to adequately associate a virtual sphere to the femoral head, find its centre, and reference it as the centre of rotation of the femur. This can be made visually: the 3D model being opened, a virtual sphere is added to the part and fitted in a way that seem to correspond best to the femoral head. Apparently it might not be the optimal way of finding the hip centre; however it has some great advantages. It is a quick method, and the high quality of 3D models might display a great amount of details. Furthermore, the human brain is rather good at estimating the adequacy of small details like the quality of a sphere-on-sphere fitting. If we want to rely more on a computer-based analysis, and eliminate any bias that could emerge from a human analysis, it is also possible to extrapolate the spherical structure directly from the bone structure. To do so, we can use a least square fitting technique to generate the sphere that is closest to the femoral head anatomy. Once this step is achieved, the centre of the sphere can be considered to be the centre of rotation.

In a different way, we could try to rely more on the **anatomical asperities** to find the centre of rotation. The technique would be to find at least three reliable points that we can consider as equidistant from the centre of the femoral head. Unfortunately, this seems highly unlikely, and the selection of these specific points would be controversial. We could also try to use the bone axes. The centre of rotation should be on the axis of the femoral neck, and then we would only need to find two bone

asperities equidistant to the rotation centre to find its location. However, all these techniques seem rather hazardous since it relies on a very small number of anatomical landmarks. This problem is reinforced by the fact that the patients suffer from articular diseases that might deform the physiological asperities of the bone. Therefore the use of less reference points increases the risk of finding an inaccurate rotation centre.

The last possibility is to exploit external data. The previous CT slices could be considered as external information if measured separately. With the different pictures it would be possible to take measurements at different levels and then determine the X, Y and Z location of the centre. After that, it would however be necessary to recreate this centre in the 3D file by entering the appropriate coordinates in the 3D part. If available, it could also be possible to take a direct measurement of the hip centre with the well-known ultrasound technique, and then again to re-enter these coordinates in our 3D femoral model. To be realistic, in this project we have no access to the patients so this specific possibility seems unlikely. At the contrary, CTs are available and the measurements can be done easily on them, so it might be a good solution.

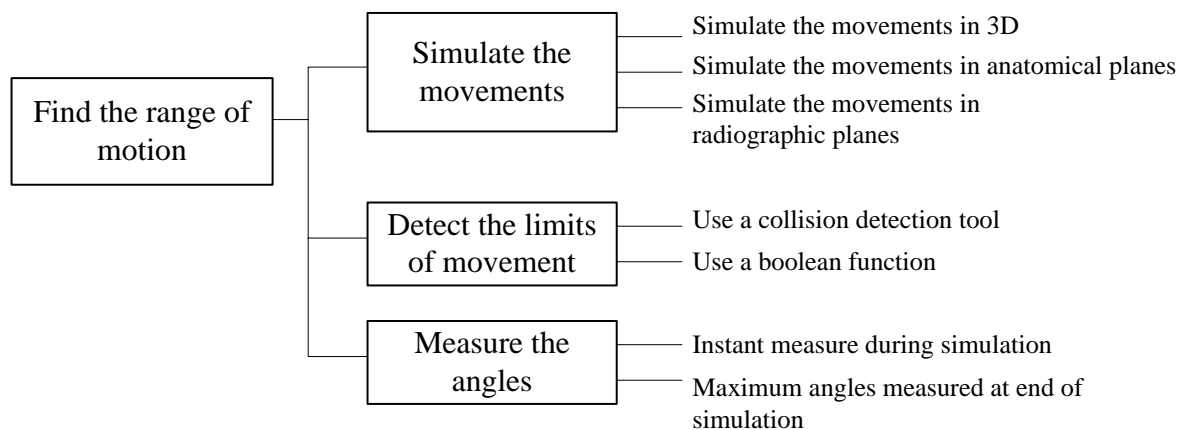


Figure 18: Breakdown of the first degree technical function “Find the range of motion” into second degree technical functions leading to concrete solutions

Once the two previous steps are achieved, the system is ready for the simulation. We have now two parts, the femur and the pelvis, adequately positioned in space and fitted together, and we also have the precise rotation centre.

In order to determine the range of movement achievable without dislocation, we must estimate the range of motion that is possible without impact between the femur and the pelvis (otherwise it creates a lever and leads to dislocation). Three technical functions allow us to find this range of motion as shown in figure 18.

First we obviously have to **simulate the movements**. Three main possibilities emerged: we can do a 3D cinematic analysis or a series of 2D cinematic analysis by describing the movements plane by plane using the anatomical or radiographic planes. The 3D viewing of the movements might appear more realistic, and be more appealing for the surgeon by showing complex hip movements. However, it is also possible that this type of 3D motion might be a little confusing if the user is not familiar with 3D views, since it is only a partial reconstruction of the bone structure (neither the femur nor the pelvis are entirely shown). From this point of view, relying on pre-established planes that respect international conventions might give a clearer overview of the achievable movements. Two plane systems can be used in this perspective. We can choose to display the movements in the anatomical planes, which is convenient because it basically respects the default positioning of the 3D parts once they are extracted from the CT scans. The downside is that this is generally not the way movements are depicted clinically. To be closest to the reality, it might be a good idea to show the range of motion in radiological planes. This implies to rotate the 3D parts to respect these specific planes, therefore to increase the length of the process, but most of the medical staff is more used to these references.

Detecting the limits of the movements, and therefore deducting the angular amplitudes, is an essential technical function. Two main tools can help us achieve this. We could use a collision detection tool integrated to a CAD software. This type of tool allows the user to know when surfaces or volumes that belong to distinct parts collide. It can either restrict the motion or not depending on the programming choice of the user. This solution could be a rather effective way to restrict the movement during our simulation. The other way to achieve that would be to use directly Boolean functions. The use of Boolean functions is integrated in the collision detection tool, so here we would have to use them to reprogram the same kind of tool

that we already have. It would not be appropriate for now but could be a good alternative in case we have serious problems using the existing tool.

The last step to achieve is effectively measure the different angular amplitudes of movement. Two possibilities emerge: it can be an instant measure or a final measure. The advantage of measuring the angles during the simulation is to visualise the evolution of the amplitudes in real time; however it might also be visually disturbing and not extremely relevant. Obtain the final amplitudes at the end of simulation seems to make more sense, and should be clearer for the user since the angles will not be changing every second. Furthermore, the relevant numbers are indeed the final amplitudes, and not the instant angular measures.

3.32 C1: Be compatible with the 3D format.

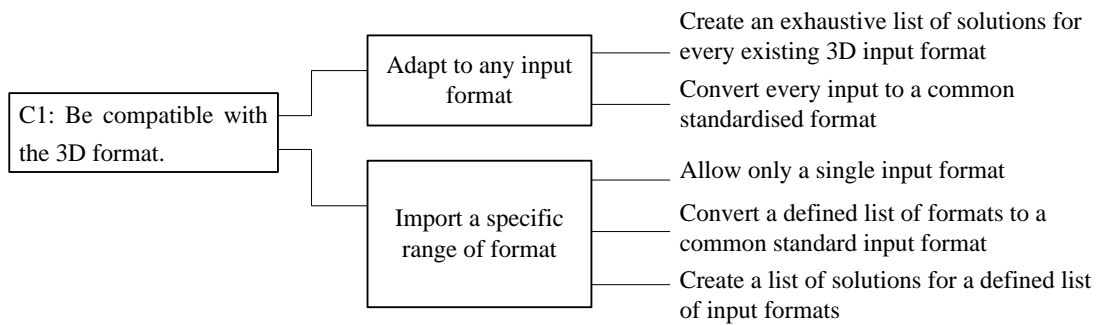


Figure 19: Analysis of the constraint “C1: Be compatible with the 3D format” by using technical functions leading to concrete solutions

Our product requires a compatibility with the 3D format of the files exported from Mimics, otherwise it would be incapable to process it. Two choices can be made (figure 19): we can either allow the product to process any format, or restrict its use by only allowing a specific range of format.

The primary hypothesis suggests that we could try to **adapt to any format**. This can be done in two ways. The first one consists in creating a specific solution for every existing output format of Mimics. It seems pretty obvious that this is not a very efficient way to solve the problem. It would take a very long time, and the resulting program would be excessively heavy. The other solution is to be able to convert any Mimics format to a standardised one that will be processed by our program. Although the process is simpler than the previous one, it still requires a huge amount

of work to achieve a subsidiary task. In consequence, the “universal adaptation” seems like a poor answer to our compatibility requirement.

Therefore, we will try to find a better solution by exploring the other possibility: only **import a specific range of format**. We could try to adopt a sort of compromise with the first hypothesis, by limiting the list of formats we could process. Once again, it could be performed either by preparing a different solution for each format or by converting a small list of Mimics formats to an easier-to-process standard format. The same problem remains, however, because such work is highly time-consuming. That is why allowing only one 3D format appears to be the best solution. It is complex enough to elaborate a coherent way to evaluate the 3D range of motion of the hip, trying to reiterate the same work for a totally different format within ten weeks would be counterproductive. Besides, this section focuses only on the *compatibility* and therefore does not take all the other constraints into account.

3.33 C2: Display the results to the user.

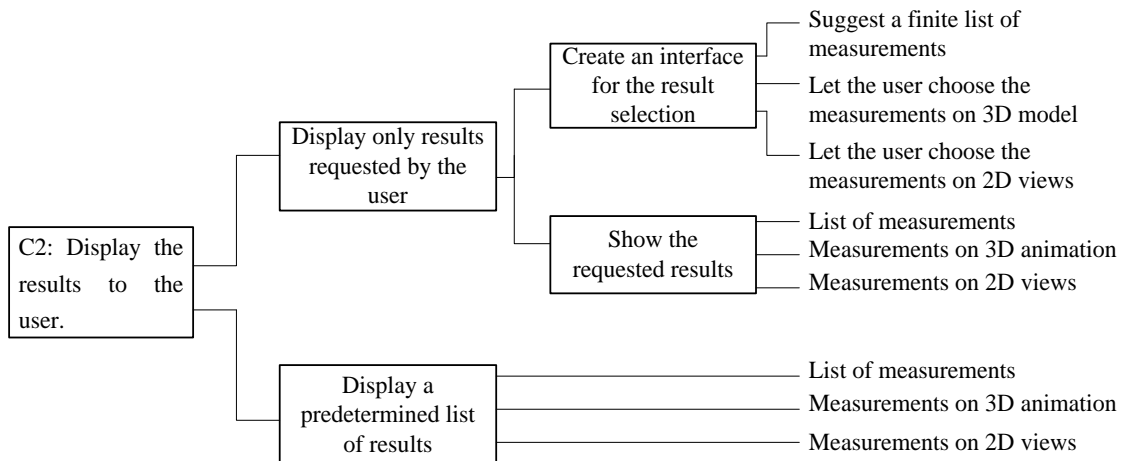


Figure 20: Analysis of the constraint “C2: Display the results to the user” by using technical functions leading to concrete solutions

Once the range of motion is calculated, the results should be displayed to the user as shown in figure 20. It can be done in two different ways. We can either let the user choose which results he or she wants to see, or display a fixed amount of information.

Let's consider the possibility **to let the user request the results** he or she wants. In that case, an intermediate step must be added. There should be first an **interface to allow the result selection** to take place. To select the measurements, a list of measurements could be proposed in plain text. The user would only have to tick boxes corresponding to the requested movements ("adduction-abduction range" for instance). The advantage of it would be the flexibility of the system, but the text interface could be a bit confusing for the user if he or she does not have the possibility to visualise the planes used for the measurements. Therefore, it might be clearer to let the user choose directly the angles on the 3D view of the bone assembly. The problem however would be to select the right directions, because many people are unfamiliar with a 3D environment. Hence a good compromise in this case would be to display 2D views of each of the 3 planes, where the user could benefit from a graphical display with familiar views of the articulation.

Once the user has chosen which angles he or she wanted to measure, the program must display the results. Once again, we have three possibilities, rather similar to the ones in the previous paragraph. The different measures could appear in plain text ("adduction-abduction range: 60°" for example). It seems first rather clear, but the referential problem remains. It is important to always keep in mind that all the articular measurements must be done in reference to a specific plane in order to be accurately interpreted. That is why a graphical display of the results is probably more relevant. As described before, it would theoretically be possible to show the results in a 3D view of the articulation, but no doubt there would be some confusion between the different angles shown in such image, especially if several different measurements are made on the same model. It appears once again that the best solution would be to use 2D views that would display the range of motion plane by plane.

These personalised results can appear appealing, but it might not be the most adapted solution. The aim of the project is to estimate the range of motion of the hip articulation previous to surgery; therefore we can assume that there would be no use of a choice interface. The medical staff susceptible to use this program would need all the available measurements, therefore putting efforts in creating an interface that

no one requires would be an error. That is why we will more consider the alternative possibility: automatically **display a predetermined list of results**, hopefully sufficient to describe all the amplitudes. The most logical list of measurements is the one the orthopaedists use to assess their patients. The critics about the way we could display the results is the same as the previous paragraph: we could use plain text or 3D views but it might be confusing, so the 2D display plane by plane would be better.

3.34 C3: Cost nothing.

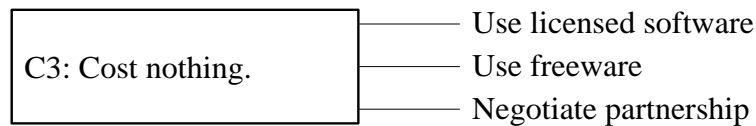


Figure 21: Analysis of the constraint “C3: Cost nothing” by using technical functions leading to concrete solutions

As indicated at the beginning of the “Functional specifications” section, cost is an indirect issue in this project. It is tightly related to the time we have and the available resources. But it is nevertheless interesting to think about this specific aspect (see figure 21), because it is a fundamental (or indeed the most important) parameter in an industry or research project.

To limit the costs in this project, we have to use “free” software. It can be done by limiting our use to licensed software. They are not free, but the University already paid the licensed so it is a sort of “integrated cost”. At the contrary, not using them would even be a waste of resources, because these software are often quite powerful. It is therefore interesting to rely on the possibilities offered by the University. The CAD software easily available at Strathclyde are Autocad, PTC Creo (formerly Pro/ENGINEER) and Solidworks.

Another possibility would be to use freeware. Flexibility and availability are two of their advantages, since they can be installed for free on any computer and undergo constant improvements online. Furthermore, it is really easy to find help about their use since their functionalities are generally fully detailed by active communities of users. It seems tempting; however it is far from perfect. The first problem is the

permanence of the results. Since the freeware are not managed by a specific company, there is no guarantee it will remain compatible with former versions in time, therefore we cannot be assured that we will still be able to run our program at long term. Another issue is to find a CAD freeware capable of cinematic simulation. This specific module is quite complex, hence not mainstream in the CAD freeware. Once again, it is much simpler, and more reliable, to use the licensed CAD software for this project.

The last possibility would be to negotiate a partnership in order to associate the project with a CAD software (Dassault System’s Catia CAD software for instance), but of course it would be very unrealistic for this project. We do not have the time nor the leverage to negotiate such a partnership, but it is interesting to think of this possibility as a reminder for further projects.

3.35 C4: Be compatible with the computer capacities.

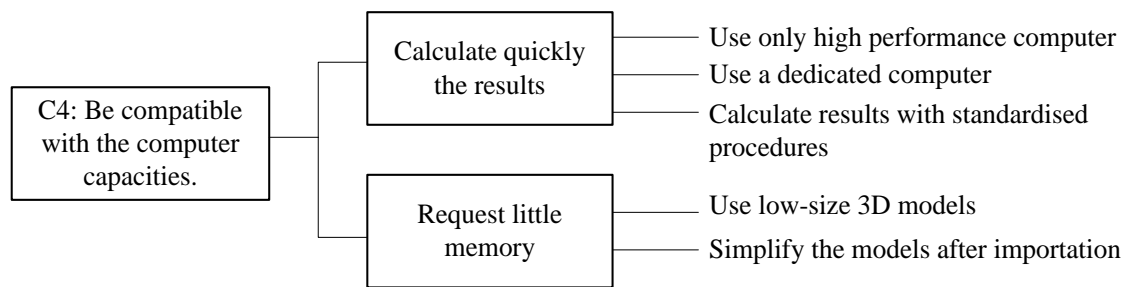


Figure 22: Analysis of the constraint “C4: Be compatible with the computer capacities” by using technical functions leading to concrete solutions

It seems rather straightforward that the computer running the program should be able to do so. Nevertheless, it is important to think about this parameter as displayed in figure 22. It is indeed easy to create a program that requires too much time to be really useful. The product resulting of this project is designed to help surgeons or other medical staff, so they really cannot spend hours waiting for the results to appear.

To be sure that the computation time will remain minimal, two conditions must be verified. The memory requested should be small, and the results should be calculated quickly.

To **obtain rapid processing**, we have mainly two options. One is to rely on the computer capacities. If we use a high performance computer or dedicate a computer only to this task, the computational time should remain low. However, such solutions are not conceivable. Firstly, we have no guarantee that a high performance computer will be available, and even if it was the case it would surely be assigned to other tasks that also require a high speed of information treatment. As to dedicating a computer to our program, it would be a waste of resources. So in the end the only realistic way to maintain a high computational speed is to use standardised procedures to run our program. To achieve this goal, it is important not to try to be exhaustive about the possibilities of the cinematic analysis. Simplicity remains the best path to efficiency.

In order to **limit the amount of memory requested** for the motion analysis, the 3D models should also remain low-sized. The first possibility is to choose a low definition 3D output while exporting the 3D parts from Mimics. Obviously, a wireframe model will take less memory space than a surface model, which will take less memory space than a volume model, since the amount of information enclosed in the file is not the same. It is also possible to convert a complex model to a simpler one, within the CAD software, but ironically this will increase the computational time. Besides, it would be not be logical to convert a file instead of exporting it directly in an optimised format.

3.36 Review of the solutions

In order to reach a coherent solution for the project, the different functions and constraints must be reviewed. We must keep in mind that sometimes an individual solution would be the best answer to a specific constraint, but will not be efficient for the global solution. As an example, we can think of a car: it must be resistant to impacts but also require protecting the passengers. Obviously, a highly rigid structure would be extremely resistant to impacts, but it would be very dangerous if the outer

structure could not absorb the shocks. Therefore, the structure must be resistant but deformable enough to ensure the protection of the passengers. The selection of the individual solutions must rely on priorities in order to reach the best possible solution in a given context.

Since the different solutions have already been discussed, now is the time to combine them to find our optimum response.

SF1: Determine automatically the range of motion from the 3D files.

Importing the femur and the pelvis as two separate structures seems more appropriate, since it spares computational time in the following operation. The possibility to export these models in the IGES (surface) format also seems pertinent, because of its compatibility with CAD software. As to put the two parts in the right position, relying on the default CT positioning and a simple measurement on CT slices also appears as the quickest and simplest solution.

Finding the hip centre will be more accurate and easier with a spherical least square regression fitting to the structure. It is also coherent with the literature review results that showed the reliability of this technique.

At last, the range of motion should be estimated by using a collision detection tool. It is adapted to the surface IGES format, and it already exists in CAD software. Hence it will not be necessary to create a new algorithm to achieve this function.

C1: Be compatible with the 3D format.

The best way to ensure the compatibility of the files created with Mimics with the following software is to export them in a specified format. Furthermore, it is a huge time gain since it allows us to elaborate a common solution for every file.

C2: Display the results to the user.

The previous analysis showed that suggesting a list of results to the user was essentially an unnecessary complication. It is more logical to display directly a predetermined list of results. To ensure the results will be accurately interpreted, the solution could be a combination of two of the solutions. Displaying a 3D view of the

different movements as well as a plane-by-plane radiographic view to illustrate the measurements might be a good compromise.

C3: Cost nothing.

It seems quite logical to rely on the University available software. The CAD freely accessible to the students (Autocad, PTC Creo and Solidworks) could all be good candidates for our motion analysis. However the author does not have experience of any of these software packages, so the precise choice of software will only take place after further investigation.

C4: Be compatible with the computer capacities.

To ensure the final result of the project will be compatible with any computer, the limitation of the requested memory seems the best solution. With standard IGES files, the models should be light enough to achieve this goal. The use of a preprogrammed collision detection tool as chosen in the SF1 will also make the final analysis easier from this point of view.

Part 4

Project progression

The aim in section is to explain how the project was conducted. All the work has been realised on computer and the use of different software was required. Many different steps has been realised and will be explained in order to enlighten the reader.

4.1 DICOM viewer and analysis of CT images

4.11 First set of CT scans

Understanding and accurately interpret the CT scans regarding the bone structure was the first step. The initial available material was composed of 2 anonymised CT-scans performed on the lower body (CT207 and CT208). From the aspect of the different pictures (figure 23) I assumed that they were originally designed to focus on knee replacement prosthesis.



Figure 23: Frontal views of the CT207 (left) and CT208 (right) centred on the knee implants

It is important to notice that the knee prostheses are generally made of metal and polymers (Song *et al.*, 2013⁴⁵), which implies that the CT settings were not optimised for viewing the bone or soft tissue structures.

4.111 Hounsfield units

The CTs images are generated by using the Hounsfield units. It is a measurement system that assigns a grayscale value to a specific density of tissue. The Hounsfield scale in the human body goes from -1000 (air) to more than +3000 (cortical bone), the zero value being clear distilled water at standard temperature (as defined by the NCI CDISC – National Cancer Institute, Clinical Data Interchange Standards Consortium⁴⁶). Every voxel (volume pixel generated with computed tomography) will therefore have a specific Hounsfield value assigned to it.



Figure 24: A low-quality slice from CT208 (series 2) displaying the CT parameters on each side and corner

A computer screen generally displays 256 grey values, therefore it is not possible to visualise the entire range of Hounsfield units on a single image. To fully exploit the sensitivity of the CT scans, some adjustments can be made to select the range of values converted to adapt the screen capacity and the middle value on which the data are centred. The range of data is displayed as the width W, and the centre value is shown under the label C. Default settings on CT scans for W and C depend on the nature of the examination.

On figure 24 we can see in the bottom left corner that the parameters chosen for this specific CT208 are W: 400 and C: 40 (these settings are identical for the CT207); but it is possible to modulate these values to optimise the images of the bone structures.

4.112 DICOM viewer

The images of the CTs are displayed with a DICOM (Digital Imaging and COmmunications in Medicine⁴⁷) viewer. In addition to the W and C parameters, we have other information displayed on the main window as shown in figure 25.

The most relevant parts for us are:

- The W and C, which can be modified by the user on the viewer
- The series number and the slice number, that need to be retained in order to select the best set of data (see further)
- The directions which orientate the slice. [A] is anterior, [P] posterior, [R] right and [L] left. We can notice here that a CT slice is always shown from a “top bottom view”, as if we were looking from the feet of the patient to the transverse slice.
- The thickness of the slice. This parameter is set during the examination, and remains the same for the whole CT. The importance of the thickness will be highlighted later on, when the 3D reconstruction and interpolation will be described.

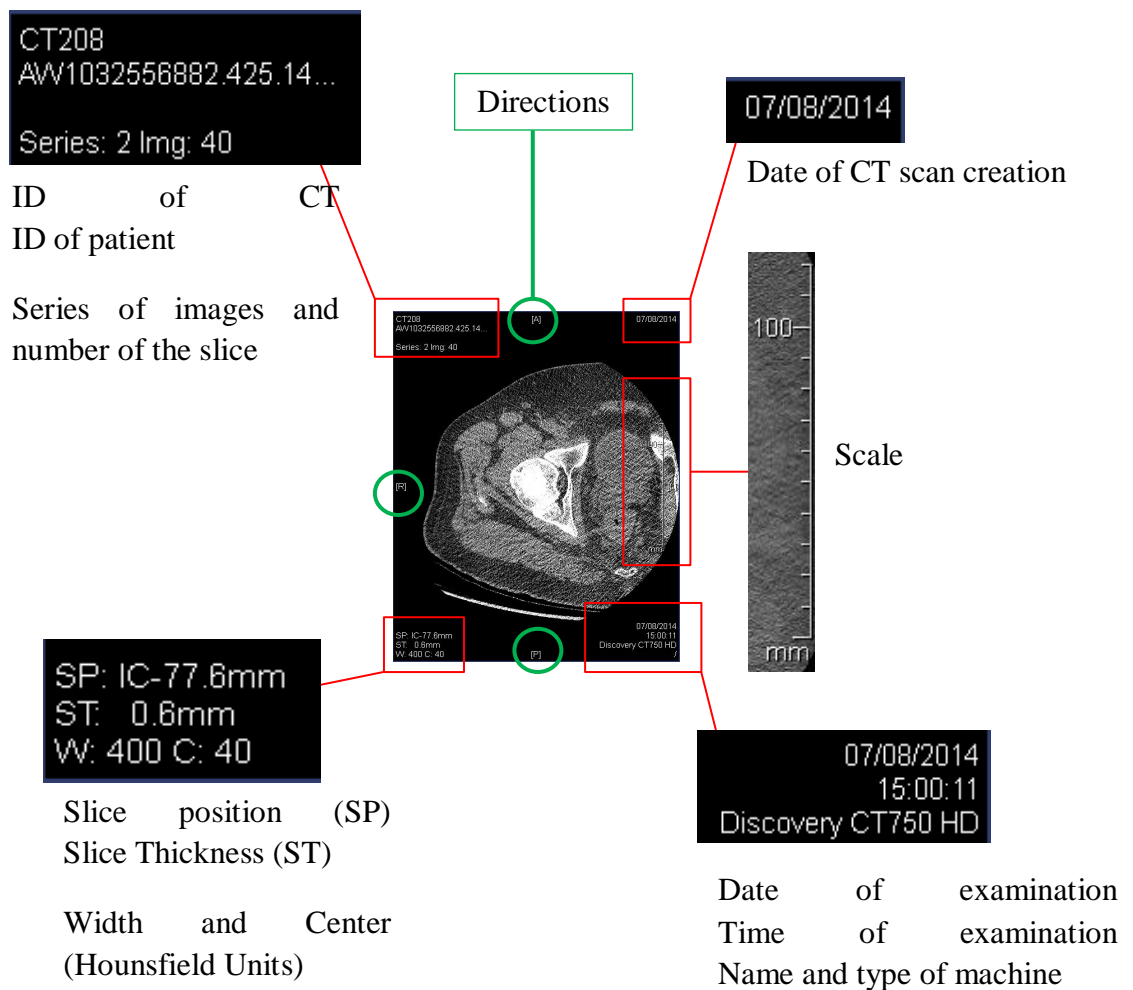


Figure 25: Explanation of the parameters displayed on a CT slice

Both CTs have two series of data I could potentially use for 3D-reconstruction, the series 2 and 3. The series 1 displays sagittal and coronal views of the entire leg, irrelevant to our reconstruction purpose. To achieve a realistic Mimics 3D-reconstruction it is necessary to choose the most accurate set of CT slices. To obtain the better quality I chose the set which had the clearer bone contrast by analysing the CTs with the viewer. In order to see the bone more clearly, I changed the W: 400 and C: 40 to the recommended parameters for bone visualisation, W: 2000 and C: 250 (Nahum, 2013⁴⁸). The compared images are shown in figure 26.

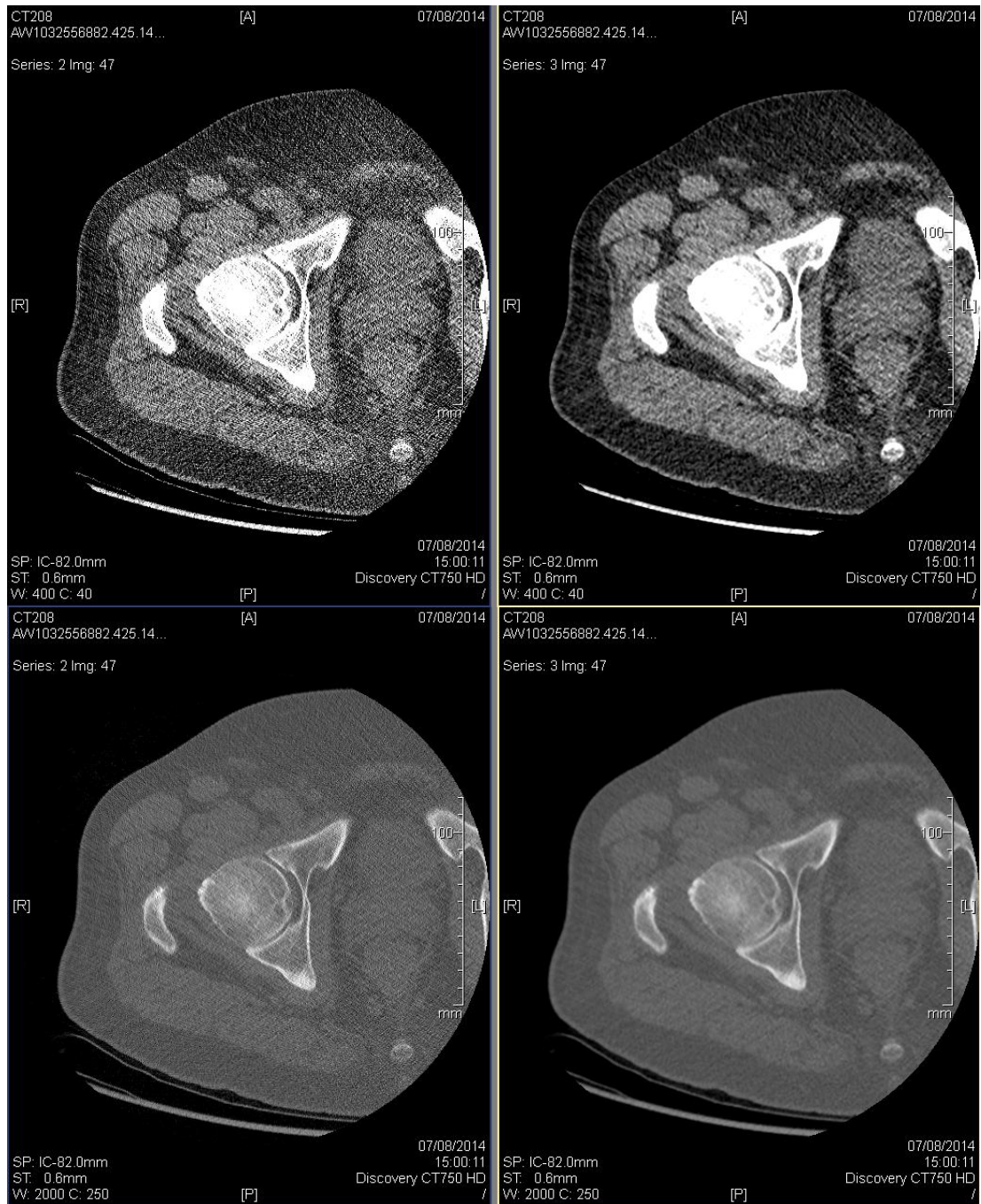


Figure 26: Default settings (top) and bone settings (bottom) of series 2 (left) and 3 (right), CT208. The bone settings improve the visualisation of the bone structures.

We can see that the change of settings improves indeed the visualisation of the bone. The images 1 to 81 allow us to focus on the hip area, but it is important to notice that the superior limit is tangent to the acetabulum, so we do not have much structural

information about the surrounding structures. The pelvis cannot be reconstructed entirely, and the acetabulum is not totally shown. It is therefore not an ideal CT set.

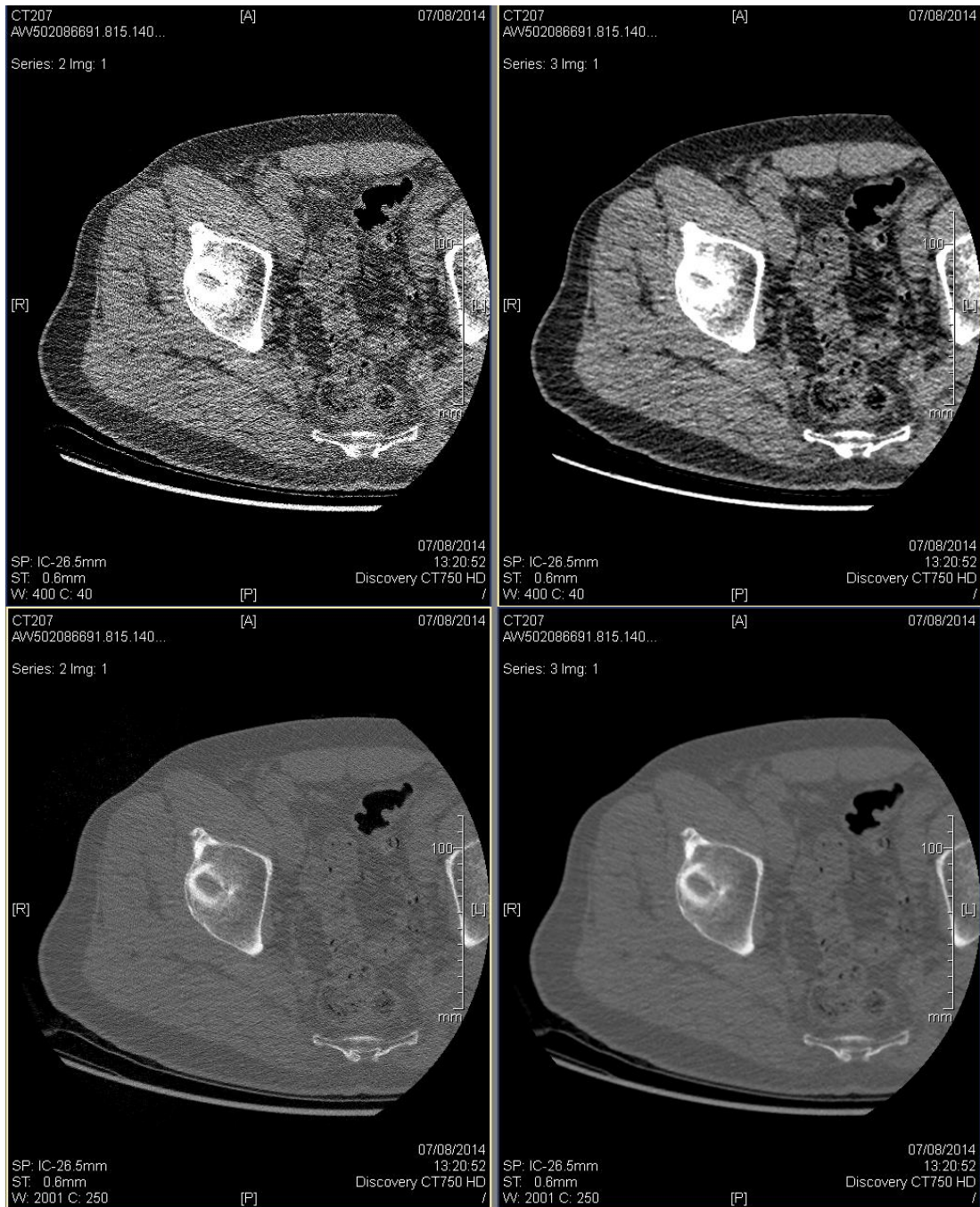


Figure 27: Default settings (top) and bone settings (bottom) of series 2 (left) and 3 (right), CT207. The bone contours appear sharper in the series 2 than in the series 3.

The series 3 (also images 1 to 81) is almost identical to series 2 but was performed with a different contrast that makes the grain of the bones blurrier. It implies a less precise set of data regarding the bone surface; therefore the sharper series 2 should allow us to access more information about the precise bone limits.

The CT207 contains also 3 series that seem to be identical to the CT208 ones. The clinical picture is the same (imaging of knee replacement).

Once again, the series 2 seems more appropriate to clearly distinguish the bone contours. The figure 27 shows the difference of contrast. These pictures are the first of the series, so we can also highlight the fact that the CTs are not even tangent to the acetabulum, which is a problem if we want an accurate model of the hip articulation and its surrounding structures.

4.12 Second set of CT images

If the first set of images was really useful for the beginning of the project, I needed new scans with a better quality to reconstruct good 3D models that could be later animated with 3D motion. Two parameters in particular needed to be improved: the initial quality and sensitivity of the CT images, and the anatomical extent of the scans. The first series stopped at the superior acetabular level, whereas I needed to have a good view of the pelvis.

With the help of Angela Deakin, Jon Clarke and Alistair Ewen from the Golden Jubilee National Hospital, I had the chance to obtain two new sets of CT scans which filled these criteria.

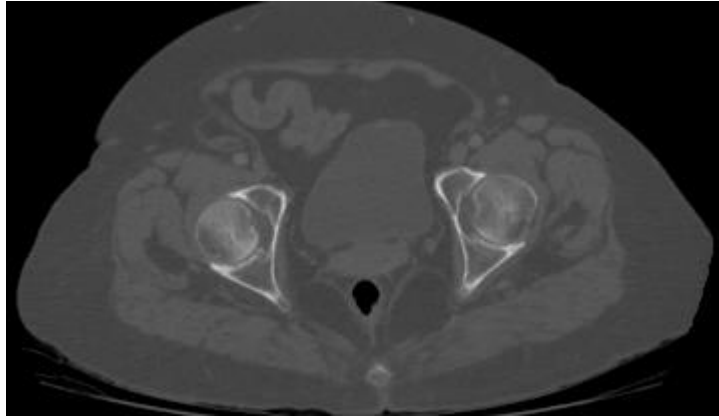


Figure 28: High quality of details shown by a CT slice from the second data set

The figure 28 shows an improved quality of the CTs. It becomes obvious when reconstructing the 3D structure with Mimics.

4.2 Mimics Software

The chosen series of pictures must then be imported to Mimics. The first set of pictures (CT207 and CT208) will not be particularly shown in this section, because of their poor quality. Nevertheless, they were really useful to the project because they were the only available material during the first weeks of the project.

4.21 Principle of Mimics

The Mimics software first task is to reconstruct sagittal and coronal views from the CT transverses slices. Following this initial step, it allows the user to perform a process called segmentation to reconstruct 3D-views of chosen structures.

The result can be a surface model. The surface output format is STL (commonly used in stereolithography). It contains the coordinates of a finite number of interconnected triangles and their facet normal vector, forming a mesh that describes the surface. The simplicity of the algorithm makes it easy to modify in order to adapt efficiently to the real structure by performing manual or computer-aided remeshing.

The segmentation process in itself leads to the generation of the STL file. The basic principle is to gather the parts of the CT scans that have similar grayscale values. These values are distinguished by Hounsfield units in CTs.

The generation of volume models is also possible: tetrahedral structures are then described and interconnected to form a volume mesh. With this option, material properties can be assigned to the different parts of the model by assigning a specific material to each grayscale value.

Independently of the nature of the described structure (surface or volume), the data can be converted to the IGES format (parametric file), allowing the user to export them to any CAD (Computer Aided Design) or CAE (Computer Aided Engineering) software. With a parametric file, the surface is fully described, so it is no longer simulated with a finite number of facets.

4.22 Importing the images

As previously explained, the CT slices are images of the patient's inner organs viewed in the transverse plane. Successive pictures are taken with a constant thickness, which is the distance between two of those transverse planes.

When the images are loaded into the software, the user must indicate the orientation of the pictures by pointing the anterior/posterior and left/right directions. Then, Mimics automatically processes the CT slices to create coronal and sagittal views of the patient. This task is performed by interpolation, which converts a series of discrete values into a continuous field. This step is realised by minimising the errors between the discrete values.

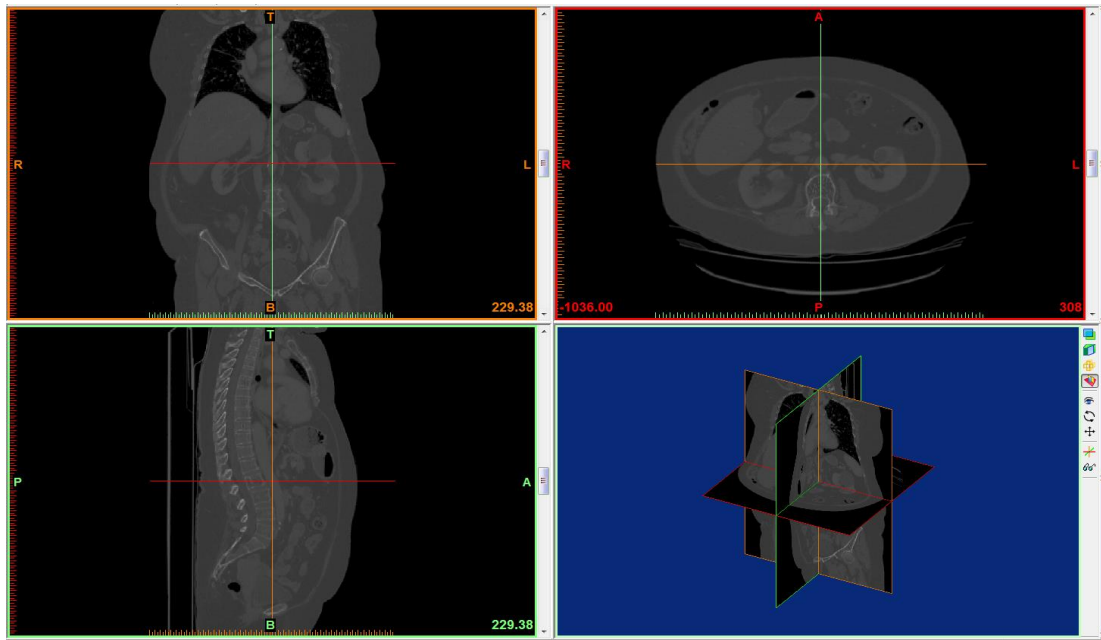


Figure 29: Main windows of the Mimics software showing the original CT slices (top right) and the reconstructed coronal (top left) and sagittal (bottom left) views of the patient. The bottom right window shows the same views in 3D.

Once the interpolation is done, Mimics displays the results of this operation as shown in figure 29. The top right window shows the original CT slices from which the other views have been constructed. The top left displays a coronal view whereas the bottom left shows a sagittal picture. The last quadrant is a perspective display of the different planes combined together. The green, red and orange lines in the different windows show the location of the other displayed planes.

4.23 Understanding the Mimics interface

Before trying to perform 3D reconstruction, it is fundamental to understand the main functions and menus of the software.

The lateral windows are the main indicators of the current work. The figure 30 shows these windows. The four parts form the project management toolbar which allows creating, editing and deleting the different entities.

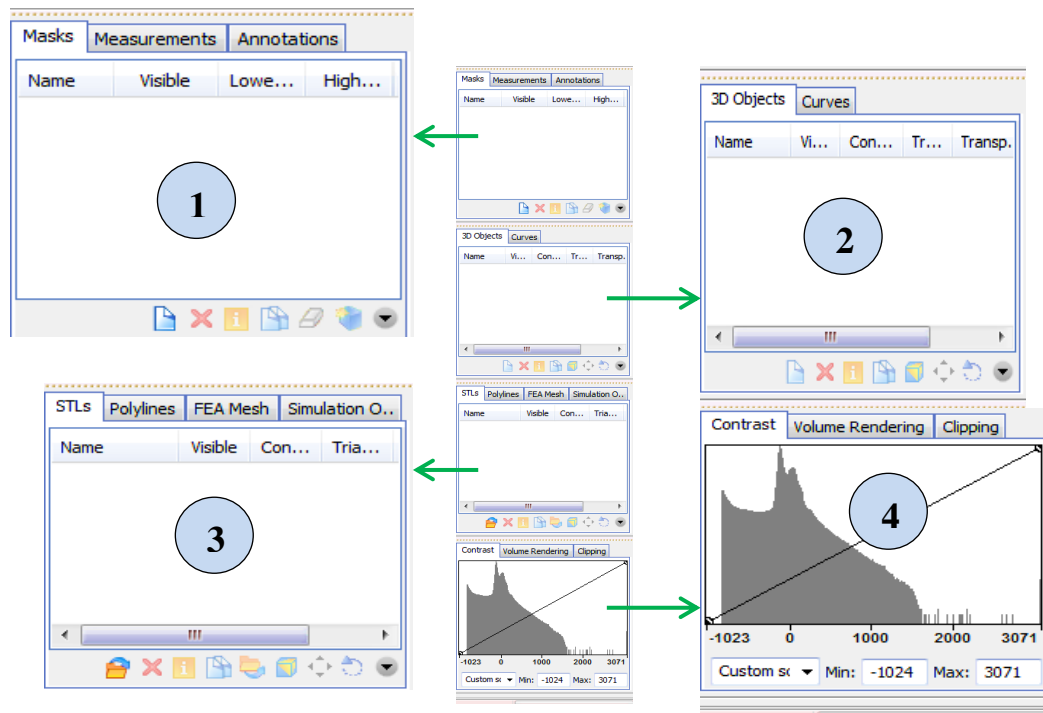


Figure 30: Main control windows of Mimics. The window 1 shows the work made directly on the CT slices, the window 2 shows the extrapolated 3D structures, the window 3 allows the user to generate contours and surfaces and the window 4 allow managing the visualisation parameters.

The window labelled **1** allows the user to manage the masks, measurements and annotations on the current project. Basically, masks are filtered images that regroup all the Hounsfield units with the same value. Measurements and annotations can be made directly on the different views, and appear as a list in the dedicated tabs.

The window **2** displays the existing 3D objects and curves that can be generated from the masks previously created.

The part **3** is designed to allow further analysis and extrapolation from either the masks or the 3D objects/curves. The first possibility is to generate STLs. It is a surface-based descriptive entity made of interconnected triangles which orientations are defined by vectors. The result is a mesh. Another possibility is to create polylines that help the user to draw the contours of the masks. The particularity of this tool is the possibility to outline the irregularities or holes that appear in the masks. With polylines, it is also possible to recreate a 3D object. Finally, some FEA (Finite

Element Analysis) or Simulation Objects can be generated, but it is of no use in this project.

The window 4 contains the tools that allow the user to change the visual aspects of the project. The contrast changes the range of grayscale that are displayed on screen. It is labelled in Hounsfield units, so the settings can be rather close to the ones used in the DICOM viewer at the beginning. However, a large amount of experiments with Mimics taught me that the exact DICOM Hounsfield range of units is not always the best range of values to obtain the optimum result. Other tools in this fourth box are about volume rendering, and do not matter here.

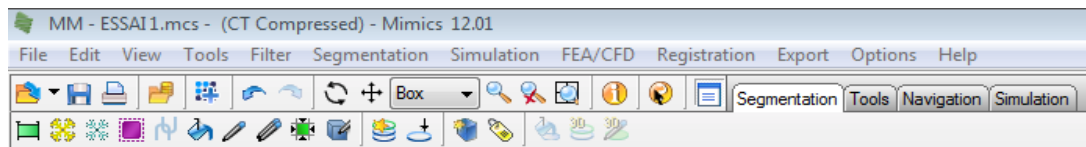


Figure 31: The main tools are displayed in the top toolbars of Mimics

The other toolbars, figure 31, are located at the top of the screen. The segmentation tools allow the user to create and edit masks, 3D structures or polylines. The aim is to create entities that are separated from the rest of the images, hence the name segmentation. The other tabs contain mainly the same tools as the lateral windows (measurements, annotations...) and simulation tools that we do not require to use in this project.

4.24 Creating a mask

The very first step to 3D reconstruction is the creation of an initial mask. A mask will highlight all the voxels with the same grayscale value. This operation requires what is called a “thresholding” in Mimics.

This thresholding should allow us to isolate and display the bone structure. It can be done in two different ways; combining them is the most efficient way to get a good initial approximation.

The first (and most direct) possibility is to select the threshold command (figure 32) in the top “segmentation” toolbar. The command displays the range of grayscale values detected in the CT slices and their frequency. The user can then select the range of values that must remain in the mask.

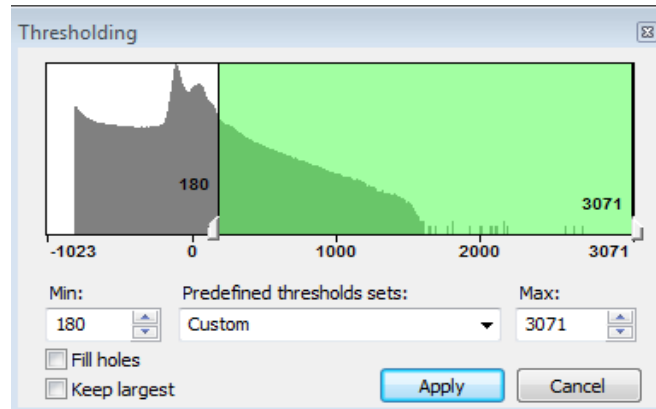


Figure 32: The thresholding command as displayed in Mimics. The threshold limits can be adjusted between -1023 and 3071 Hounsfield units manually or selected from predefined thresholds sets.

It is possible to select the “Bone scale” in the predefined thresholds sets, but it is often not that accurate. To improve this thresholding, a good tool is the “Profile Line”. By drawing a line through a bone on the CT (The femoral head for instance), the Hounsfield profile of the crossed elements appears in a separated window. It allows the user to know the Hounsfield values of the voxels attached to the selected structure and their frequency, and hence to refine the range of values needed for a good thresholding. Some peaks indicate the high frequency of gray values that are of interest for the specified structure.

The first thresholding realised with this process gives an overview of the bone structure as shown in figure 33 when we apply the “convert to 3D structure” tool. The result is far from perfect. Many floating pixels are scattered through the image, the entire bone structure appears even if we only need the hip articulation and parts of what seems to be the table of the CT scanner (dorsal to the skeleton) are included in the model.

To get rid of the majority of artefacts, it is possible to do a “dynamic region growing” following the thresholding. This process is based on an automated comparative method. Basically, the software compares the grayscale values of each area to the values of the adjacent voxels and determines the best local threshold to apply. The result is a cleaner model.

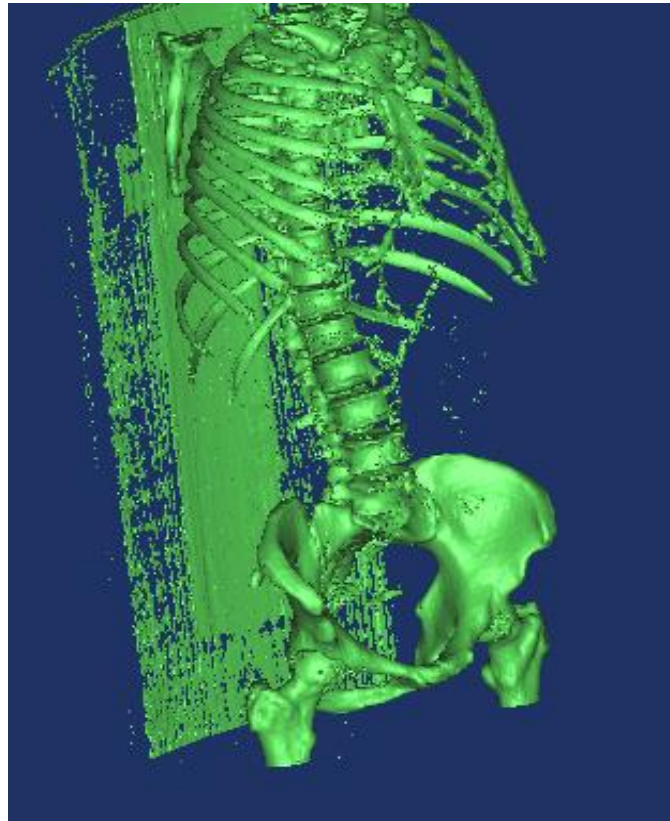


Figure 33: Generated 3D model after first thresholding. Many artefacts are scattered through the model, the table appears posteriorly to the skeleton and the model is not limited to the hip articulation.

The last operation required for this first mask is performing a “crop mask”, which allows erasing the unnecessary parts of the 3D model. The result in figure 34 is a right hip joint articulation isolated from the rest of the skeleton. This first modelling aims to isolate the right femur; hence the cropping limits have been set to include the femoral head. The diaphysis of the femur has not been cut; it corresponds to the inferior limit of the CT slices.

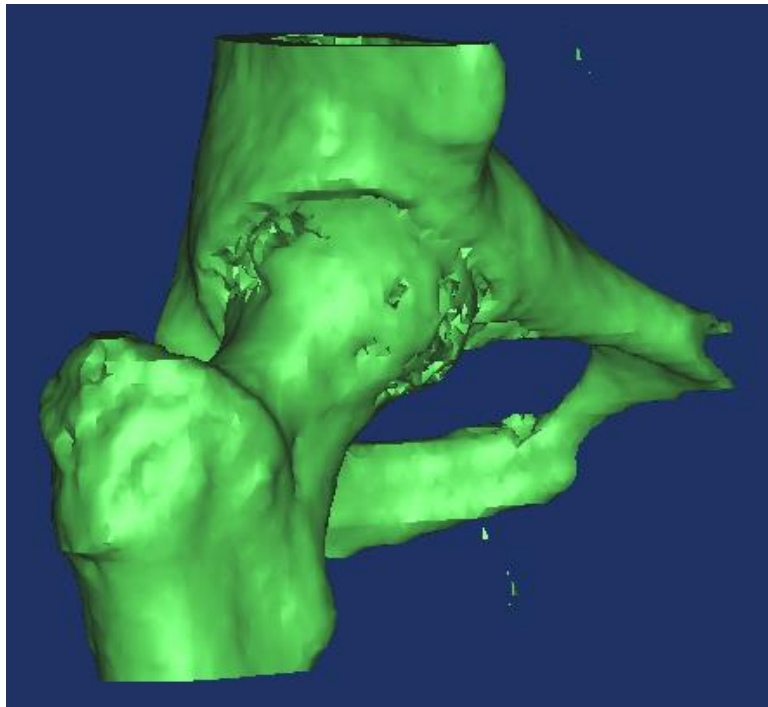


Figure 34: Cropped 3D model of the right femur. Abnormal holes appear on the femoral head, and fused areas are visible between the femur and the pelvis.

We can already see the problems that emerge from this series of initial steps. The femur is not isolated from the pelvis and at the contrary some areas of those two bones appear fused in the model. Floating pixels remain around the main structure. Large holes are present on the surface of the femur and the overall surface seems not optimal. The 3D reconstruction is far from perfect and still requires a lot of processing.

4.25 Isolating the femur

Once this preliminary work is done, the aim is to isolate and then refine the 3D model of the femur. It is important to bear in mind that knowing how to read a CT scan and be able to visualise the precise shape of a human femur are the key to an accurate reconstruction here.

A very important tool of Mimics is the “polylines” function. Once a mask is created, the “polylines” tool draws the contour of the mask in every slice of the CT. This set of polylines appears in the polylines window after this operation. It is then possible to apply a “cavity fill from polylines” to this set of data.

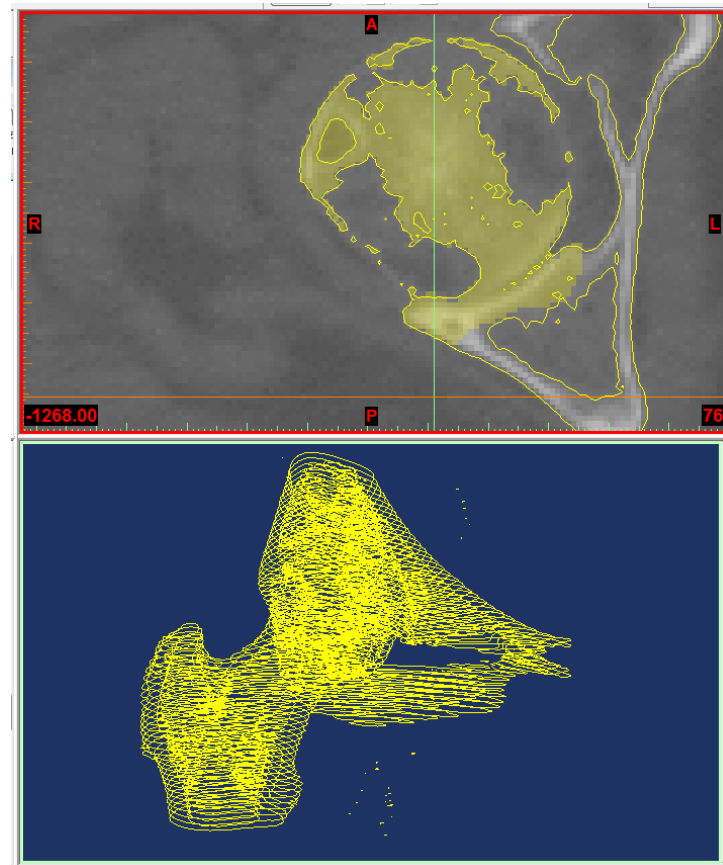


Figure 35: The first polylines set (bottom) shows the contours generated from the first 3D model. It allows the new mask being edited (top) to suppress the pelvis in the next 3D model.

This “cavity fill” will perform a reverse operation: it creates a new mask from the polylines, and in principle most of the abnormal holes that remained in the model are now filled. In reality, it requires more work. In figure 35, we can see the first set of polylines created from the original mask at the bottom and the newly generated mask at the top. Note that no 3D model has been generated from this new mask because some editing must be realised on it beforehand. On this figure 35, the new mask is shown while being edited. The yellow outer lines are the polylines generated from the first mask and appear in the top and bottom windows. The new mask only appears in the top window: it is the clear yellow filling that mainly covers the

femoral head. When the new mask is generated, all the space inside the polylines is automatically filled. It is then necessary to erase the parts that belong to the pelvis and to fill the abnormal cavities located on the femur. With this operation, the femur becomes isolated from the hip and its outer surface become uniform. It takes a non-negligible time since this operation must be done on every CT slice, but once every image is edited a new 3D model can be generated and compared to the previous one (figure 36).

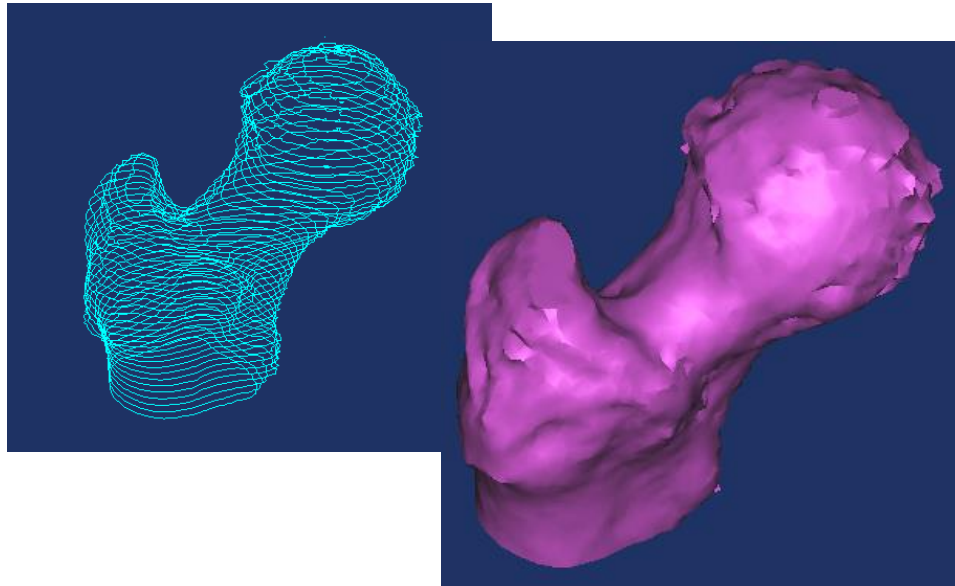


Figure 36: The new set of polylines (left) does not include the pelvis. It is then converted to a new 3D model (right) generated from a new mask.

Despite the length of the operation, the most efficient way to end up with an acceptable 3D model is to reiterate this operation a few times (figure 37). The major difficulty is to distinguish the limits of the bone in the CT slices. Since the patients will be suffering from articular disease, the theoretical anatomical knowledge might not be exactly the same as the “real” bone structure of the patient. At this point, it would be interesting to be aware of the clinical background of the patient in order to analyse the CT in the most accurate way.

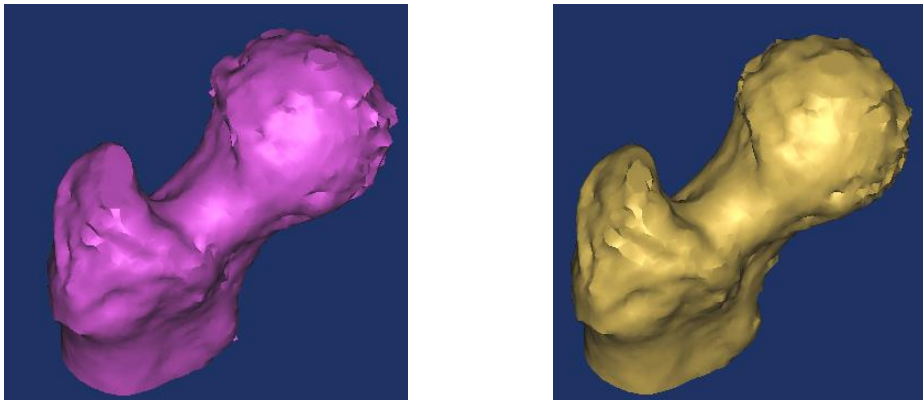


Figure 37: Evolution of the 3D model before (left) and after (right) one iteration of the refine process. The surface is more detailed after the iteration, but the difference is subtle, so many iterations are necessary to have a good model.

The left femur is then generated with the same process (figure 38).

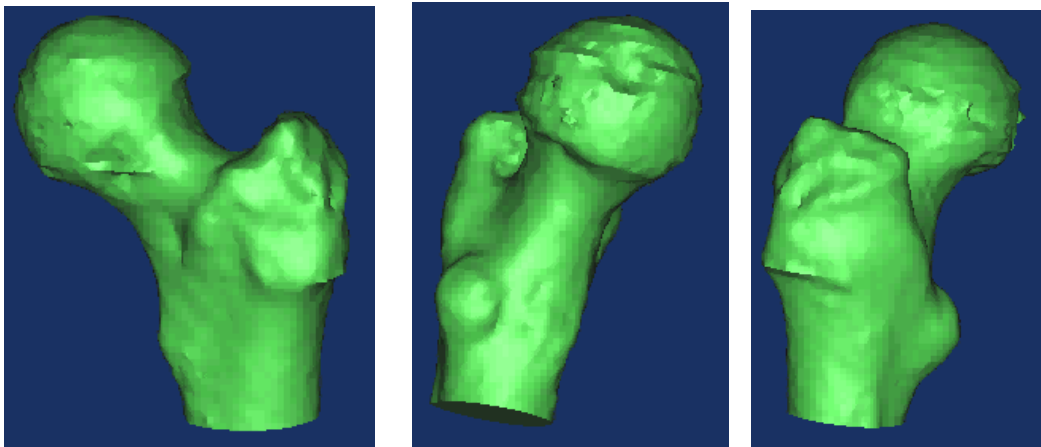


Figure 38: Views of 3D model of the left femur after the final iteration, showing a good surface grain and an anatomically accurate bone.

4.26 Processing the pelvis

The pelvis is processed with the same steps as the femurs. The main difference is its size, making this operation a lot longer than the precedent.

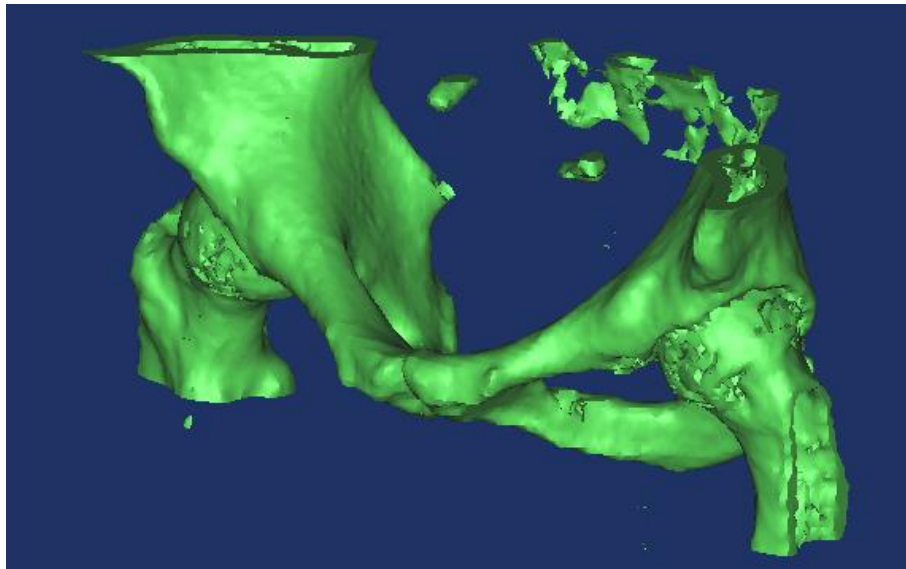


Figure 39: “Crop mask” operation on pelvis preserving the pelvic asperities susceptible to lead to impingements with the femur during the motion simulation.

From the first 3D model (generated with the initial mask), a different “crop mask” operation is done to focus on the pelvis (figure 39). The limitations of the cropping are now different. It is not necessary to preserve the femur structure on one hand; On the other hand, the pelvis is not entirely preserved either. The important structures that need to remain are the acetabular cavities that form the articular surface and the bone asperities that are susceptible to lead to impingement.

The defects present in this model are the same we observed for the femur: merged femoral and pelvic areas, holes, floating pixels, inaccuracy of the surface. In the same way than the femur, the iterative process is then applied: polylines, creation of a new mask, slice-by-slice edition of the new mask, generation of a new model, then new set of polylines etc. This process is showed in figures 40 to 43 inclusive.

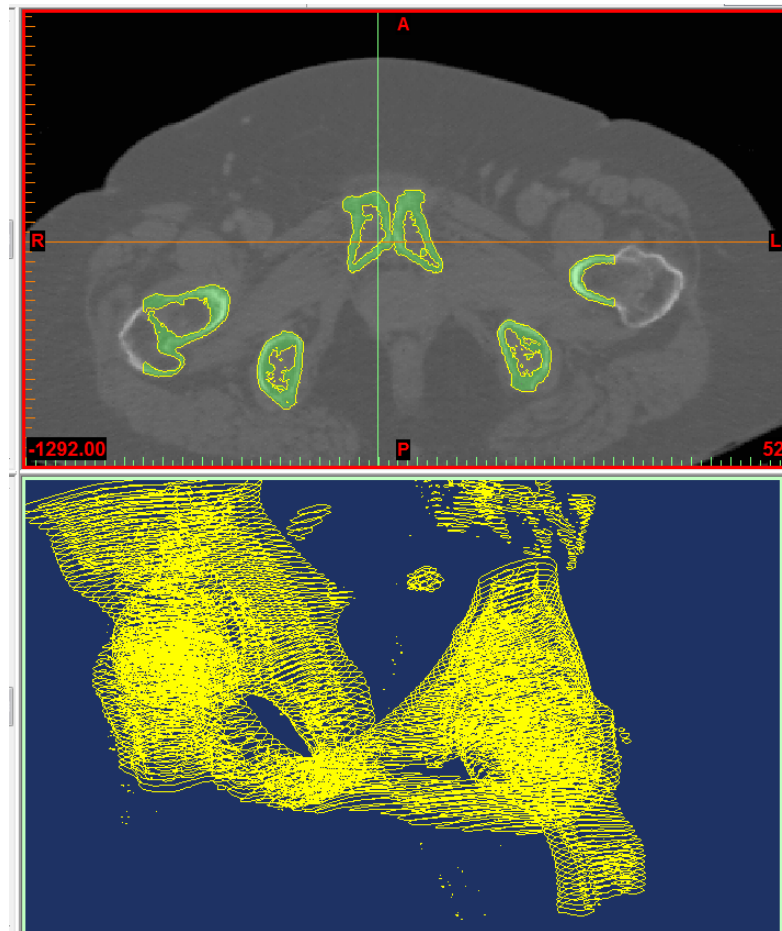


Figure 40: The first mask (light green, top) includes many different bone structures and shows numerous holes that should not appear. The polylines extrapolated from this mask (yellow lines, top and bottom) reflect this problem.

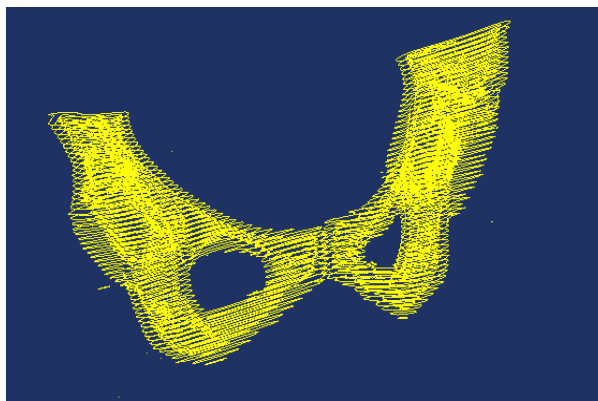


Figure 41: The first iteration consists in a removal of the femurs, the sacrum and the main artefacts. The polylines are recalculated and shown here: the model is clearer.

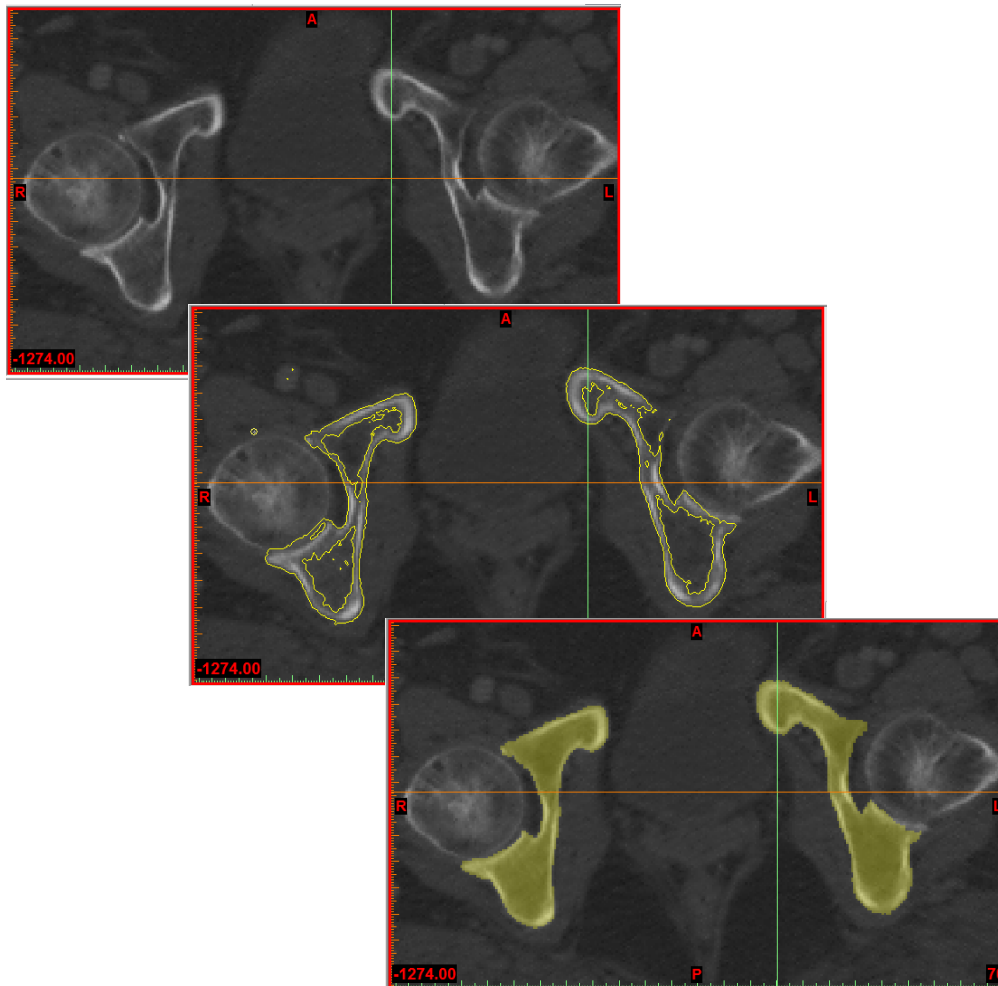


Figure 42: From the rough CT slice (top left) the extrapolated polylines define automatically the contours of the bone (middle), but the process is far from perfect (holes and inadequate shapes). Therefore the user has to recreate the mask manually (bottom right) based on the polylines and measurements on the CT slices.

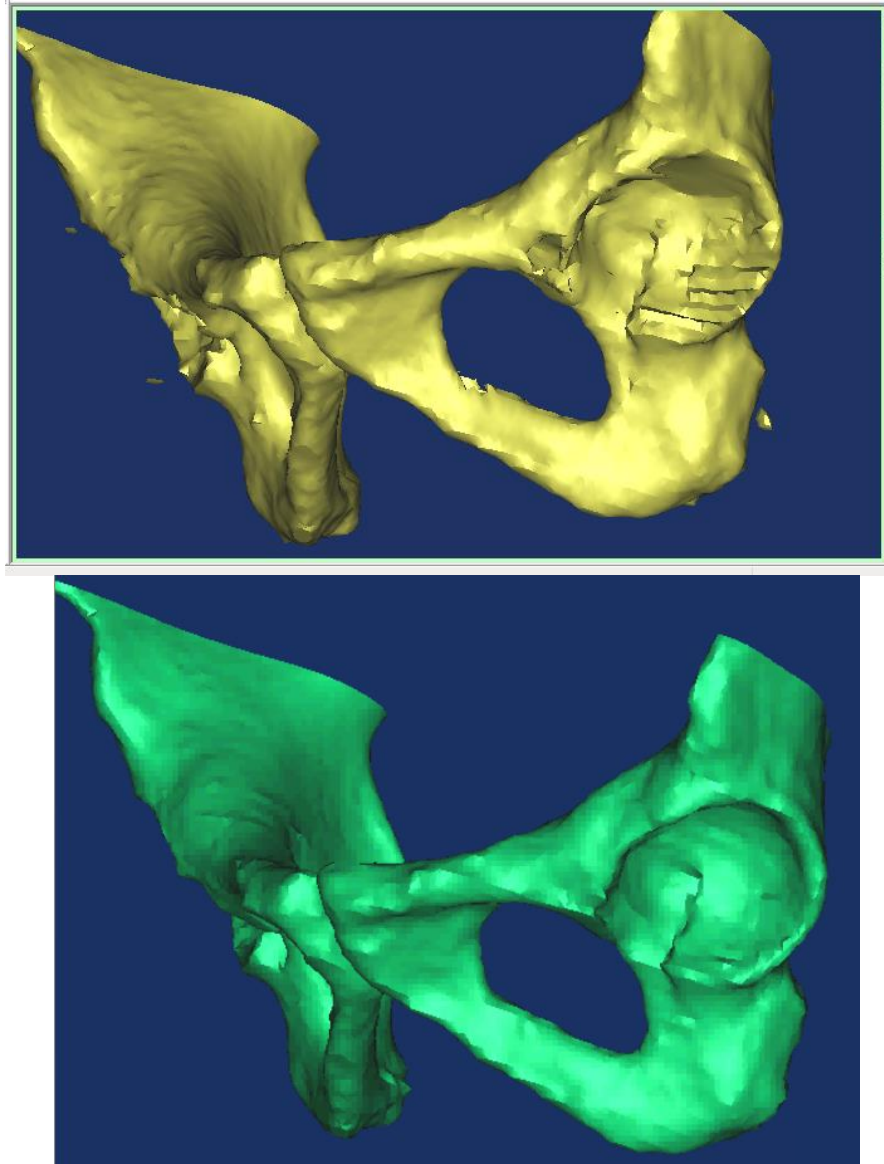


Figure 43: There is a clear improvement in the quality of the 3D model of the pelvis before (top) and after an iteration (bottom). The surface is smoother, artefacts are removed and abnormal holes are filled.

We now have a complete model for the pelvis and the femurs. They are stored as MCS files that can only be opened with Mimics. To use the models in a CAD analysis, it is necessary to convert these files to an IGES format that can be readily imported to any CAD software. To perform this, it is necessary to use the Mimics module called MedCAD.

4.27 MedCAD module

It is necessary to perform the same steps to convert the pelvic and femoral model, hence both models will be shown in the following explanations.

4.271 Smoothing the models

Despite the iterations during the segmentation process with Mimics, it is noticeable that the models have been created from CT slices. Indeed, the 3D models show some acute angles where the surface is supposed to be smooth (surface of the femoral head for example). The first useful tool of MedCAD is the smoothing function shown in figure 44. It allows us to reduce this rough aspect by performing an automated average of the surface.

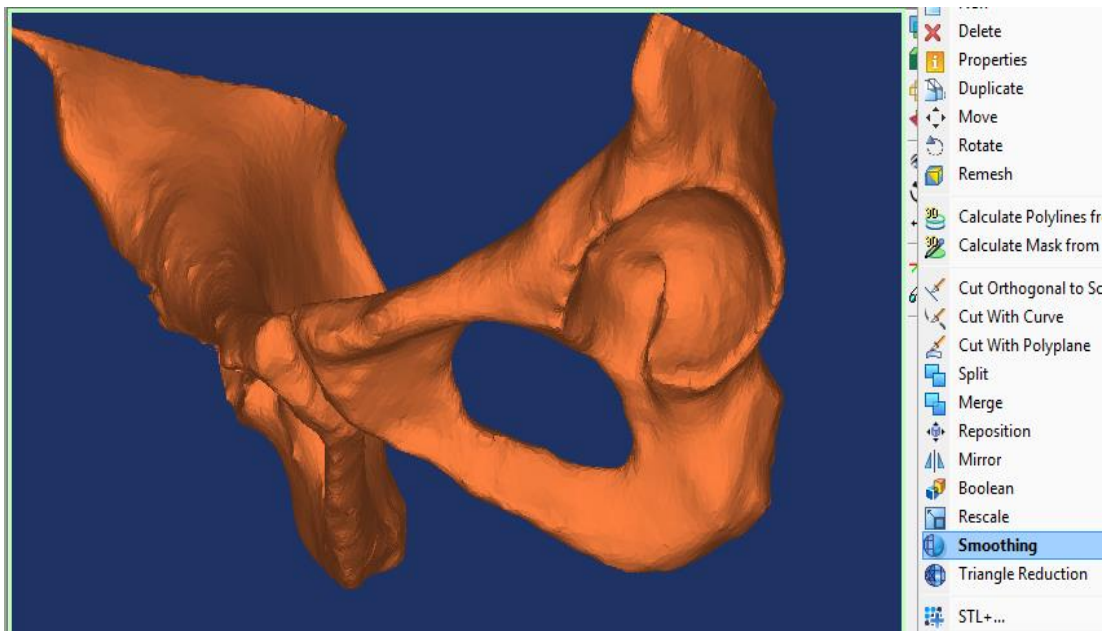


Figure 44: Smoothened model of the pelvic bone showing a realistic rendering of the bone surface.

The amount of lost information due to this process is hard to evaluate, because the reference dimensions are measured on the CT slices. Since the edges of the bones are always blurry on the slices, the reference measurements are always slightly subjective. However, repeated measurements have been done to ensure the accuracy of the approximation and the relative error between the CT and the 3D models never

exceeded 4.55%. The error on articular surfaces was always maintained below 1% (maximum relative error: 0.96%).

It is then possible to extract the polylines from the smoothed model. This operation determines the contour or the new part slice by slice and displays those contours on the CT slices. We can see on figure 45 a zoom on the polylines calculated on the model of the pelvis. The polylines extrapolated here will serve as a guide for the surface creation.

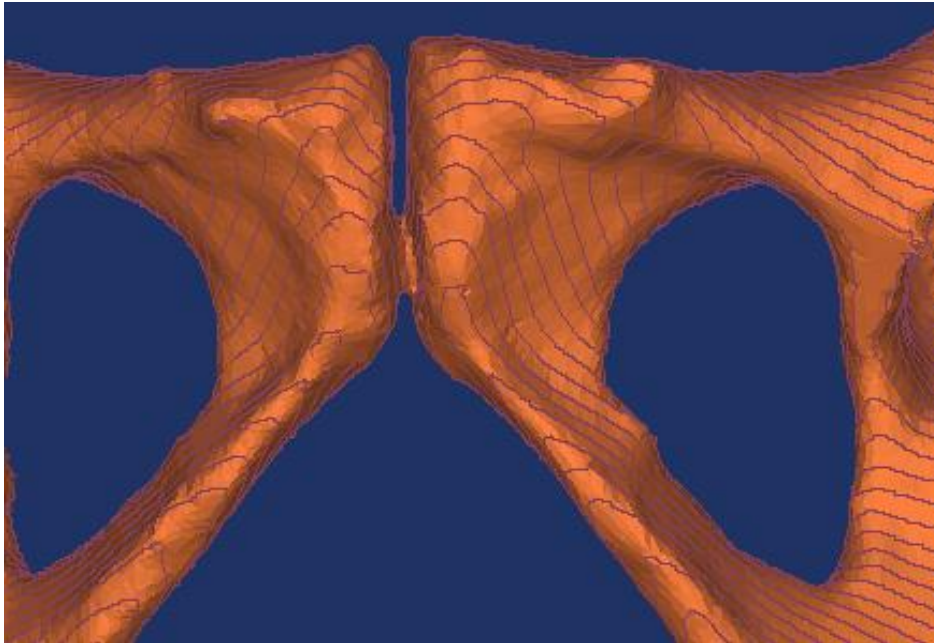


Figure 45: By zooming on polylines calculated from the new pelvic model, we can see how they are extrapolated directly from the 3D model.

4.272 Polyline growing and surface fitting

Our aim is to obtain a surface description of the femur and the pelvis that will be used to detect collisions during the CAD analysis based on the obtained polylines. Therefore, the accuracy of the surface is important, especially regarding the bone processes that are most likely to interfere with each other. Since we are working with real bones, we cannot use the standard geometrical shapes like spheres or cylinders that are available with MedCAD for modelling the surfaces. We have to apply the “freeform surface” function, which is more complex. To use this tool, it is necessary to perform some “polyline growing”. This function allows the user to perform a selection of successive polylines on a previous polylines set (see figure 46). It is

fundamental for one reason: the freeform surface fitting can only be performed if every contour resembles the one in the previous slice. That is why we have a correlation parameter in the polyline growing function, which determines the percentage of resemblance between slices that is considered acceptable for the current selection. This parameter default value is 97%, hence two successive contours will not be considered as part of the same polyline growing set if there is less than a 97% correlation between them: there cannot be any discontinuity between the profiles. It implies that we will have to perform several surface fittings for the 3D models.

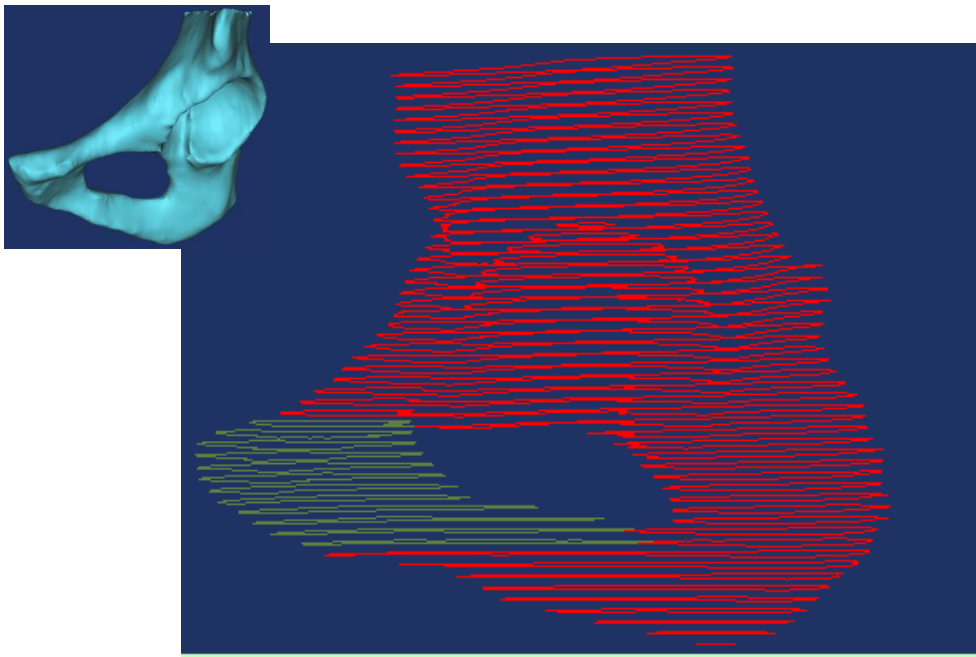


Figure 46: By doing a polyline growing (green lines) from polylines of the left pelvis (red lines), only a part of the pelvis is selected.

As shown in figure 47, the femur will be decomposed into 3 distinct elements called “head” (head and neck), “crest” (greater trochanter) and “stem” (proximal diaphysis). The left pelvis will be decomposed into 4 parts: “superior part” (mainly acetabulum), “inferior part” (inferior part of ischium), “medial part” (pubis) and “lateral part” (junction between ischium and acetabulum). The choice of segmentation was made using several criteria. The bones had to be divided in a minimal number of parts in order to simplify the reconstruction afterwards. The different parts had to be

separated with transverse limits since the dividing process uses the transverse slices to generate new polylines sets. Finally, only one structure can appear in a transverse slice, therefore parallel structure like the “head” and “crest” parts of the femur (figure 47) must be identified as two separate structures.

We can see in this figure 47 that the continuity is preserved: each part contains only one series of profile lines. To do so, it is sometimes necessary to manually reselect a polyline in a slice (or several successive slices) that contains more than one polyline.

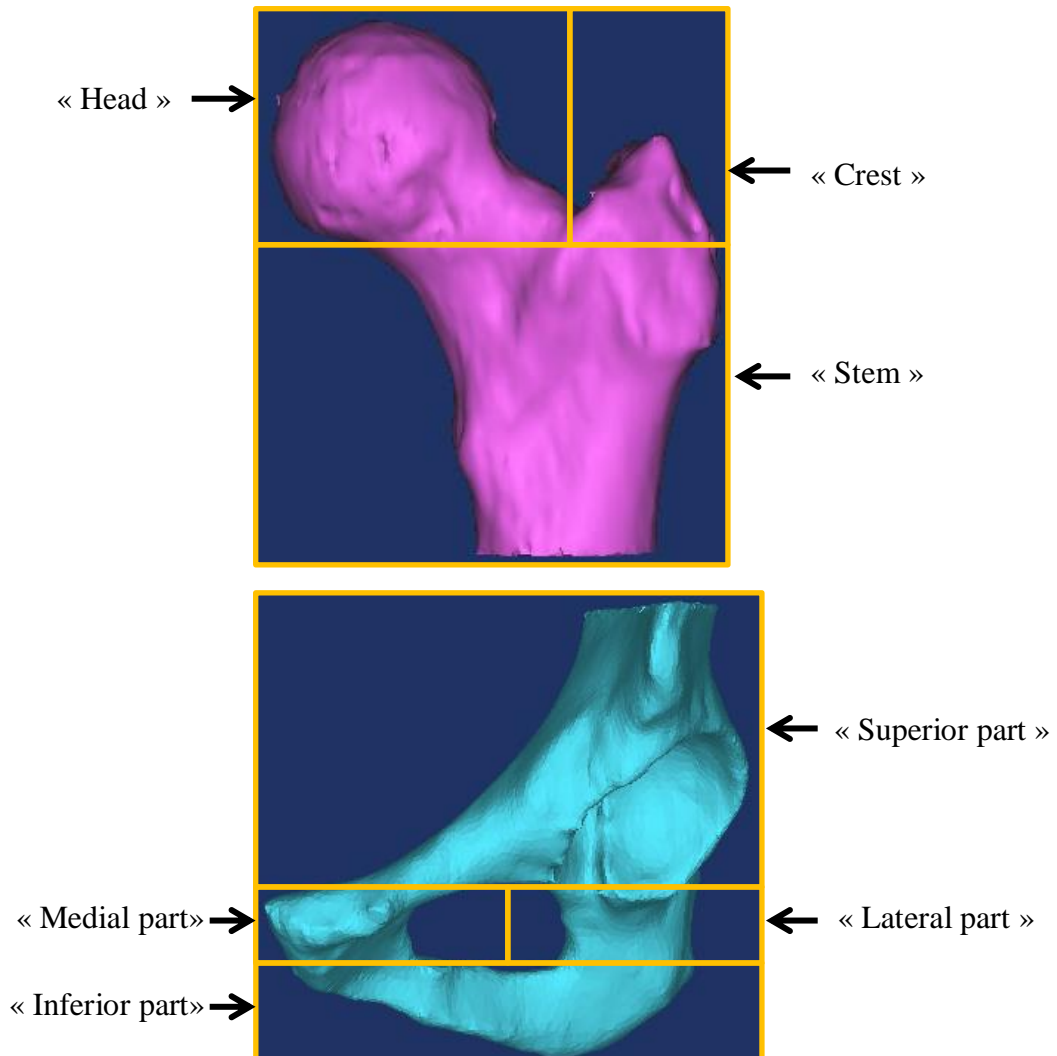


Figure 47: Definitive location of the different polyline growing sets for the left femur (top) and left pelvis (bottom). This segmentation has to be done with horizontal limits since it is based on polylines which are in the transverse plane.

On figure 48 we can observe the reselection of the “head” part of the femur in the current polyline growing.

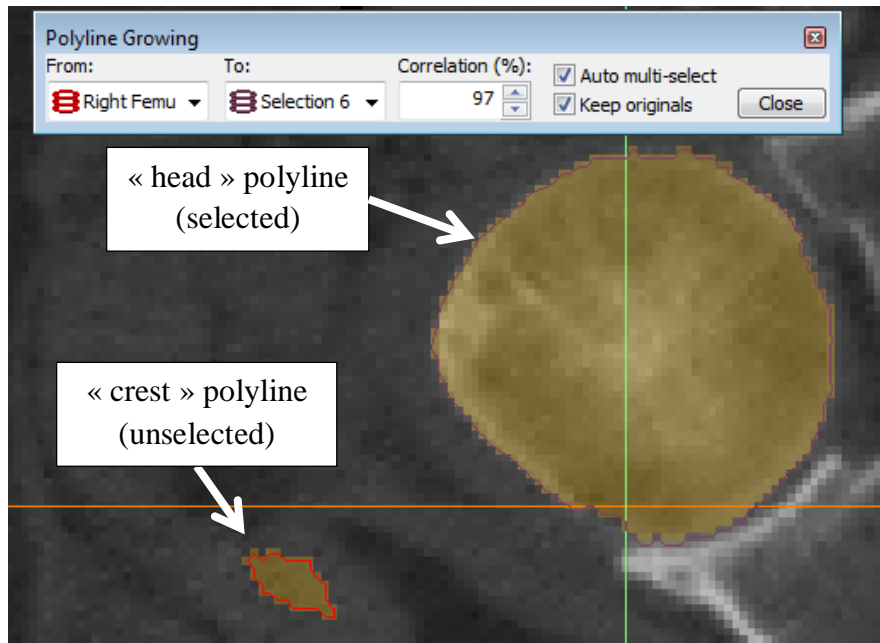


Figure 48: Selection of a polyline in a slice during polyline growing process. If two different closed contours were selected in the same slice of a single polylines set, the following surface generation could not be solved by the Mimics algorithm.

The “crest” part will be selected in another polyline growing process to obtain two separated surfaces. Once these different parts have been converted to polyline sets, the “freeform surface” fitting can be used. If the polyline grow has been done accurately, the window shown figure 49 appears and indicates “Set OK”. It means the different polylines present in the selected set are similar enough to allow a surface fitting. The user is then allowed to change the u-parameters and v-parameters. These are the two mathematical entities that are used to calculate a surface from a set of control points. The order and the number of control points that must be used to calculate the surface can be manually adjusted. The order will define the complexity of the resulting surface. The control points are points that must be included in the resulting surface.

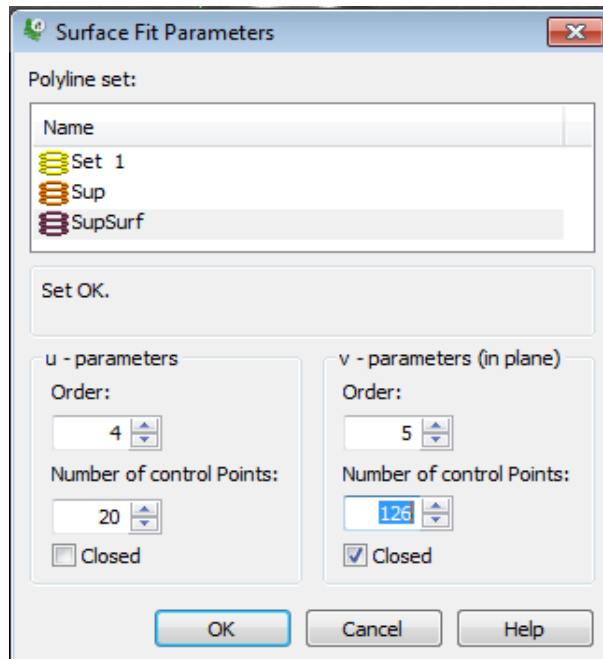


Figure 49: Freeform surface fitting interface allowing the user to choose the order and number of control points to be used for the surface fitting.

Contrary to what one might think, choosing the maximum order and control point values is not necessarily the best solution. If too many control points are selected for modelling a small surface, it can lead to local distortions for example, like shown in figure 50. In this example, the problem was reinforced by the shape of the inferior polylines which were too large compared to the superior ones. It proves that even with a correlation limit in the polyline growing tool, some inaccuracies can remain within the polyline sets.

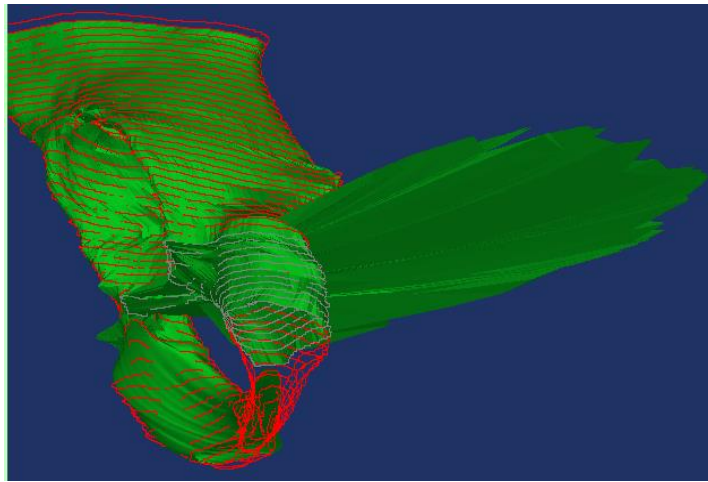


Figure 50: Surface artefact due mainly to an inaccurate number of control points, making the generated surface inadequate for further analysis.

Another problem that can emerge with the surface fitting function is the junction between the different parts. The different polyline sets must overlap, otherwise holes will remain between the surfaces (see figure 51).

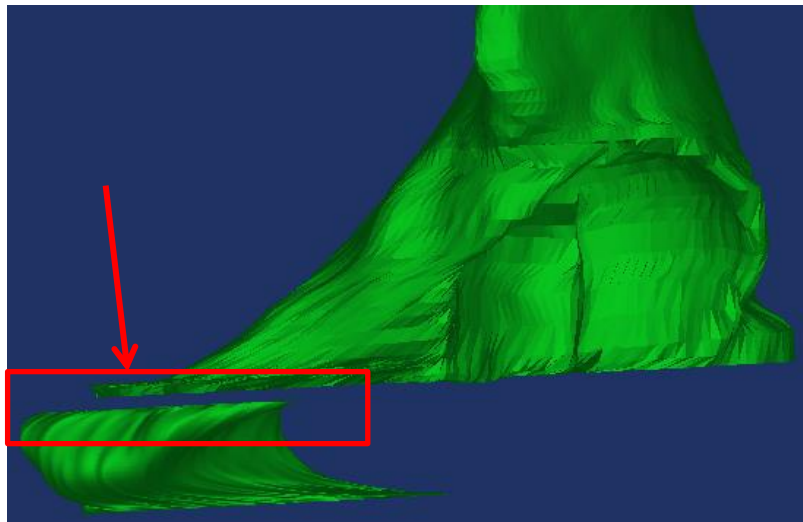


Figure 51: Gap between superior and medial part of left pelvis due to lack of polylines overlap. The resulting assembly is not suitable for analysis since there is a lack of surface information.

The most important objective here is to obtain an accurate representation of the asperities of the bone, especially on the articular and bone asperities areas. To do so,

several attempts are required and direct comparisons on the original 3D model are a good way to verify this accuracy. The figure 52 is a good example of the evolution of the surface fitting on the left pelvis. It shows the changes that can be obtained by modifying the u- and v-parameters.

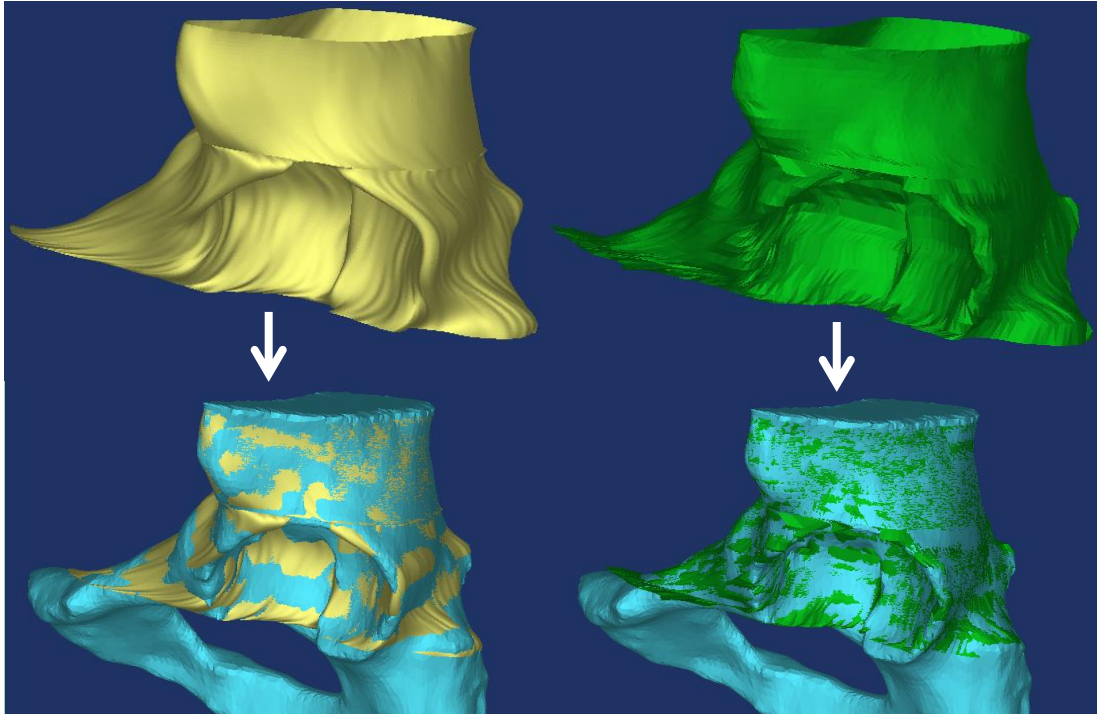


Figure 52: Fitted surface before (left) and after (right) “order” and “control point” adjustments. After the adjustments, the surface is fitted closer to the 3D model hence it is a better representation of the real surface.

We can see that the new surface is closer to the 3D model than the previous one. This process is done for every part of the femur and the pelvis, until the entire 3D model is converted to surfaces. The results are shown in figure 53. We can distinguish the horizontal lines that separate the different surfaces, but it is not critical for the quality of the model. These lines will be softened with the CAD software.

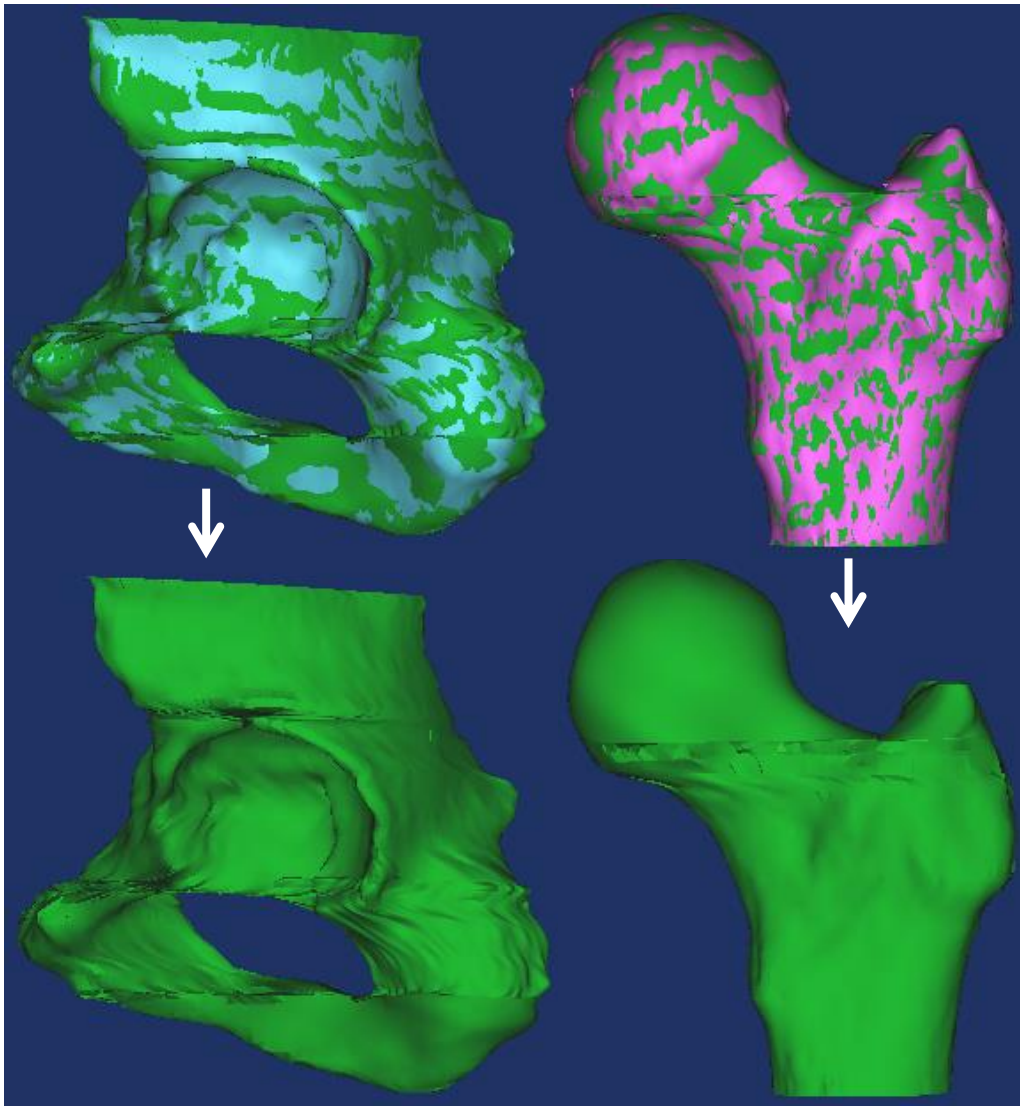


Figure 53: Extracted surfaces of the left pelvis (left) and the left femur (right) shown with (top) or without the original 3D model (bottom). For these surface models, the most important parameter is to fit closely to the 3D model.

Once the surfaces have been generated, it is then possible to save them as IGES files (.igs extension files). Note that each surface is saved as a single file; it will therefore be necessary to reconstruct the two bones from the separate surfaces before any other processing can be made.

The last operation that we have to perform with MedCAD is determining geometrical references that will help the CAD modelling in the next step. We have to find the hip centre and the axis of the femoral neck to ensure a correct positioning of the bone parts. Within MedCAD, a sphere fitting can be performed directly on the models to find the hip centre. By selecting at least four reference points on the 3D model, the sphere is pre-positioned and can be adjusted by using the images in the three anatomical planes displayed on figure 54.

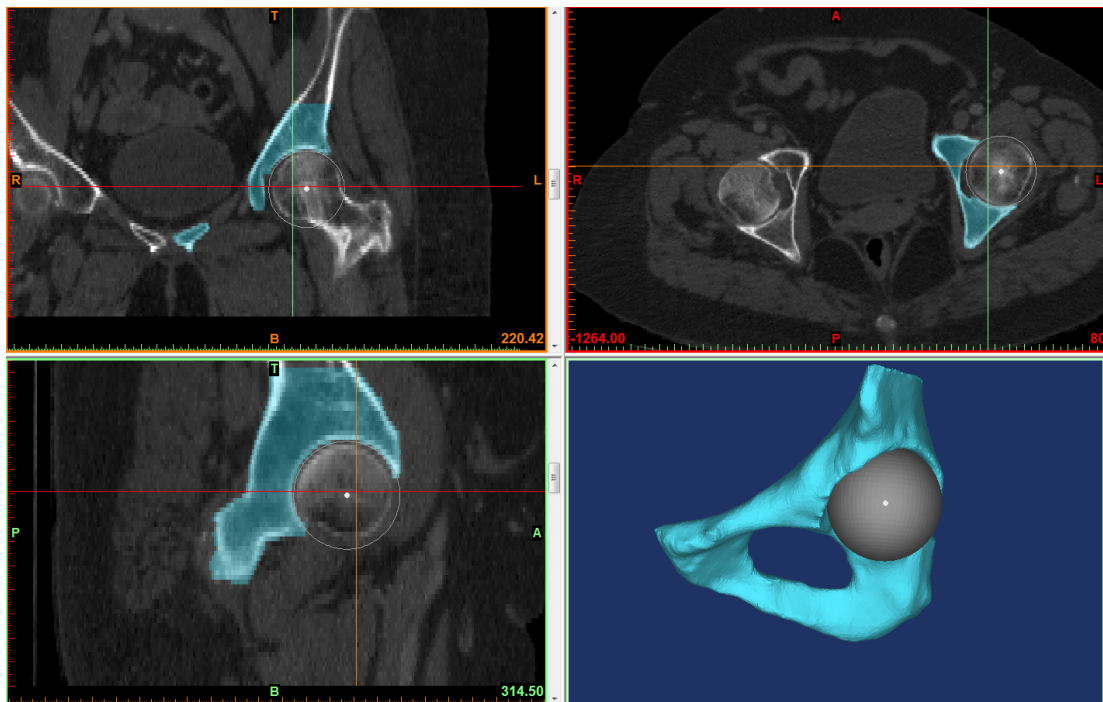


Figure 54: Sphere fitted on the acetabular surface and its projection in coronal (top left), transverse (top right) and sagittal plane (bottom left). Simple measurements on the slices allow positioning the sphere accurately in the different planes.

Once the sphere is fitted on the structure, its properties must be displayed to obtain the following measurements: coordinates of the centre, radius and deviation. The same operation is conducted on the femoral head and the results are shown in figure 55.

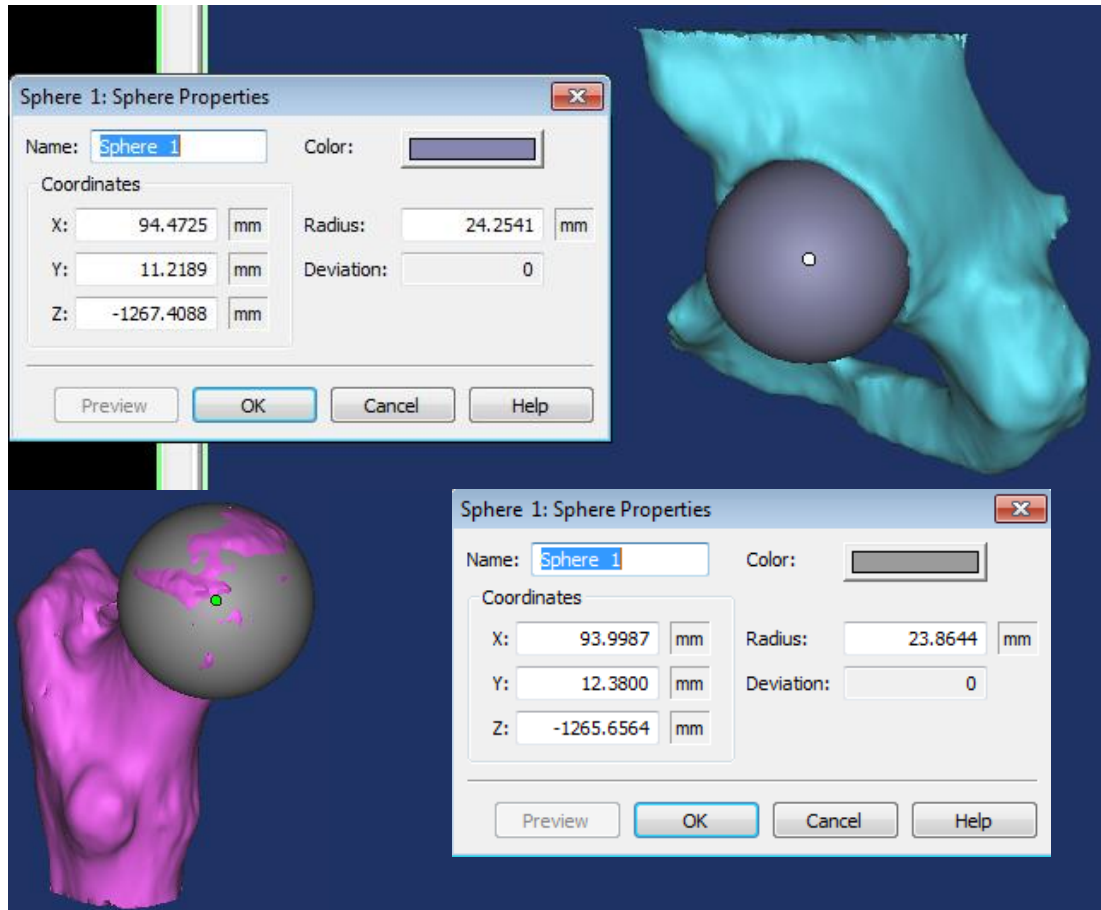


Figure 55: Measurements on the acetabular (top) and femoral sphere (bottom). The location of the hip centre based on the femoral head is consistent with the one based on acetabular cavity. The acetabular fitted sphere is logically slightly larger than the femoral head one.

We can notice that the radius of the sphere fitted in the acetabulum (24.25mm) is slightly larger than one fitted on the femoral head (23.86mm) and the relative difference is 2.25%, which is consistent with the articular role of these parts. The coordinates of the hip centre also differ between the two entities, but the difference is not very important: 0.47mm on X, 1.16mm on Y and 1.74mm on Z. These variations

are linked to anatomical variations as well as 3D approximations and can be considered small enough not to impact significantly the results.

The last geometrical measurements that are relevant to the CAD analysis are the directions of the femoral neck and the femoral diaphysis. These parameters can be extracted by fitting cylinders to the 3D model of the femur in the same way we fitted the sphere, as shown in figure 56. Some reference points are selected first, and a cylinder is then automatically fitted; it is then possible to modify its location through the different views displayed in Mimics.

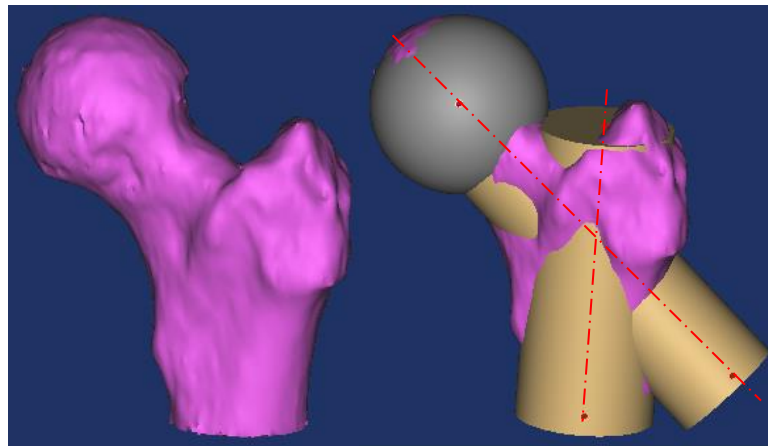


Figure 56: Fitted sphere, cylinders and axes on left femur 3D model defining the geometrical parameters of the bone.

The direction of the axes can be found under the cylinder properties. By copying the parameters we can generate the axes and then save the file in an IGES format. The other measures relative to the cylinders (length, radius and coordinates of the centre of extremities) are not relevant for this study.

The spheres and axes created therefore are saved as IGES and will be imported in the CAD software to create the hip assembly.

4.3 CAD modelling with Solidworks

4.31 Basic principle of Solidworks

Solidworks is a CAD that allows many different processes. Mainly, it is possible to create or import some parts (individual models) or assemblies (which unite several

parts) to either realise some static analysis or some cinematic/dynamic studies. The parts can be volumes or solids depending on the type of study required. The “history” of every file is displayed on the side of the screen as showed on figure 57 and therefore it is possible to modify any parameter during the study by acting directly on the lateral tree. For an assembly, it shows the parts involved, the mates between the parts (which allow to position the parts relatively to each other), the references like planes or axes, the annotations made on the assembly if any, the movements of the different parts, the materials properties and all other parameters than have been added to the assembly.

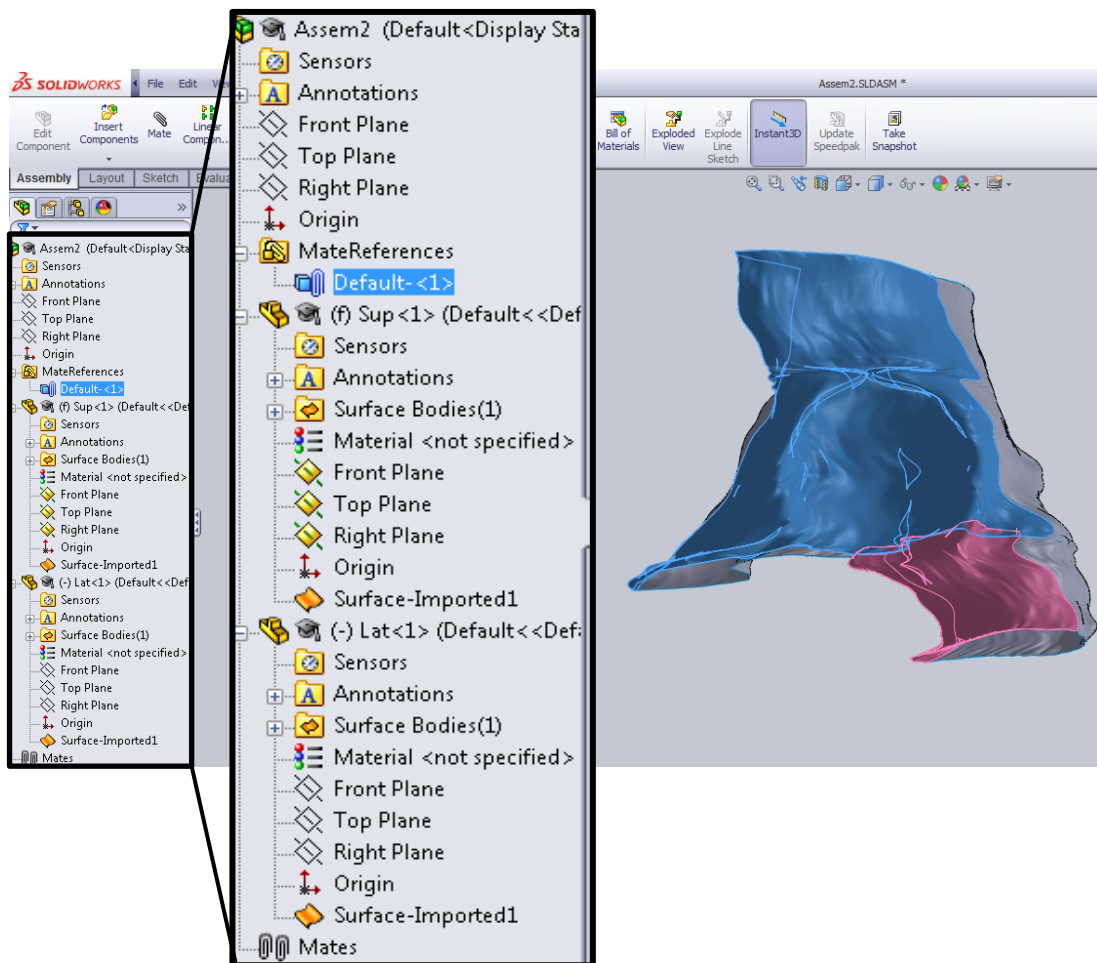


Figure 57: Early assembly tree of a 2-parts assembly (“superior” part partially blue and “lateral” part partially pink) in Solidworks. Many parameters already appear in the tree despite the simplicity of the overall structure, and must be managed to ensure the stability of the assembly.

In the figure 57, only 2 parts are present in the assembly, hence the assembly tree is short, but it enlarges quickly as soon as we add other parts, mates and references. It is important to know how to integrate a new part or reference and then being able to find it back in case a parameter must be redefined.

4.32 Reconstruction of the pelvic part

As explained in the Mimics section, the bones have been recreated with IGES surfaces, but it was necessary to generate several different files to describe a single bone. Therefore we have to unite the different parts into a single entity with SolidWorks. The aim of the CAD simulation is to estimate the range of motion of the hip articulation; hence we will measure the movements of a bone relatively to another. It seems logical to lock the pelvis in anatomical position and then allow the femur to rotate freely around the hip centre in order to achieve this. That is why the four surfaces of the pelvic bone will be reunited within an assembly. It will allow us to locate the different parts, check their orientation and lock them in the right position.

The four surfaces of the left pelvis (“superior”, “medial”, “lateral” and “inferior”) must be imported individually to the software first. While a surface is imported, an analysis is automatically performed by SolidWorks and the user has several choices, as shown in figure 58. The diagnostic is standardised, so some of the “problems” are parameters that we want to maintain in our model. It is the case for the “gaps between faces”, which will be connected to similar “gaps” present on the other surface parts. At the contrary, the “faulty faces” message indicates small defects present on the surfaces generated with Mimics; it is desirable to repair these.

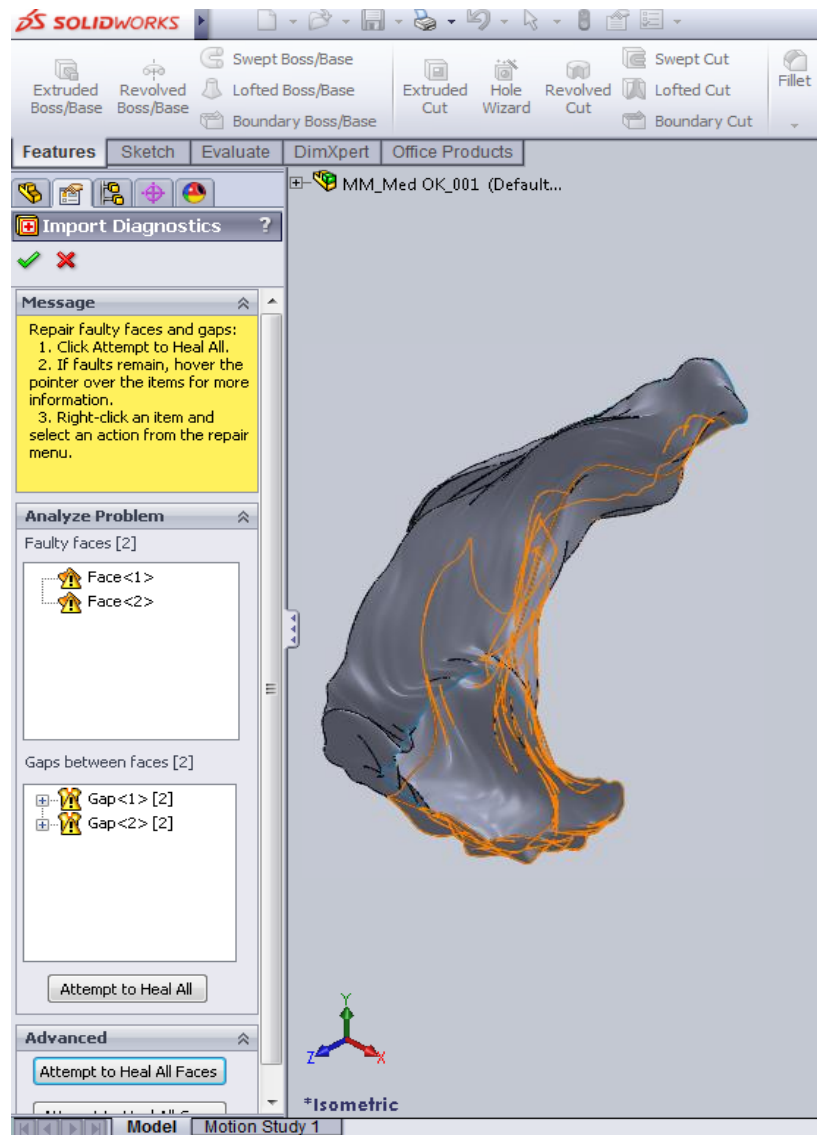


Figure 58: Import diagnostic window analysing the "medial" surface of left pelvic bone. The “faulty faces” are unwanted defects of the Mimics generated surfaces whereas the “gaps between faces” are to be connected with the “superior” and “inferior” parts of the pelvis.

In this case, we will therefore select the “Attempt to heal all faces” function and not the “Attempt to close all holes” one. The part is then ready to be added to an assembly. Therefore, once all four parts of the pelvis have been analysed and repaired, they have been imported to a new assembly. The figure 59 shows the result. The fitting between the different parts was based on various techniques. The surfaces have been generated from polylines that appear on transverse slices in the CT, so the upper and/or lower limit(s) of the surfaces are all parallel. Making the same planes parallel in the assembly is the first step to an accurate positioning.

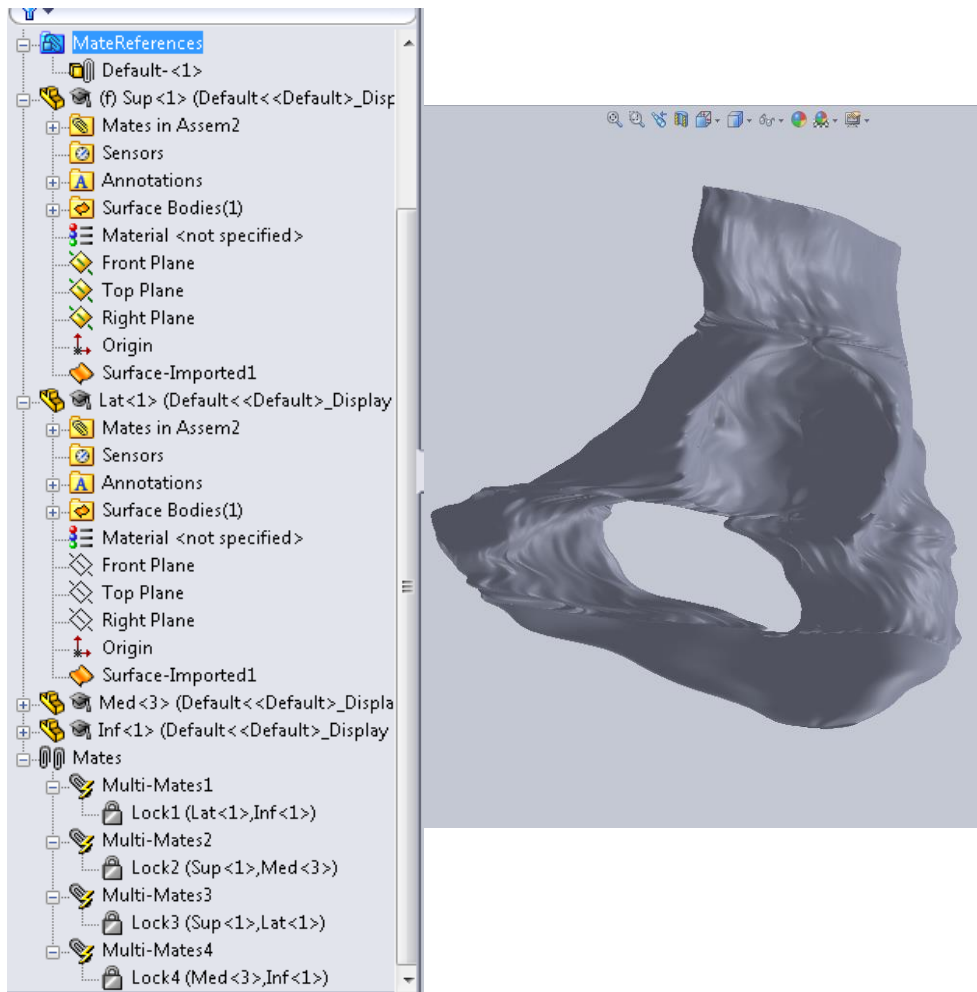


Figure 59: Assembly of the four pelvic surfaces and associated assembly tree. At the bottom of the tree, we see the four “Lock” mates that ensure the immobility of the pelvis.

The surfaces have been created with an overlap, so the edges cannot be constrained with a coincidental mate. The only way to connect them is to ensure the tangency of the parts. Once the position is correct, all the parts have been locked to fix the assembly. It is also shown on the figure 59. At the bottom of the assembly tree, we can see that four “lock” functions have been assigned. The superior part (“Sup<1>”) is locked with the lateral (“Lat<1>”) and medial part (“Med<3>”), which are both locked with the inferior part (“Inf<1>”). The result is a rigid surface model.

The last step shown in figure 60 is the import of the sphere we previously fitted to the acetabulum. The sphere itself is obviously not part of the joint, but its centre allows us to define easily the articulation centre as part of the assembly. A problem emerged though: the coordinates of the sphere centre could not be entered so it was

not possible to locate this sphere by entering them. Instead, collision detection was used. This tool detects the interaction between the surfaces of two separate parts. By selecting the option “stop at collision”, it is possible to replace the sphere inside the acetabulum, tangent to the external part of the surface. The centre of mass was then calculated and added to the sphere part to be used as the reference centre.

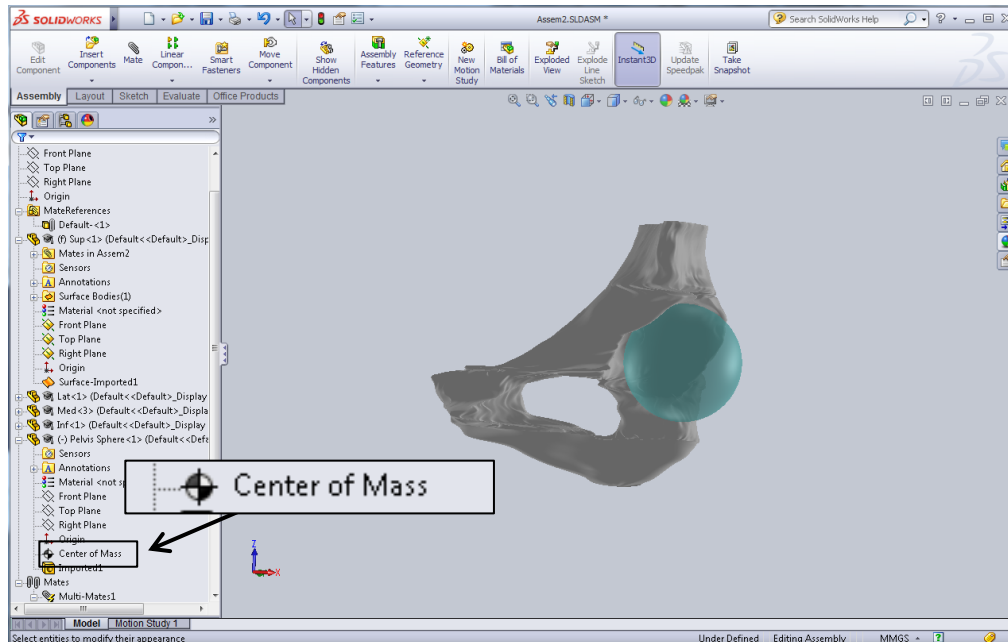


Figure 60: Complete left pelvic bone with fitted sphere. The centre of mass has been recalculated within Solidworks to redefine the centre of the hip articulation.

4.33 Reconstruction of the femur part

The femur must not be a rigid stationary part. It should be able to rotate freely around the hip centre during the simulation. Therefore we will not use the assembly function. Instead, the three different surfaces generated with Mimics (head, crest and stem) will be imported as free surfaces and united within a single part file. However, the first step remains the same: it is necessary to import and analyse each surface first. After the automated repair of surface has occurred, it is possible to unite the three surfaces and improve the quality of the details. The assembly of the surfaces within a part is similar to the assembly of parts. The “limits” of the surfaces (edges)

that separate the upper (crest and head) and lower (stem) surfaces are parallel to each other since they were separated with polylines, which are all in a transverse plane. It allows the user to do a primary positioning. The tangency between the surfaces is then used to put the surfaces in right place. Once the three surfaces are accurately positioned, the main repair consists in filling some remaining holes on the model. A remaining hole at the top of the crest was filled as shown in figure 61 with the filling function. Continuous edges must be selected to allow the “patching” to take place. Some other holes have been filled in a similar way, between the stem and the crest/head surfaces.

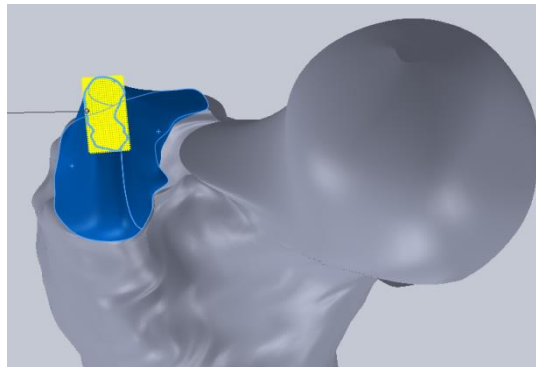


Figure 61: "Patch boundary" being performed on the upper limit of the "crest" part. This will repair the surface by closing a residual hole on the model.

After these repairs, the sphere should also be fitted to the femur to determine the articulation centre. Once again, it was not possible to enter the centre coordinates to locate the sphere, only here we could not use the collision detection. It is logical since the sphere fits around the femoral head and therefore “interferes” with it.

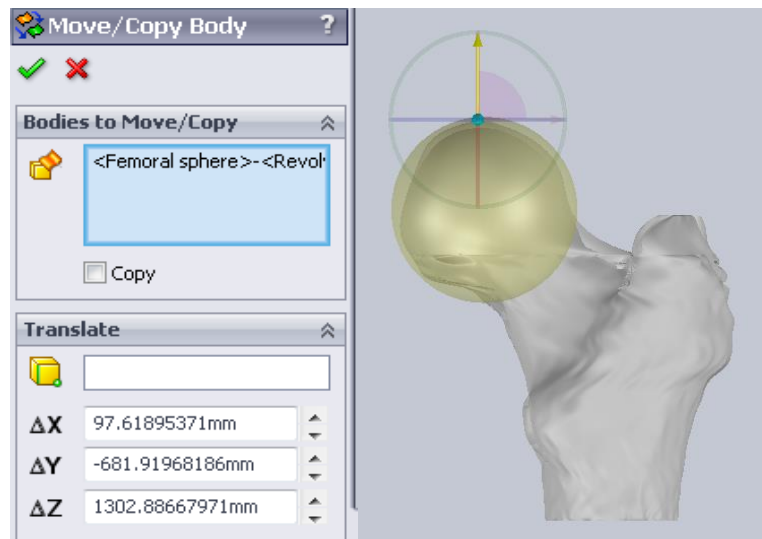


Figure 62: Femoral sphere positioning, anterior view of coronal plane. The translation is very carefully controlled by the left window (up to 0.1nm precision).

In reality it would obviously not collide since it is a virtual part. Therefore the position of the femoral sphere was determined visually, while comparing the views in Solidworks with the plane by plane pictures from Mimics. The CAD software allows very precise positioning, up to 0.1nm (see figure 62).

From this positioning the head centre was calculated and added to the “femur” part as a reference point.

The axis of the neck was also supposed to be added to the “femur” part, but it was also not accurately defined in the new environment. It was necessary to find an alternative way to recover this axis. It was performed with geometrical operations based on control points on the edges of the surface shown in figure 63. First, two points here named “A” and “B” were selected in the neck area. The selection of those two points was made by measurements and comparison to the Mimics files. In the Mimics views, the neck axis was traceable in the different views. On the different views, it has been shown that the direction determined by those two points A and B formed a right angle with the neck axis.

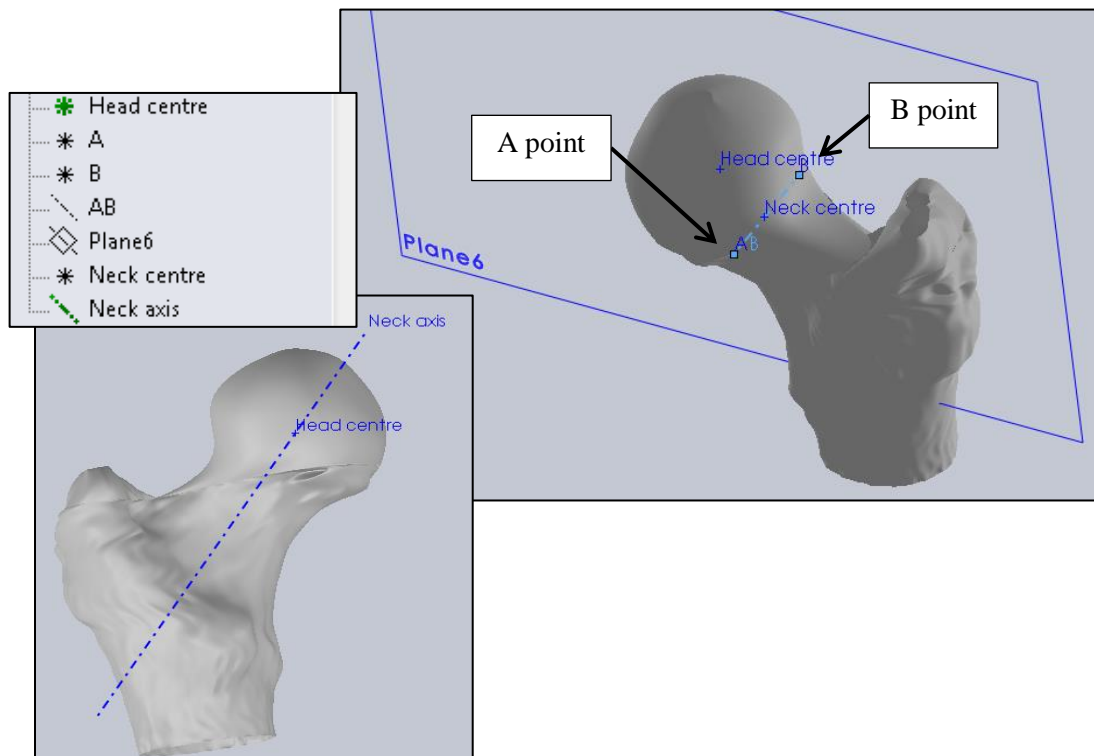


Figure 63: Geometrical parameters leading to the reconstruction of the neck axis. The neck centre is extrapolated from two neck points (A and B) which coordinates were measured on CT slices and the plane normal to the AB axis that passes through the head centre.

We also know that the neck axis goes through the head centre. Therefore, first we had to define a new plane with a point (head centre) and a normal direction (AB direction). Once this plane was created, the projection of the AB segment was made on this new plane and named “neck centre”. Finally, an new axis passing through the head centre and the neck centre was created and named “neck axis”. All these operations are recorded chronologically in the part tree also displayed in figure 63.

4.34 Assembling the articulation

The femur is now complete and can be imported as a part to the main assembly containing the fixed pelvic bone. Since the femoral head centre and the acetabular centre have been defined as references, it is now possible to mate the femur and the pelvis by defining a coincidence between these two points (figure 64). The relative position of the femur and the pelvis was automatic, since they kept their default orientation i.e. the CT orientation.

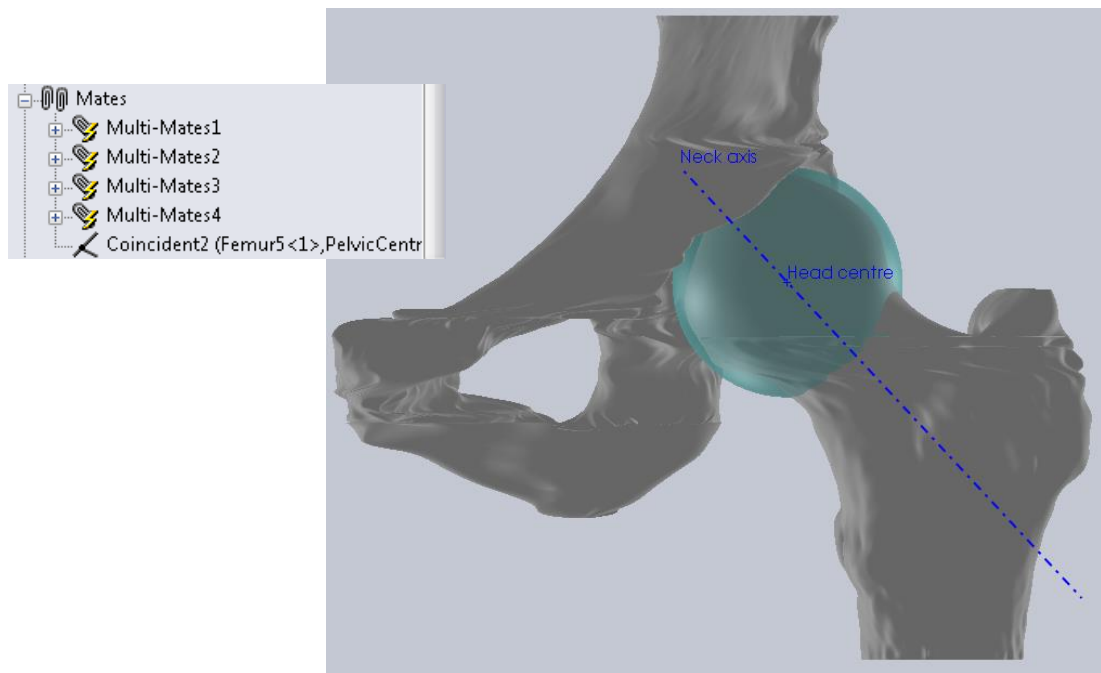


Figure 64: Hip articulation assembly and associated mates The “Multi-Mates” 1 to 4 are the “Lock” mates that fix the pelvis. The last mate (“Coincident”) is the coincidence of the femoral head centre and the acetabular centre.

To prepare the motion simulation in different planes, it was necessary to create new planes and axes. Indeed, with a free rotation of the femur around the hip centre and no other references, it is not possible to parameter plane-by-plane displacements. First some new planes have been defined. They are the anatomical planes that pass through the hip centre (figure 65). This has been performed by creating a linear translation of the three original reference planes (located at CT scanner origin) until the hip centre point. By using an intersection process between these new planes, three axes can be generated. They were referenced “TranSagAxis” at the intersection of the transverse and the sagittal planes, “SagCorAxis” at the intersection of the sagittal and coronal planes and “CorTransAxis” at the intersection of the coronal and transverse planes (see figure 66).

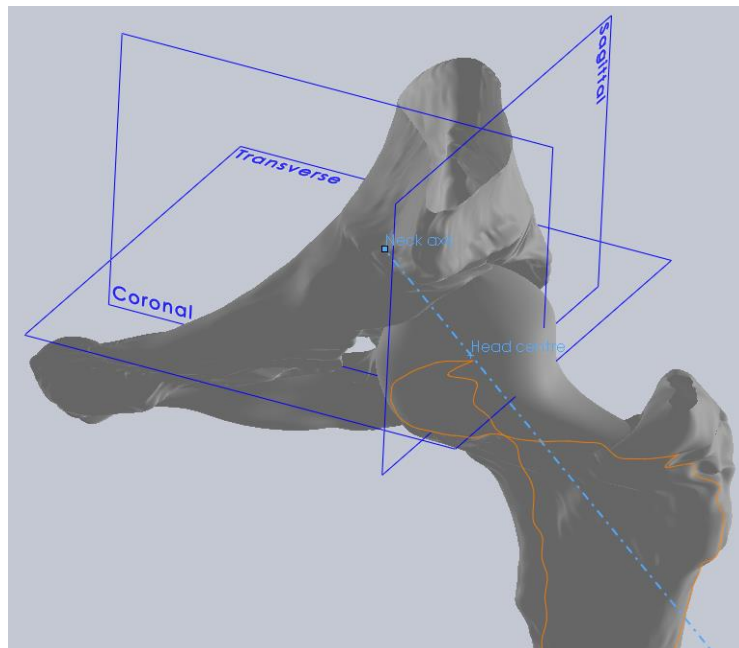


Figure 65: Anatomical planes passing through the hip centre. These planes are to be used for projecting the measured angles of the hip articulation after the motion simulation.

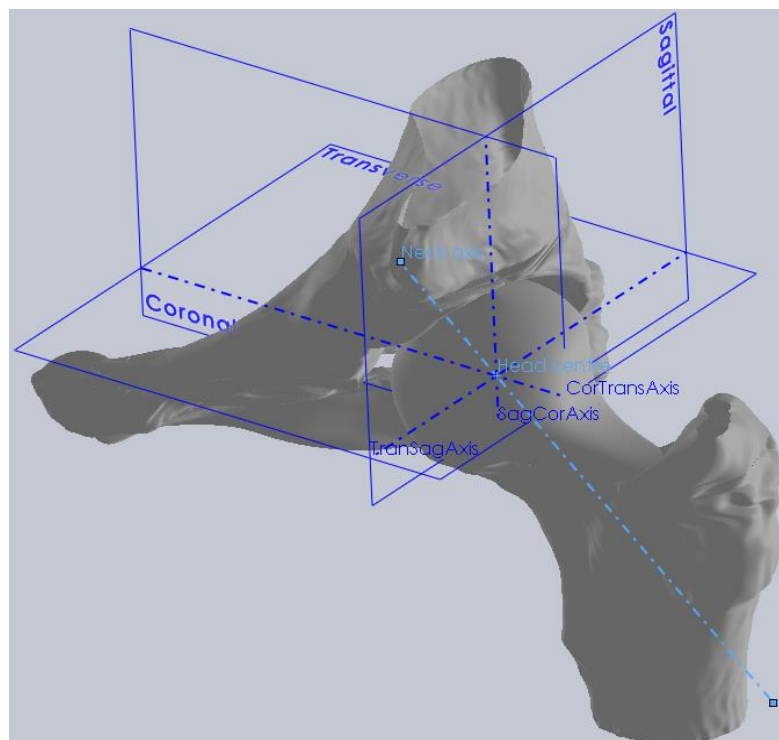


Figure 66: Hip articulation with new axes and anatomical planes. These new axes are designed to be used as rotation axes for the femur during the motion simulation.

4.35 Cinematic analysis

The range of motion must be measured between the neck axis and the different anatomical planes. Therefore the motion analysis should be set with variable parameters that allow the femur to rotate around its head centre in the various planes. To do so, three angular mates can be created between the new axes and the neck axis (figure 67).

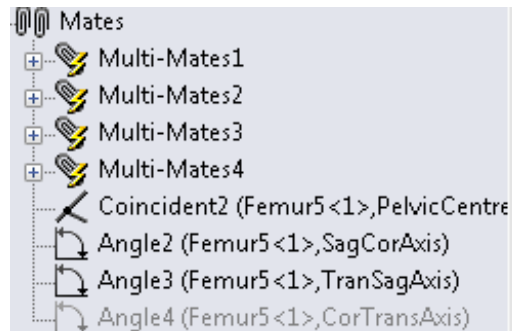


Figure 67: Updated mates showing the three new angular parameters (bottom) that can be modified in order to control the displacements of the femur during the motion analysis.

We can see in this figure that the last angular parameter is displayed in grey. It means the mate is “supressed”, which means not active. This is because the assembly is “fully defined” geometrically by the coincidence of the acetabular and femoral head centre and two angular parameters (it is isostatic). Therefore this last angular parameter can appear redundant in this static situation. It is nevertheless useful to keep this parameter, because some adjustments can be made with it during the motion analysis as it will be explained later on.

At first, these angles are fixed in the default (anatomical) position as shown in figure 68. The motion simulation can be performed by modifying the values of the angles in the “motion study” manager of Solidworks.

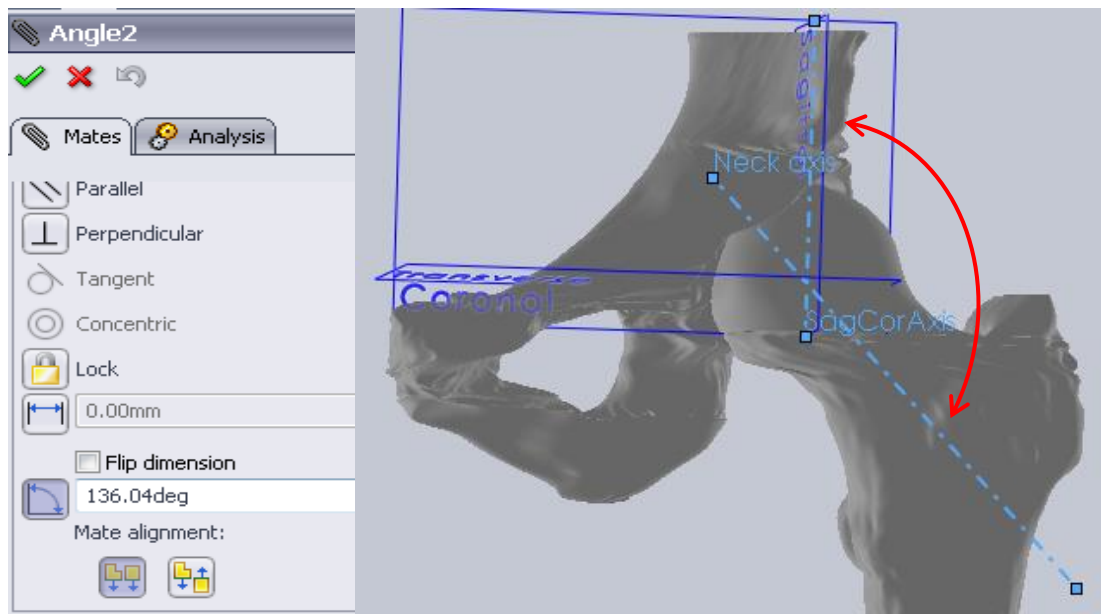


Figure 68: Setting the default value of the angle between the neck axis and the vertical axis (SagCorAxis). We see that the default anatomical angle is set at 136.04° in the coronal view.

As a result of the simulation, we want to measure the range of motion achievable without any impingement between the femur and the pelvic bone. Hence we have to select the “collision detection” associated with the “stop at collision” option. This will prevent the femur to rotate further if any collision with the pelvis is detected during the simulation.

To allow the model to move automatically, we must use the “motion study” manager. This module appears at the bottom of the main screen as shown in figure 69. In this figure, the motion analysis is already set. The successive blue bars correspond to different time phases, each one related to a particular angular motion.

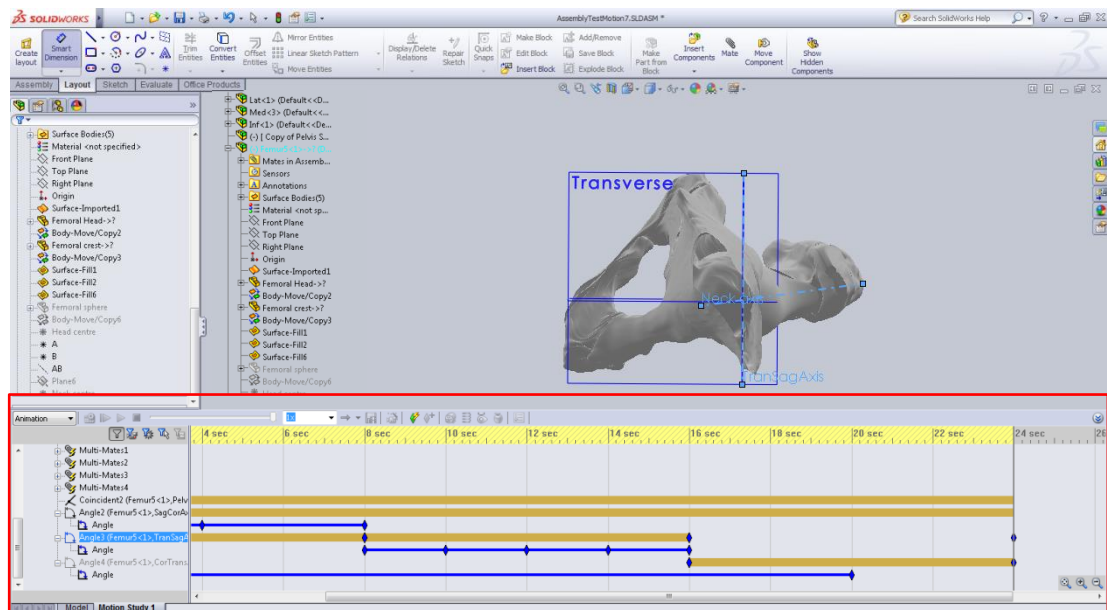


Figure 69: Full Solidworks screenshot showing the Motion Study manager (red frame). This module must be managed in time, hence the blue and brown lines extending in front of each parameter that represent the setting changes in time.

The motion study manager displays on the left tree all parameters that can be defined (therefore changed in time) during the analysis. The mates are of particular interest for us because the rotation of the femur will be controlled by changes in the values of the angular mates. The successive blue bars in the time track indicate the angular control of motion for each angular mate. As said before, only two angular mates can be active at the same time to fully define the position of the femur in space. By deactivating one of the two first angular mates, it is then possible to activate the last one and change its parameters during time. In this analysis, the extreme values of all angles were set to 360° to attempt a maximal movement. The analysis being set with the “stop at collision” parameter, the full 360° rotation is never achieved during simulation though.

4.36 Results of simulation.

When looking at the simulation, we can detect two major bone impingements during the movement. The first one (figure 70) occurs between the greater trochanter of the femur and the antero-superior iliac spine.

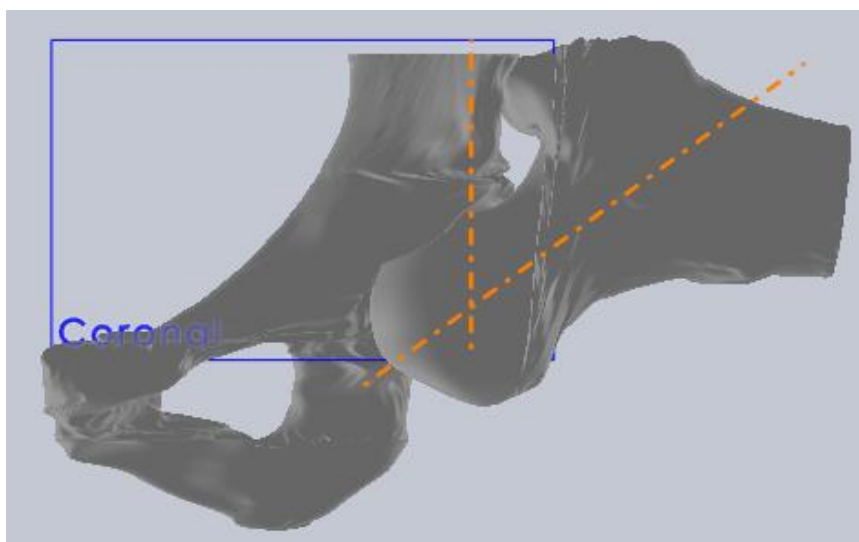


Figure 70: First impingement during simulation between the greater trochanter and the antero-superior iliac spine, coronal view.

This type of impingement is consistent with clinical reports if we bear in mind that the bones are never in direct contact within the real articulation. The pelvis and femur are surrounded by a great amount of soft tissues in the hip area. Therefore a real dislocation with this type of impingement would occur with the femur being in a much lower position and probably less rotated around its neck axis.

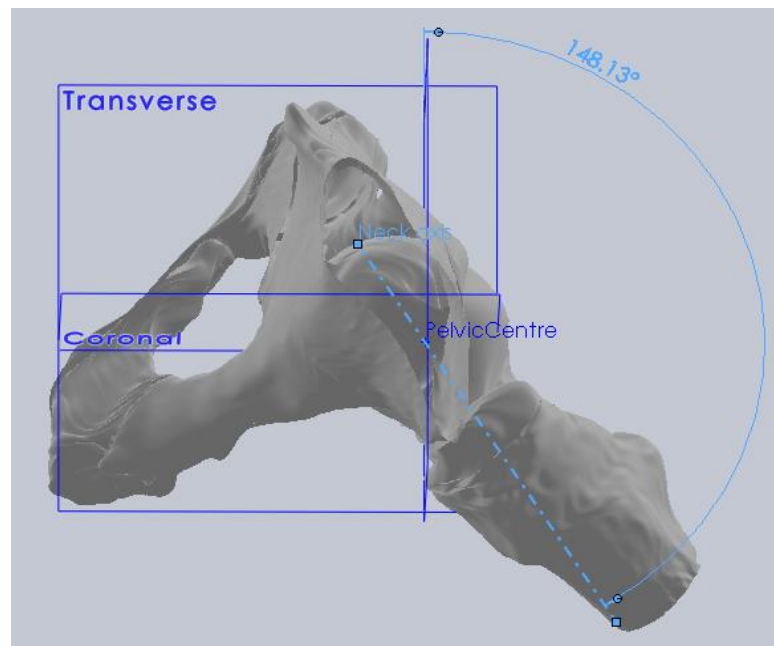


Figure 71: Angular measure between neck axis and sagittal plane at first impingement, superior view. The femur has rotated internally around the hip centre towards the pubis from the anatomical position.

We can then obtain a measure of the different angles between the neck axis and the different planes we referenced before as shown in figure 71 showing the impact moment from a superior view. This is possible by selecting the “smart dimension” tool.

The second impingement implies the lesser trochanter and the ischium. The moment of collision is displayed in figure 72 where we can see the contact between the bones. This is also a clinically referenced risk of real impingement. Once again, the soft tissues of the hip also play a role in clinics but only the bone structure is studied here.

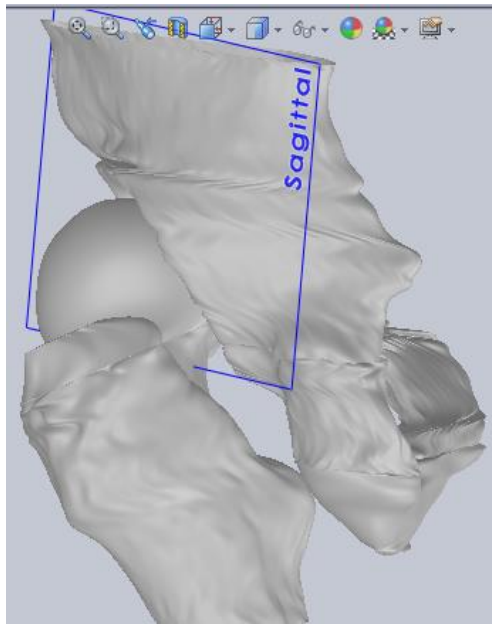


Figure 72: Second impingement, between the lesser trochanter and the ischium, during the simulation.

Then again it is possible to measure the angles between the neck axis and the different planes at collision time. The resulting angles are summarised in the figure 73 and 74.

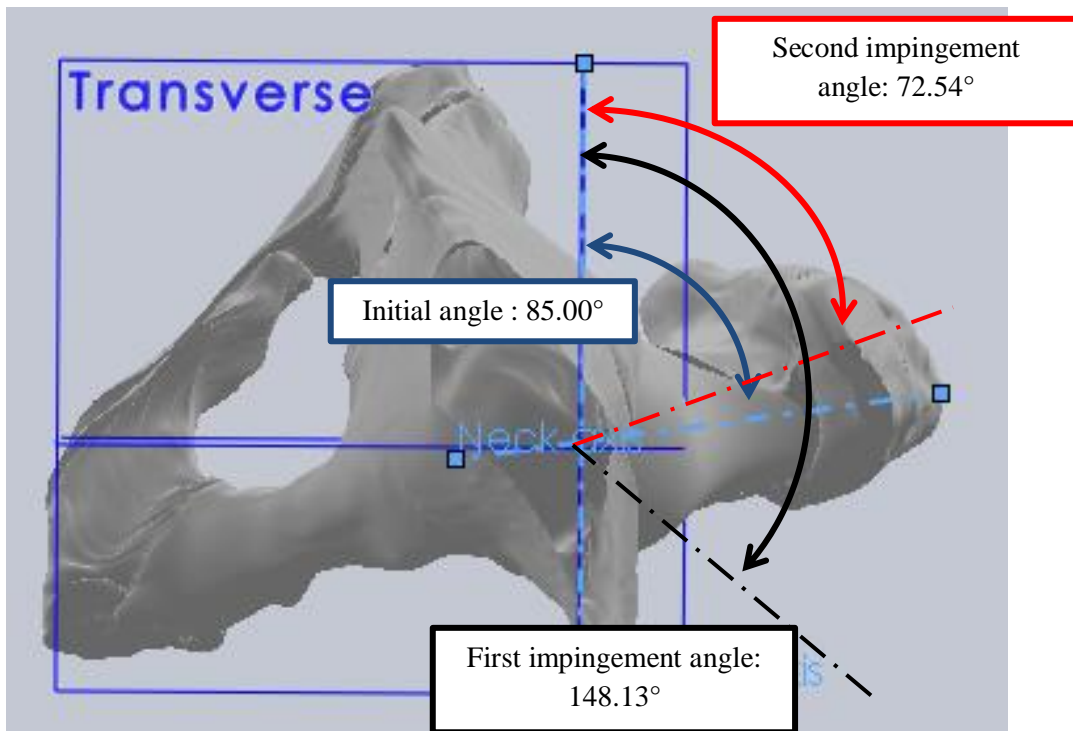


Figure 73: Maximum angles between neck axis and sagittal plane measured in a transverse view. The total range of motion in this view is 75.59° if we consider the two impingement angles as the extremums.

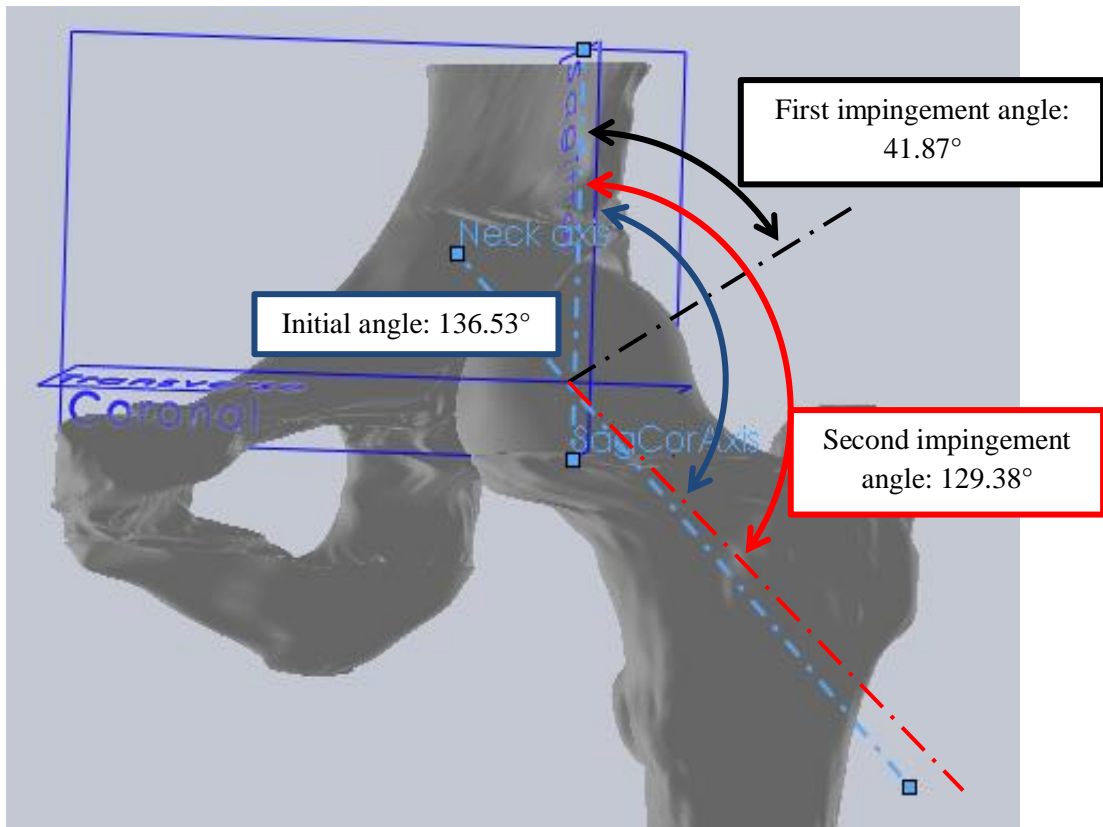


Figure 74: Maximum angles between neck axis and sagittal plane in a coronal view. The range of motion is 94.66° between the initial angle and the first impingement angle. The second impingement angle is inferior to the initial angle because of a rotation of the femur around its neck axis restricting the motion of the bone.

Part 5

Discussion

As explained in the introduction, this project was not only aiming to determine the range of motion of the hip articulation but also to define the path to achieve it. Therefore the different steps of this process must be reviewed and analysed.

5.1 Available CTs

The first set of CT scans was not optimal for an accurate 3D modelling of the hip articulation. The fact that the pelvis upper limit was tangent to the acetabular surface combined with the inadequacy of the contrast regarding the bone structure led to a very poor 3D reconstruction. Nevertheless, the availability of these files permitted an early contact with the Mimics software.

The second set of CTs was good material. The contrast was adapted and the extent of the slices at the hip level was sufficient to clearly identify every bone asperity that is typical of the proximal femur and the pelvis.

To be able to properly analyse and interpret the CTs, it is important to have a fairly good anatomical knowledge. The use of anatomy books is useful in addition to prior medical knowledge. It would be interesting to ask members of the medical staff like orthopaedic surgeons or radiologists for help at the beginning of the project in order to become rapidly familiar with the CT readings.

5.2 Mimics software

The first step was importing the images from the CTs. Theoretically it is possible to import only a selection of CT slices from the DICOM files. This operation was performed correctly with the first CTs but not with the most recent ones. For an unexplained reason, it was only possible to import the whole series of CT slices with those. The DICOM viewer that automatically opens with the CT files was different from the previous one, but the features of the viewer seemed the same. Maybe some options within the Mimics software could be found and selected to resolve this issue. Two consequences emerged from this particular issue. Firstly, the computational time required by Mimics to interpolate the data and create the sagittal and coronal views of the CTs was significantly higher. Secondly, the “crop mask” tool has been

used extensively on the newest models to get rid of the unnecessary parts of the model.

The thresholdings on the imported data have been done with a mixed technique, using the “threshold” command refined with the “profile line” tool. This mixed approach led to fairly good first 3D models compared to those obtained with a single approach (threshold or profile line technique alone). It is an efficient technique that deserves to be generally used when creating a new model from the CTs.

To isolate the 3D models and improve their quality, iterations have been performed with the tools available in the segmentation toolbar of the software. Those iterations (polylines, creation of a new mask, slice-by-slice edition of the new mask, generation of a new model, then new set of polylines) were quite time-consuming. Furthermore, the surface of the 3D files obtained with this method was not as satisfactory as expected. If the closure of the abnormal holes present on the models was really well achieved, the overall surface remained irregular and granular. As performed later in the project, it might have been better to do less iteration during this step of the process and increase the number of smoothing iteration while working with the MedCAD module.

The surface fitting was a complex process. Choosing accurately the decomposition of the model is fundamental. The complexity of this decomposition led to a simplification of the 3D model. Originally the entire pelvis was supposed to appear in order to recreate both right and left hip articulations in the CAD software. This is why both femurs, as well as the whole pelvic structure, appear in the project prior to the surface fitting process. Several surface fittings have been attempted with a complete pelvis but could not even be resolved by the software. In order to counter the problem, the project has been redefined. It has been decided to focus on the left articulation, which femur had the best resolution. The next challenge was about the u- and v-parameters. If the Mimics software lets the user choose the order and the number of control points to be used, it is not always easy to anticipate the result. Knowing the meaning of these parameters is not synonym of knowing the outcome of their selection. The only real way to see the impact of different settings is to try and compare the result. It is reinforced by the fact that settings leading to a good

surface approximation for a given set of polylines might lead to a very bad surface approximation on another set. The level of segmentation overlap between the different surfaces of a single model (either the femur or the pelvic bone) was really good however. Two surfaces that had to be connected in reality always had one supplementary CT slice overlapping the other surface. This overlapping slice added to each polyline growing set led to a very good match between surfaces during the “reconstruction” of the model during the CAD process. It preserved a similar curvature of the surfaces at the edges which facilitated the tangency detection between adjacent surfaces and hence their positioning within Solidworks.

The sphere fittings on the model were easily and accurately performed. It was disappointing not to be able to use directly the centre coordinates to locate the model in Solidworks, however the presence of the spheres precisely sized to fit the articular surfaces of both the femur and the pelvis was extremely useful. Unfortunately, the two axes created in Mimics to represent the neck and the diaphysis directions could not be adequately imported to Solidworks. Therefore, more work had to be done to recreate new references in the CAD analysis. Notwithstanding, it is the presence of the axes on the Mimics images that allowed performing the adequate measurements to recreate the neck axis on Solidworks. In consequence, the determination of the axes with Mimics was a useful step that could not have been avoided.

5.3 Solidworks software

Two ways have been employed to reunite the different surfaces into a complete model. The four surfaces describing the pelvic bone have been integrated to an assembly with fixed mates joining the different parts together. The result was a rigid structure that could not be easily relocated or rotated in the virtual space. It was not an absolute necessity in our project since the pelvic part itself served as reference for the complete hip articulation assembly; however this method might limit further possibilities. If we wanted to use again the same model to simulate other movements or adding other structures (soft tissues for instance), it might become problematic. Furthermore, the resulting assembly tree was quite large. Once again, our assembly was small enough to allow this without major issues, but it might be an exponential

problem if we wanted to add a greater number of structures. A large assembly tree containing many parts increases the calculation times during analysis, implies to requisition a large storage memory, and most of all increases the risk of inconsistency in the assembly. Inconsistencies appear when mates between the parts of an assembly are not compatible, too numerous or not adequate in the assembly context. They can also emerge from under-defined geometries. A lack of consistency leads to post-processing failures, for example the motion analysis is no longer possible. It is therefore highly recommended to have a well-built assembly tree, and reducing the number of parts that are present in the assembly seems a simple way to reduce the risk of inconsistency. The femur was rebuilt in a single part by joining the three surfaces directly. This has simplified the assembly tree in one hand, and in the other hand it allowed us to make the femur move within the assembly. This was a good solution and should be the preferred solution for reconstructing a single surface model from various surface files.

The sphere fittings took some time, since it was not possible to locate the spheres directly with coordinates. The collision detection was a rather straightforward way to fit the sphere to the pelvic bone, but the sphere fitted to the femoral head took longer to locate. It would be useful to plan this location by taking measurements from Mimics during the initial sphere fitting process in the 3 anatomical planes that cross the hip centre.

The impossibility to import the neck and diaphysis axes of the femur led to a major problem. In order to simplify the result, the neck axis only has been rebuilt. The rebuild itself has been well performed, and the geometrical determination of this axis was coherent and robust. However, without the diaphysis axis, no orientation of the femur has been performed around the neck axis. Therefore, the femur could freely rotate around the neck axis without any precise parameter to control it. It is problematic for the simulation as well as for the results, since we could not measure this parameter after the simulation.

The creation of three anatomical planes centred on the hip articulation centre was very useful. It led to a clearer visualisation and allowed us generating rotation axes around which the femur was moved during simulation. The simulation itself was

controlled with a low number of parameters. It should simplify the analysis, unfortunately the absence of orientation of the femur around its neck axis made this simulation problematic. During the motion the femur is not fully controlled, therefore some unexpected movements occur during the sequence.

Nevertheless, the collision detection has accurately been performed during the simulation. We saw the expected impingements and some measurements have been done to estimate the range of motion. The issue there was the accuracy of the results. The angular measurements have been done between the neck axis and the planes, but it is not certain that the results displayed are the angles we wish to measure. It depends on how Solidworks calculates the angle between the plane and the axis. To have a well-defined measure of the angles between the femur and the three anatomical planes, some additional references were necessary. Once again, the diaphysis axis would have been useful. Combined with the neck axis, it would have defined a new reference plane for the femur. Then it would have been possible to measure the angles between this new plane and the anatomical planes, and hence all ambiguities about the angles would have been eliminated. The spatial orientation of the femur would be completely traceable.

Part 6

Further work and conclusion

This project was ambitious and required many different steps to be fully over. The aim was to create an estimation of the range of hip motion that could be used by medical staff in order to reduce the dislocation rate after the surgery. Mainly, it was about measuring the range of hip motion achievable without bone impingement. The final result is not totally satisfactory regarding this requirement, but a good result could be soon achieved. Some recommendations for the future work could help with this objective by drastically reducing the time that was lost in unsuccessful trials and abandoned solutions.

The first important thing to do is finding good quality CTs from the beginning. It was easier to perform 3D reconstructions with good CTs since all the segmentation and therefore thresholding processes rely on the quality of the scans. The final models obtained with the newest CTs are pretty accurate, as attested by the good adequacy between the dimensions of the femoral head and the acetabular surface. It is also important to learn rapidly how to interpret the CTs. The help of medical staff, surgeons or radiologists for example, would surely be an asset. It would also be useful to access “real” 3D models (either real bones or facsimile of the articulation) to have a better understanding of the bone structure. Another interesting thing to do is focusing on a single articulation from the beginning of the Mimics process.

To perform the thresholding, the mixed use of the “threshold” and “profile line” tools is recommended. Once the first 3D model is generated, the number of iteration (polylines, creation of a new mask, slice-by-slice edition of the new mask, generation of a new model, then new set of polylines) should be limited to 2 at most. It might even be interesting to perform only one new analysis and then try to refine the model with the “smoothing” tool later in MedCAD. Maybe this will be sufficient to recreate the overall shape of the bone with an acceptable approximation.

The surface fitting has to be done with the “polyline growing” tool. The use of a systematic one-slice-thick overlap between two connected polyline sets proved to give very satisfactory results when it comes to reconnect the generated surfaces in the CAD environment. Regarding the u- and v-parameters (order and number of control points), it is unfortunately difficult to provide an accurate advice. Testing different parameters and compare the results remains the best solution so far.

Nevertheless, it is highly recommended to begin with low parameters and then increase them progressively, since the computational time increases very rapidly when the parameters are raised. Once the surfaces are generated, fitting spheres to the articular surfaces is encouraged. Recording the coordinates of their centre is not required though, since it cannot be used in Solidworks. In the same way, the determination of the neck and diaphysis axes of the femur might not be very useful while using Mimics. Perhaps some work could be done on this particular problem, in order to find an easy and quick way to extrapolate the neck and diaphysis orientation in Solidworks based on a complex surface.

To recreate the bone structures within Solidworks, the different surfaces that belong to the same bone should be combined in a single part. The spheres created with Mimics should also be imported in their matching part. Fitting the acetabular sphere is easily done with a collision detection combined with the “stop at collision” option. The femoral sphere requires more work. The previously suggested solution was to take precise measurements on the CT slices, but some further work on this issue might lead to a better solution. Once this step is done, the two parts should then be imported in an assembly and mated with the coincidence of the sphere centres.

Defining the anatomical planes and associated axes is very interesting. It allows the user to set multiple angular parameters before the simulation, and after that to take all the measurements that will define the range of motion of the hip articulation before impingement. The important thing is to find a way to know the orientation of the femur around its neck axis at all time. Some further work should be done to find the better way to achieve this function. Fully define the angular measurements and ensure they correspond to the actual position of the femur regarding the different anatomical planes is another necessary improvement.

During the simulation, two clinically relevant impingements have been detected. The two situations are encountered in extreme positions of the bones and can both lead to dislocation, especially when the soft tissues surrounding the articulation facilitate this process. The angles measured with Solidworks show the precise range of motion in two planes and can be communicated to surgeons to help them having a better understanding of the patient hip’s mobility. These measurements can be improved by

projecting the angles in new planes that are more clinically used: the radiological planes.

Therefore, once these steps have been resolved, further research paths could be investigated. It would be interesting to use different reference planes, depending on the requirements of the medical staff. The simulation could also be performed on both hip articulations of the patient in order to compare the results and give more information to surgeons. But the biggest challenge would be the addition of soft tissues to the current single-articulation hip model. Many parameters would change with such hypothesis, but it is likely that the bigger difference would be the 3D models used for the soft tissues. It would probably be necessary to import them not as surface models but as volume models, in order to be able to assign various material and mechanical properties to them. As a consequence, the motion analysis could no longer be based on simple collision detection since it should include material deformations. Maybe asking for advice to tissue mechanics specialists could be a good start. It would be a real improvement because the medical staff in confronted to real patient hence the hip motion simulation will never be totally realistic without the soft tissues.

Therefore, even if much work has been done on this project, many further improvements can be achieved, or at last investigated. The humblest one would be achieving a clearer measurement of the various angles on the bone model. The most ambitious research path would be integrating the soft structures to the bone parts in order to take realistic measurements of the hip motion.

Associated video files

Six video files (.avi files) are available in addition to this thesis in order to illustrate some Mimics and Solidworks steps. The following material is attached to the thesis:

2015waltermcscbioeng_video1.avi

Mimics video showing the 3D structure generated from the cropped mask on the left hip articulation (green 3D model) in association with the extrapolated polylines (yellow curves). We can notice the artefacts, holes and merged areas of the model.

2015waltermcscbioeng_video2.avi

Mimics video that compares the pelvis before (yellow) and after (green) an iteration or the refining process. The surface quality improves, holes are closed and artefacts are suppressed. The acetabular surfaces in particular are meticulously redefined.

2015waltermcscbioeng_video3.avi

Mimics video displaying a rotating view of the 3D left femur model before the smoothing operation.

2015waltermcscbioeng_video4.avi, 2015waltermcscbioeng_video5.avi and

2015waltermcscbioeng_video6.avi

These are Solidworks videos showing the final motion analysis simulation. First impingement occurs at 4 seconds, second impingement occurs at 20 seconds. Anatomical planes are displayed at the hip centre level without labels on **video4**, and with transverse, sagittal and coronal labels on **video5**. Finally, the simulation is shown without the planes on **video6**.

References

- ¹ <http://www.arthritisresearchuk.org/arthritis-information/surgery/hip-replacement-surgery/> accessed on June 2015
- ² http://www.ons.gov.uk/ons/dcp171776_258607.pdf, Population Ageing in the United Kingdom, its Constituent Countries and the European Union, 2012 accessed on June 2015
- ³ <http://www.njrcentre.org.uk> accessed on June 2015
- ⁴ James L. Nutt, Kleomenis Papanikolaou, Catherine F. Kellett, Complications of total hip arthroplasty, Orthopaedics and Trauma, Volume 27, Issue 5, October 2013, Pages 272-276, ISSN 1877-1327
- ⁵ Robert Pivec, Aaron J. Johnson, Simon C. Mears, Michael A. Mont, Reprint of “Hip arthroplasty”, International Journal of Orthopaedic and Trauma Nursing, Volume 17, Issue 2, May 2013, Pages 65-78, ISSN 1878-1241,
- ⁶ <http://www.nhs.uk> accessed on June 2015
- ⁷ W. J. Hozack, J. Parvizi, B. Bender, W.B. Saunders, Surgical Treatment of Hip Arthritis, Philadelphia, 2009, Elsevier ISBN 9781416058984
- ⁸ Michael Nogler, Saunders, The Direct Anterior Approach, Philadelphia, 2009, Elsevier ISBN 9781416058984
- ⁹ Donald S. Garbuz, Gurdeep S. Biring, and Clive P. Duncan, Saunders, The Anterolateral Minimal/Limited Incision Intermuscular Approach, Philadelphia, 2009, Elsevier ISBN 9781416058984

¹⁰ Ormonde M. Mahoney, Tracy L. Kinsey, Saunders, The Direct Lateral Approach, Philadelphia, 2009, Elsevier ISBN 9781416058984

¹¹ P.J. Lusty, W.L. Walter, D. Young, Saunders, Posterior and Posteroinferior Approaches, Philadelphia, 2009, Elsevier ISBN 9781416058984

¹² Jeya Palan, David J. Beard, David W. Murray, J. G. Andrew, and John Nolan, Which Approach for Total Hip Arthroplasty: Anterolateral or Posterior? FRCS (Orth) Clinical Orthopaedics and Related Research, Feb 2009; 467(2): 473–477.

¹³ A. Ploumis, K. Tapsis, I. Papageorgiou, I. Terzidis, D Pouliopoulos and A. Christodoulou, Comparative study between posterior and lateral approach of total hip arthroplasty in patients with osteoarthritis. Journal of Bone & Joint Surgery 2003 vol. 85-B no. SUPP III 225-226

¹⁴ Kwon, Michael; Kuskowski, Michael; Mulhall, Kevin; Macaulay, William; Brown, Thomas; Saleh, Khaled; Does Surgical Approach Affect Total Hip Arthroplasty Dislocation Rates? Clinical Orthopaedics & Related Research June 2006 - Volume 447 - Issue - pp 34-38 DOI: 10.1097/01.blo.0000218746.84494.df

¹⁵ Witzleb, Stephan, Krummenauer, Neuke, Günther, Short-term outcome after posterior versus lateral surgical approach for total hip arthroplasty - A randomized clinical trial, (2009) European Journal of Medical Research, 14 (6), pp. 256-263.

¹⁶ Demos, Rorabeck, Bourne, MacDonald, McCalden, Instability in primary total hip arthroplasty with the direct lateral approach, (2001) Clinical Orthopaedics and Related Research, (393), pp. 168-180.

¹⁷ E. Kaivosoja, V.-M. Tiainen, Y. Takakubo, B. Rajchel, J. Sobiecki, Y.T. Kontinen and M. Takagi, Materials used for hip and knee implants, edited by Saverio Affatato, Woodhead Publishing, 2013, Pages 178-218, Wear of Orthopaedic Implants and Artificial Joints, ISBN 9780857091284

-
- ¹⁸ B Sonny Bal; Santaram Vallurupalli, Ceramic Bearings in Total Joint Arthroplasty, updated June 2014, <http://emedicine.medscape.com> accessed on June 2015
- ¹⁹ E. Kaivosoja, V.-M. Tiainen, Y. Takakubo, B. Rajchel, J. Sobiecki, Y.T. Konttinen and M. Takagi, Materials used for hip and knee implants, edited by Saverio Affatato, Woodhead Publishing, 2013, Pages 178-218, Wear of Orthopaedic Implants and Artificial Joints, ISBN 9780857091284
- ²⁰ .B. Pedersen, F. Mehnert, L.I. Havelin, O. Furnes, P. Herberts, J. Kärrholm, G. Garellick, K. Mäkela, A. Eskelinen, S. Overgaard, Association between fixation technique and revision risk in total hip arthroplasty patients younger than 55 years of age. Results from the Nordic Arthroplasty Register Association, Osteoarthritis and Cartilage, Volume 22, Issue 5, May 2014, Pages 659-667, ISSN 1063-4584,
- ²¹ L.V. Wilches, J.A. Uribe, A. Toro, Wear of materials used for artificial joints in total hip replacements, Wear Volume 265, Issues 1–2, 25 June 2008, Pages 143–149 doi:10.1016/j.wear.2007.09.010
- ²² Darryl D. D’Lima, Andrew G. Urquhart, Knute O. Buehler, Richard H. Walker, Clifford W. Colwell Jr., The Effect of the Orientation of the Acetabular and Femoral Components on the Range of Motion of the Hip at Different Head-Neck Ratios, The Journal of Bone and Joint Surgery, VOL. 82-A, NO. 3, March 2000
- ²³ Aamer Malik, MD, Aditya Maheshwari, MD, and Lawrence D. Dorr, MD, Impingement with Total Hip Replacement, The Journal Of Bone And Joint Surgery 2007;89:1832-42 doi:10.2106/JBJS.F.01313
- ²⁴ K.-H. Widmer, B. Zurfluh, Compliant positioning of total hip components for optimal range of motion, Journal of Orthopaedic Research 22 (2004) 815-821, 2003
- ²⁵ S.W. Veitch, S.A. Jones, Prevention of dislocation in hip arthroplasty, Orthopaedics and Trauma, Volume 23, Issue 1, February 2009, Pages 35-39, ISSN 1877-1327

²⁶ G. E. Lewinnek, J. L. Lewis, R. Tarr, C. L. Compere and J. R. Zimmerman, Dislocations after Total Hip-Replacement Arthroplasties, in *The Journal of Bone and Joint Surgery* vol. 60-A, NO. 2. MARCH 1978

²⁷ Is there really a "safe zone" for the placement of total hip components? By Bioceramics and alternative bearings in joint arthroplasty 11th BIOLOX Symposium, Rome, June 30 - July 1, 2006

²⁸ Hirohito Abe, Takashi Sakai, Masaki Takao, Takashi Nishii, Nobuo Nakamura, Nobuhiko Sugano, Difference in Stem Alignment Between the Direct Anterior Approach and the Posterolateral Approach in Total Hip Arthroplasty, *The Journal of Arthroplasty*, Available online 24 April 2015, ISSN 0883-5403

²⁹ Widmer, K.-H., Zurfluh, B., Compliant positioning of total hip components for optimal range of motion (2004) *Journal of Orthopaedic Research*, 22 (4), pp. 815-821. DOI: 10.1016/j.orthres.2003.11.001

³⁰ <https://www.clinicalgraphics.com/> accessed on March 2015

³¹ Ehsan Arbabi, Ronan Boulic and Daniel Thalmann, A Fast Method for Finding Range of Motion in the Human Joints, 29th Annual International Conference of the IEEE EMBS Cité Internationale, Lyon, France August 23-26, 2007

³² Fumihiro Yoshimine, Ko Ginbayashib, A mathematical formula to calculate the theoretical range of motion for total hip replacement, *Journal of Biomechanics* 35 (2002) 989–993

³³ Sahar Aghayan, Calculation and Visualization of Range of Motion of Hip Joint from MRI, Thesis submitted to the Faculty of Graduate and Postdoctoral Studies for the degree Master of Computer Science, Ottawa, Canada, 2014

-
- ³⁴ Keisuke Hagio, Nobuhiko Sugano, Takashi Nishii, Hidenobu Miki, Yoshito Otake, Asaki Hattori, Naoki Suzuki, Kazuo Yonenobu, Hideki Yoshikawa, Takahiro Ochi, A novel system of four-dimensional motion analysis after total hip arthroplasty, Journal of Orthopaedic Research, Volume 22, Issue 3, May 2004, Pages 665-670, ISSN 0736-0266
- ³⁵ Jianping Wang, Ming Ye, Zhongtang Liu, Chengtao Wang, Precision of cortical bone reconstruction based on 3D CT scans, Computerized Medical Imaging and Graphics, Volume 33, Issue 3, April 2009, Pages 235-241, ISSN 0895-6111
- ³⁶ Kanchana Rathnayaka, Konstantin I. Momot, Hansrudi Noser, Andrew Volp, Michael A. Schuetz, Tony Sahama, Beat Schmutz, Quantification of the accuracy of MRI generated 3D models of long bones compared to CT generated 3D models, Medical Engineering & Physics, Volume 34, Issue 3, April 2012, Pages 357-363, ISSN 1350-4533
- ³⁷ Jacek Starzynski, Zuzanna Krawczyk, Bartosz Chaber, Robert Szmurlo, Morphing algorithm for building individualized 3D skeleton model from CT data, Applied Mathematics and Computation, Available online 14 January 2015, ISSN 0096-3003
- ³⁸ Shay Kels, Nira Dyn, Reconstruction of 3D objects from 2D cross-sections with the 4-point subdivision scheme adapted to sets, Computers & Graphics, Volume 35, Issue 3, June 2011, Pages 741-746, ISSN 0097-8493,
- ³⁹ Anthony Viste , Franck Trouillet, Rodolphe Testa, Laurence Chèze, Romain Desmarchelier and Michel-Henri Fessy, An evaluation of CT-scan to locate the femoral head centre and its implication for hip surgeons, Surgical and Radiologic Anatomy 2013, 36:1172 DOI: 10.1007/s00276-013-1172-7
- ⁴⁰ Hans Kainz, Christopher P. Carty, Luca Modenese, Roslyn N. Boyd, David G. Lloyd, Estimation of the hip joint centre in human motion analysis: A systematic

review, *Clinical Biomechanics*, Volume 30, Issue 4, May 2015, Pages 319-329, ISSN 0268-0033

⁴¹ M.E. Harrington, A.B. Zavatsky, S.E. Lawson, Z. Yuan, T.N. Theologis
Prediction of the hip joint centre in adults, children, and patients with cerebral palsy based on magnetic resonance imaging, *J. Biomech.*, 40 (3) (2007), pp. 595–602

⁴² Luo Sanding, Zou Zheng, Chen Yuanbing, Liu Qianlan, The 3D Data Extraction for Hip Joint Based on CT, *AASRI Procedia*, Volume 1, 2012, Pages 293-298, ISSN 2212-6716

⁴³ <http://methode-apte.com/> accessed on June 2015

⁴⁴ Yoshioka, Siu, Cooke, The anatomy and functional axes of the femur, *Journal of Bone and Joint Surgery*, 1987 Jul; 69(6):873-80.

⁴⁵ Eun-Kyoo Song, Jong-Keun Seon, Jae-Young Moon and Yim Ji- Hyoun, The Evolution of Modern Total Knee Prostheses, DOI: 10.5772/54343 in Arthroplasty – Update Edited by Plamen Kinov, ISBN 978-953-51-0995-2

⁴⁶ NCI CDISC – National Cancer Institute, Clinical Data Interchange Standards Consortium: International, non-profit organization that develops and supports global data standards for medical research (<http://www.cancer.gov/research/resources/terminology/cdisc> accessed on June 2015)

⁴⁷ <http://dicom.nema.org/> accessed on June 2015

⁴⁸ Henri Nahum, Traité d'imagerie médicale, edition: Médecine Sciences Publications, 2013m, ISBN 2257205812, 9782257205810